

2019-10

# Potential of Scoria, Pumice, and RHA as Supplementary Cementitious Materials for Reducing Setting Time and Improving Early Strength of Pozzolan Blended Composite Cement

Mboya, Hieronimi Alphonc

NM-AIST

---

<https://doi.org/10.58694/20.500.12479/955>

*Provided with love from The Nelson Mandela African Institution of Science and Technology*

**Potential of Scoria, Pumice, and RHA as Supplementary Cementitious Materials for  
Reducing Setting Time and Improving Early Strength of Pozzolan Blended Composite  
Cement**

**Hieronimi Alphonse Mboya**

**A Dissertation Submitted in Partial Fulfillment of the Requirements for the Degree of  
Doctor of Philosophy in Materials Science and Engineering of the Nelson Mandela  
African Institution of Science and Technology**

**Arusha, Tanzania**

**October, 2019**

## ABSTRACT

Tanzania has huge deposits of scoria (S-N) and pumice (P-N) minerals that can be used as supplementary cementing materials (SCMs) in cement factories to cut down the cost of cement and its pollution effect to the environment. Besides this, agricultural wastes such as rice husk produce rice husk ash (RHA) having high silica content that can be used with cement to reduce the cost of cement and its impact to environment. Performance indicators of mortar and concrete such as slump, flow, permeability, shrinkage, modulus of rupture, compressive and tensile splitting strength were tested with different proportions of SCMs. It was found out that in addition to cutting the CO<sub>2</sub> emissions, SCMs reduce energy bills and that they confer extra strength and resistance to mortar and concrete. This work only examined the properties of scoria (S-N) and pumice (P-N) and rice husk ash (RHA) as supplementary cementing materials (SCMs) for Portland cement.

The investigation considered these materials in binary and ternary module. X-ray fluorescence, X-ray diffraction, and pozzolanic activity index (PAI) tests confirmed the suitability of these materials as potential SCMs. Initial and final mean setting times observed for a binary composite cement were 166 and 285 min respectively. The setting times were longer than those of Ordinary Portland cement (OPC) but shorter when compared to Portland pozzolana cement.

Characteristic and target mean strengths of 30 and 38.2 MPa were considered. The ultimate mean compressive strengths achieved at 28 days of curing were 42.5, 44.8, and 43.0 MPa for S-N, P-N, and RHA respectively indicating the potentials of these materials as SCMs. Further observation show that, the 28-days maximum compressive strength achieved by the blended cement concrete (with 10% replacement of SCMs) were 44.2 and 43.1 MPa for S-N 10 and P-N 10, respectively. The modulus of rupture decreased with an increase in the amount of S-N. On the other hand with P-N, a maximum of 8.0 MPa at 20% replacement was observed

but then dropped to a minimum value of 6.4 MPa at 40% replacement level. This indicated potentially a superior ability of the P-N concrete to endure more sustained stress such as those caused by tremors and earthquakes and impact-related stresses. The residual compressive strength of P-N blended cement concrete samples, after subjection to a high temperatures of 600 °C, was higher compared to S-N blended cement indicating the superior resistance of P-N to higher temperatures. S-N 10, S-N 20 and S-N 30 gave coefficients of permeability, ( $K$ ), of 5.2526E-08, 5.20833E-08, and 4.9741E-08 m/s, in that order. This low permeability was attested by their dense microstructure, with implied reduced chemical attack, less carbonation, improved steel protection against corrosion, and enhanced durability of the reinforced concrete.

The maximum compressive strength of ternary materials of 53.8 MPa was attained at 10/20% P-N/RHA replacement level. The 28 days Strength Activity Index (SAI) of S-N/RHA blended cement at 30/0, 10/20, 5/25 and 0/30% S-N/RHA were above 75% recommended by ASTM. On the other hand the SAI of P-N/RHA blended cement were higher than the ASTM recommended value at all replacement levels. Therefore, 10% of S-N, P-N or RHA is recommended as the optimum replacement for Portland cement in binary materials and 10/20% P-N/RHA for ternary materials to enhance performance of cement.

## DECLARATION

I Hieronimi Alphonse Mboya do declare to the Senate of the Nelson Mandela African Institution of Science and Technology that this dissertation is my own original work and that it has neither been submitted nor concurrently submitted for the degree award in any other institution.

---

Name and signature of candidate	Date
---------------------------------	------

The above declaration is confirmed

Prof. Karoli N. Njau

---

Name and signature of candidate	Date
---------------------------------	------

Dr. Cecil Kithongo King'ondeu

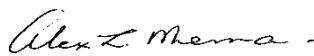


16/10/2019

---

Name and signature of candidate	Date
---------------------------------	------

Prof. Alex L. Mrema



17/10/2019

---

Name and signature of candidate	Date
---------------------------------	------

## **COPYRIGHT**

This dissertation is copyright material protected under the Berne Convention, the Copyright Act of 1999 and other international and national enactments, in that behalf, on intellectual property. It must not be reproduced by any means, in full or in part, except for short extracts in fair dealing; for researcher private study, critical scholarly review or discourse with an acknowledgement, without a written permission of the Deputy Vice Chancellor for Academic, Research and Innovation, on behalf of both the author and the Nelson Mandela African Institution of Science and Technology.

## CERTIFICATION

The undersigned certify that they have read dissertation titled “**Potential of Scoria, Pumice, and Rice Husk Ash as Supplementary Cementitious Materials for Reducing Setting Time and Improving Early Strength of Pozzolan Blended Composite Cement**”, and recommended for examination in fulfillment of the requirements for the Degree of Doctor of Philosophy of Materials Science and Engineering of the Nelson Mandela African Institution of Science and Technology.

---

Prof. Karoli N. Njau  
(Supervisor)



---

Dr. Cecil K. King'onde  
(Supervisor)



---

Prof. Alex L. Mrema  
(Supervisor)

## ACKNOWLEDGMENTS

I am indebted to convey my heartfelt thanks to all people who helped to make this dissertation possible.

It is my pleasure to offer my praise, glory and honor to the Almighty God for granting me life and benedictions. Magnificent God, delightful God, Miracle worker, King of Kings. Omnipotent Good, I respect You, Your majesty is eternally.

My heartfelt thanks to my main supervisor Prof. Karoli N. Njau for his tireless guidance, encouragement, support, and patience. He was always strengthening me where I was weak and discouraged.

I wish to convey my profound thanks to my co-supervisors, Prof. Alex L. Mrema and Dr. Cecil Kithongo King'onde for all their tireless guidance, inspiration, support, and perseverance. Their sincere and unexplainable interests in material science and engineering have been of a great inspiration to me.

I would like to thank the Government of the United Republic of Tanzania through the Nelson Mandela Institution of Science and Technology for giving me a scholarship to pursue this course.

My thanks and appreciations go to the Dean of School MEWESE for persevering with me as my lecturer and mentor all through my coursework and in this dissertation.

My gratitude goes to Professor Alexander Pogrebnoi, Professor Tatiana Pogrebnya and Dr. Askwar Hilonga my lecturers in the Department of MASE who tirelessly shared their memories and experiences that supported and expanded my knowledge and comprehensive thinking. Indeed I appreciate their cooperation.

I am grateful too to my late father Alphonse and mother Yohana for their hospitality, wisdom, enlightenment, and encouragement throughout my life. May God let the rest in eternal peace. Amen.



I am grateful to express gratitude to my beloved wife Hilda Tulanyilika for her passion and faithfulness in all years of my study and her encouragement through prayers that consistently helped to overcome my hardships and difficulty circumstances.

My heartfelt thanks go to my children Innocent, Immaculate, Irene, Isabela, Isaac, and Immanuel for their litanies and homesickness of their father through all years of study.

I finally thank my brothers T. Mboya, J. Mboya, Dr. B. Mboya and E. Mungunasi for their encouragement, moral and material support during difficult times in my life.

## **DEDICATION**

With lot of appreciation and great love I dedicate this dissertation to my beloved wife Hilda Tulanyilika and my children: Innocent, Immaculate, Irene, Isabela, Isaac, Immanuel, and Alphonse and my grandchildren: Joshua and Lightness, together with Witness whom I am her guardian for tirelessly devoting their time and efforts praying day and night for my success.

## TABLE OF CONTENTS

ABSTRACT.....	i
DECLARATION .....	iii
COPYRIGHT.....	iv
CERTIFICATION .....	v
ACKNOWLEDGMENTS .....	vi
DEDICATION .....	viii
LIST OF TABLES .....	xiii
LIST OF FIGURES .....	xiv
LIST OF ABBREVIATIONS AND SYMBOLS .....	xvi
Chapter 1 : GENERAL INTRODUCTION AND BACKGROUND .....	1
1.1    Introduction.....	1
1.2    Statement of the Problem.....	3
1.3    Research Objectives.....	3
1.3.1    Main Objective.....	3
1.3.2    Specific objectives .....	4
1.3.3    Research Questions.....	4
1.4    Scope of the Research.....	4
1.5    Rationale of the Research .....	5
1.6    Expected Outcome/Significance .....	5
Chapter 2 : THE EFFECT OF DIVERSE POZZOLAN TO THE PROPERTIES OF MORTAR AND CONCRETE.....	6
2.1    Introduction.....	6
2.1.1    Cement .....	6
2.1.2    Supplementary Cementitious Materials .....	7
2.2    Pozzolanic materials .....	8
2.2.1    Silica fume .....	9
2.2.2    Fly ash.....	10
2.2.3    Ground Granulated Blast Furnace Slag.....	10
2.2.4    Metakaolin .....	11
2.2.5    Rice Husk Ash .....	12
2.2.6    Scoria .....	13

2.2.7	Pumice.....	14
2.3	Pozzolanic reactions.....	14
2.3.1	Pozzolanic activity index .....	14
2.4	Properties of Pozzolan Blended Cement.....	18
2.4.1	Setting Times .....	18
2.4.2	Soundness .....	19
2.4.3	Effect of Alkali.....	20
2.5	Properties of mortar and concrete .....	21
2.5.1	Workability .....	21
2.6	Properties of blended cement.....	22
2.6.1	Density, Porosity and water absorption .....	22
2.6.2	Mechanical Strength .....	23
2.7	Durability of concrete containing diverse Pozzolanic materials.....	26
2.7.1	Shrinkage .....	27
2.7.2	Expansion and Alkali silica reactions .....	28
2.7.3	Carbonation.....	29
2.7.4	Chloride ion diffusion .....	30
2.7.5	Sulphate resistance.....	30

Chapter 3	: MEASUREMENT OF POZZOLANIC ACTIVITY INDEX OF SCORIA, PUMICE AND RICE HUSK ASH AS POTENTIAL SUPPLEMENTARY CEMENTITIOUS MATERIALS FOR PORTLAND CEMENT .....	31
3.1	Introduction.....	32
3.2	Materials and Methods.....	36
3.2.1	Materials .....	36
3.2.2	Experimental Procedures .....	36
3.2.3	Determination of chemical and phase composition .....	37
3.2.4	Determination of specific gravity, specific surface area, particle size distribution (PSD), and pozzolanic activity index (PAI).....	38
3.2.5	Determination of setting times and soundness.....	38
3.2.6	Determination of compressive strength .....	40
3.3	Results and discussion .....	40
3.3.1	Materials chemical composition and physical properties .....	40
3.3.2	Particle size distribution (PSD).....	46
3.3.3	Pozzolanic activity index (PAI) .....	46

3.3.4	Setting times.....	48
3.3.5	Shrinkage and Soundness.....	50
3.3.6	Compressive strength of scoria and pumice blended cement .....	52
3.4	Conclusion .....	54

**Chapter 4 : INFLUENCE OF SCORIA AND PUMICE ON KEY PERFORMANCE INDICATORS OF PORTLAND CEMENT CONCRETE .....56**

4.1	Introduction.....	58
4.1.1	Classes of Concrete.....	59
4.1.2	Economical application of Scoria and Pumice.....	60
4.2	Objectives, .....	60
4.3	Materials and Methods.....	60
4.3.1	Materials .....	60
4.3.2	Methods and laboratory experiments .....	61
4.3.3	Aggregate grading and blending .....	62
4.3.4	Concrete Mix Design .....	63
4.4	Results and Discussion .....	64
4.4.1	Properties of fresh concretes .....	64
4.4.2	Properties of hardened concretes .....	67
4.5	Conclusions.....	82

**Chapter 5 EFFECTS OF CEMENT BLENDED WITH SCORIA AND RHA OR PUMICE AND RHA TO THE PROPERTIES OF MORTAR AND CONCRETE: OPTIMIZATION OF THE BLENDING PROPORTIONS .....84**

5.1	Introduction.....	86
5.2	Materials and Methods.....	87
5.2.1	Materials .....	87
5.2.2	Methods.....	88
5.3	Results and Discussion .....	90
5.3.1	Standard consistence of cement blended with S-N, P-N and RHA .....	90
5.3.2	Setting times and Soundness of Cement blended with S-N, P-N and RHA .....	91
5.3.3	Flow of the blended cement mortar .....	93
5.3.4	Compressive strength.....	94
5.3.5	Strength Activity Index (SAI).....	98
5.3.6	Effects of Pozzolan on Cumulative SAI of Binary and Ternary Materials.....	100

5.4	Conclusions and Recommendations .....	103
5.4.1	Conclusions.....	103
5.4.2	Recommendations.....	104
Chapter 6 CONCLUSION AND RECOMMENDATIONS.....		105
6.1	CONCLUSION.....	105
6.2	RECOMMENDATIONS.....	107
REFERENCES .....		108
APPENDICES .....		116
	Appendix 1: Chemical composition in percentages (%) of Scoria, Pumice and RHA calcined at different temperatures.....	117
	Appendix 2: Specific Gravity, Gross Density and Specific Surface Area.....	118
	Appendix 3A: Conductivity and Pozzolanic Activity Index of Scoria.....	119
	Appendix 3B: Conductivity and Pozzolanic Activity Index of Pumice.....	120
	Appendix 3C: Conductivity and Pozzolanic Activity Index of RHA.....	121
	Appendix 4: Setting time, water cement ratio and soundness.....	122
	Appendix 5: Water cement ratio, % replacement, and calcining temperature.....	125
	Appendix 6: Compressive Strength.....	126
	Appendix 7: Strength Activity Index (SAI).....	129
	Appendix 8: Shrinkage (25 x 25 x 300 mm prism).....	132

## LIST OF TABLES

Table 2.1: Chemical composition of some pozzolans .....	11
Table 3.1: Chemical Compositions of Scoria, pumice, and RHA from different literatures...35	
Table 3.2: Sample Designation of notation.....	37
Table 3.3: Temperature effects on chemical composition and physical properties of the Scoria, Pumice and RHA. ....	42
Table 3.4: The influence of materials, temperature and chemical composition on initial setting times, final setting times, shrinkage, and soundness. ....	49
Table 3.5: Factors influencing compressive strength (MPa) .....	53
Table 4.1: Chemical and Physical properties of natural scoria (S-N) and pumice (P-N).....	62
Table 4.2: Physical properties of aggregates .....	62
Table 4.3: Mix proportions (kg/m <sup>3</sup> ) of an unblended and blended cement concrete.....	64
Table 4.4: Flow, density and entrapped air test results.....	67
Table 4.5: 14 days accelerated mortar bar test (AMBT) for expansion and 28 days shrinkage tests results. ....	70
Table 4.6: 28 days ultimate and residual compressive strength after 600 °C temperature exposure. ....	81
Table 5.1: Mix proportion of S-N, RHA and Portland cement.....	89
Table 5.2: Mix proportion of P-N, RHA and Portland cement.....	89
Table 5.3: Soundness of S-N/RHA and P-N/RHA blended cement.....	93

## LIST OF FIGURES

Figure 2.1: Conductivity-time relationship (McCarter <i>et al.</i> , [26]) .....	16
Figure 3.1: Disc milling machine, (a) Front view (b) Top View .....	37
Figure 3.2: XRD patterns for (a) Scoria, (b) Pumice, and (c) RHA. ....	45
Figure 3.3: PSD profiles for scoria, pumice, and RHA at different calcination temperatures.	46
Figure 3.4: PAI versus reaction time: (a) Scoria, (b) Pumice, and (c) RHA. ....	47
Figure 3.5: Influence of materials on (a) Initial setting time, and (b) Final setting time.....	49
Figure 3.6: Influence of fineness on setting times: (a) Scoria, (b) Pumice, and (c) Rice husk ash. ....	50
Figure 3.7: Effect of materials (a) Shrinkage, and (b) Soundness. ....	51
Figure 3.8: Effect of fineness on (a) Shrinkage, and (b) Soundness.....	51
Figure 3.9: Compressive strength of blended cement versus percent replacement (a) Scoria, (b) Pumice, and (c) RHA. ....	52
Figure 3.10: Effect of materials on compressive strength of blended cement.....	54
Figure 3.11: Effect of fineness on 28-days compressive strength. ....	54
Figure 4.1: Particle size distribution of scoria and pumice powder.....	61
Figure 4.2: Slump versus (a) cement replacement (b) flow versus % replacement.....	66
Figure 4.3: Modulus of rupture versus percent of cement replaced .....	72
Figure 4.4: Compressive strength growth versus curing period .....	74
Figure 4.5: Compressive strength versus percent cement replacement .....	74
Figure 4.6: 28 days (a) modulus of rupture (b) splitting tensile strength versus 28 days compressive strength for scoria and pumice blended cement concretes.....	76
Figure 4.7: Fluorescence microscope images of Portland cement, scoria and pumice blended .....	77
Figure 4.8: Permeability versus materials and percent cement replacement .....	79



Figure 5.1: Water required for the standard paste of S-N, P-N and RHA blended cement.....	91
Figure 5.2: Setting times of Portland cement blended with (a) S-N/RHA and (b) P-N/RHA.	92
Figure 5.3: Flow of blended cement mortar.....	94
Figure 5.4: Compressive Strength versus percent of cement replaced by S-N/RHA .....	96
Figure 5.5: Compressive Strength versus percent of cement replaced by P-PN/RHA.....	97
Figure 5.6: Strength Activity Index of cement blended with S-N/RHA.....	99
Figure 5.7: Strength Activity Index of cement blended with P-N/RHA.....	100
Figure 5.8: Cumulative SAI of binary materials versus percent of cement replaced .....	101
Figure 5.9: Cumulative SAI of ternary materials versus percent of cement replaced .....	102

## LIST OF ABBREVIATIONS AND SYMBOLS

BS	British Standards
BS-EN	British Standards European Norms
BTU	British thermal unit
C-A-H	Calcium aluminosilicate hydrate
CH	Calcium hydroxide or portlandite
C-S-H	Calcium silicate hydrate
GGBFS	Ground granulated blast furnace slug
OPC	Ordinary Portland cement
PI	Pozzolanic activity index
RHA	Rice husk ash
SAI	Strength activity index
SCM	Supplementary cementitious material
SCMs	Supplementary cementitious materials
SEAMIC	Southern and Eastern African Mineral Centre
SEM	Scanning Electron Microscope
TCA	Total Cement Analyzer
TGA	Thermo-gravimetric analysis
XRD	X-Ray diffraction

## Chapter 1 : GENERAL INTRODUCTION AND BACKGROUND

### 1.1 Introduction

Cement is a material that can bind aggregates in the presence of water through hydration process to form a compact structure. Portland cements for instance OPC are referred to as hydraulic cements because of their ability to set and harden under water [1]. The manufacturing of OPC is material and energy intensive and has high CO<sub>2</sub> emission [2]. All these are challenges to economy and environment that need to be resolved. During hydration of Portland cement only about 75% of the cement powder is converted into calcium silicate hydrate (C-S-H) which binds the aggregates together; the remainder (25%) is converted into portlandite/calcium hydroxide (CH) as byproduct. The CH has adverse reaction such as efflorescence to the concrete and mortar. In addition, concrete made of Portland cement deteriorates when exposed to service environment, either under normal or severe conditions [3]. Because of these problems control of CH to minimize deterioration under service condition is important. In this case composite cements blended with materials that consume CH while enhancing strength and durability of cement bonded materials are used. Composite cement is any hydraulic cement made by blending Portland cement with inorganic materials that take part in the hydration reactions and contribute to the hydration products [1]. Such materials are supplementary cementing materials (SCMs), generally referred to as pozzolans. Among them is silica fume, ground granulated blast furnace slag (GGBFS), fly ash (FA), clay, pumice, scoria, and rice husk ash. They have high amounts of SiO<sub>2</sub> and also Al<sub>2</sub>O<sub>3</sub> and are sufficiently reactive with calcium oxide (CaO) and (CH) in the presence of water to form calcium silicate hydrate (C-S-H) and calcium aluminosilicate hydrate (C-A-H). Ghassan *et al.*, [4], [5] reported that blending of Portland cement with pozzolanic materials improves properties of concrete and lower the

overall cost of structures. Also reduces energy consumption, environmental degradation caused by extraction of OPC raw materials, and CO<sub>2</sub> emission [6].

Scoria and pumice are both volcanic ash that can be used as SCMs to replace parts of cement in concrete and mortar. According to Khandaker [7], scoria is composed of silica (45-50%), alumina and iron oxide (25-33%), calcium oxide (5-8%) and alkali (Na<sub>2</sub>O and K<sub>2</sub>O) 4-6%. Pumice is highly vesicular glass generally composed of 60-70% SiO<sub>2</sub>, 12-14% Al<sub>2</sub>O<sub>3</sub>, 1-2% Fe<sub>2</sub>O<sub>3</sub> [8] and up to 12% alkali oxides [9]. Both scoria and pumice have huge potential as pozzolans that can replace parts of cement in concrete and mortar. In addition, rice husk ash (RHA) produced by burning of rice husk in an incinerator, kiln or furnace is also potential pozzolanic material. According to Della *et al.*, [10][11], RHA calcined at 700 °C has 94.95% of reactive silica. The use of RHA as SCMs is practiced in India, Thailand, Indonesia, Malaysia, and Sri Lanka [12]. In addition, combined effect of multiple pozzolans (pumice, scoria, and RHA) on the setting time and early strength of blended cement has not been reported. Since pozzolanic activity depend on the percentage of the reactive silica and alkali salts, it is vital to investigate the potential of scoria, pumice, and RHA as SCMs. Neville *et al.*, [1] reported extended setting time and lower early strength of OPC blended with GGBFS and FA. This results from slow rate of reaction with OPC probably due to low alkali content in these materials [13]. In addition, proportion of cement, fineness, temperature, and chemical composition affect the rate of reaction [13]. This is a challenge to concrete industry that needs to be solved to enhance efficiency of concrete and construction speed. This pose a need to explore the influence of RHA, scoria and pumice as supplementary cementing materials to the blended composite cement. Also the possibility of using advantages of high alkali content in scoria and pumice to decrease the setting time and promote early strength of pozzolan blended cement.

## **1.2 Statement of the Problem**

During hydration of Portland cement only about 75% of the cement powder is utilized to produce C-S-H which binds the aggregates together and the remaining 25% is converted into portlandite (CH) as byproduct that leads to adverse reactions to the concrete and mortar. Pozzolans have been used as SCMs to consume the CH and contribute to the strength of composite cement. Though, GGBFS and FA blended cement have extended setting time and lower early strength due to their low rate of reaction stemming from low reactive silica, low alkali content and low fineness among others. The use of finely grinded scoria and pumice which has high silica and alkali content could alleviate these problems. It is expected that, high silica and alkali in scoria and pumice and high fineness will supercharge the rate of reaction between pozzolan and CH from hydrating cement to produce C-S-H and C-A-H. Such materials are readily available in Tanzania but they are not utilized. Furthermore, they have been reported to have properties that can improve setting time, strength, and durability yet they have not been comprehensively studied. Therefore investigation of scoria, pumice, and RHA as potential SCMs is of great interest in the manufacturing of high quality blended composite cement. Our central hypothesis in the proposed work is that the alkali salts in scoria and pumice will substantially reduce setting time and improve early strength without compromising other properties of OPC.

## **1.3 Research Objectives**

### **1.3.1 Main Objective**

To explore the potential of scoria, pumice, and RHA as supplement cementitious materials in reducing setting time and improving early strength of pozzolan blended composite cement.

### **1.3.2 Specific objectives**

1. To characterize scoria, pumice, and RHA at natural state and at different calcining temperatures.
2. To determine the influence of alkali salts in scoria and pumice on setting time, early strength developments, and expansion of pozzolan blended composite cement.
3. To investigate the influence of blended scoria and pumice with RHA to the setting time and early strength development of pozzolan blended composite cement.
4. To optimize calcining conditions for scoria, pumice, and RHA (such as temperature, air supply, rate of burning, soaking period, and rate of cooling) and the composition of the blended cement (blending ratios of scoria, pumice, or RHA and OPC clinker).

### **1.3.3 Research Questions**

- 1) What are the chemical compositions of scoria, pumice, and RHA at natural state and how are they influenced by calcining temperature?
- 2) What are the influence of alkali salts in scoria and pumice in setting time, early strength developments, and expansion of pozzolan blended composite cement?
- 3) How scoria or pumice blended with RHA affect setting time and early strength development of pozzolan blended composite cement?
- 4) How calcining conditions of scoria, pumice, and RHA (such as temperature, air supply, rate of burning, curing, and rate of cooling) and the composite cement (blending ratios of scoria, pumice, clay or RHA and OPC clinker) can be optimized?

## **1.4 Scope of the Research**

The focus of this research is Tanzania mainland mainly in the Regions of Mbeya, Kilimanjaro, Arusha and Dares Salaam. Materials for this research shall include Scoria from Uchira-Moshi, Pumice, and Rice Husk Ash from Mbeya. Test experiments has been done at Twiga Cement

Company Quality Assurance Laboratory, Nyati cement Laboratory, Mbeya University of Science and Technology Chemistry and Materials Laboratories and the University of Dar es Salaam Building Materials Laboratory.

### **1.5 Rationale of the Research**

The rationale of this study is to improve strength and durability of building structures by blending conversional cement with natural occurring pozzolan. This will lead to a stronger and stable structure which are resistant to aggressive environment. Also, the need to reduce the setting time and achieving early strength development of pozzolan blended cement. Furthermore, the mitigation for environmental degradation and the scarcity of cement since more cement will be produced.

### **1.6 Expected Outcome/Significance**

At the end of this research it is expected that, chemical composition of scoria, pumice, and RHA at different calcining conditions (such as temperature, curing, air supply, rate of burning, and rate of cooling) will be established and at natural states. Also the percentage replacement of parts of OPC will be established for each of Tanzanian pozzolanic materials involved (scoria, pumice, and RHA). In addition, reduced setting time of pozzolan blended cement and enhanced early strength development will be achieved. Moreover, the use of pozzolan blended cement will increase accessibility of cement and raw materials for ordinary Portland cement manufacturing.

## **Chapter 2 : THE EFFECT OF DIVERSE POZZOLAN TO THE PROPERTIES OF MORTAR AND CONCRETE**

### **2.1 Introduction**

#### **2.1.1 Cement**

Cement is a building material used to bind solid particles such as sand and gravel in the presence of water through hydration process to form a compact structure. In the concrete industry, Portland cements are commonly known as hydraulic cements because of their ability to set and harden in the presence of water [1]. According to Taylor [14], Portland cement (PC) comprises of four main phases which are alite (50-70% tricalcium silicate -  $\text{Ca}_3\text{SiO}_5$ ), belite (15-30% di-calcium silicate -  $\text{Ca}_2\text{SiO}_4$ ), aluminate (5-10% tri-calcium aluminate -  $\text{Ca}_3\text{Al}_2\text{O}_6$ ) and ferrite (5-15% tetra-calcium aluminoferrite  $\text{Ca}_2\text{AlFeO}_5$ ). They are frequently manufactured from calcareous raw materials comprising of silicates, aluminates and iron oxides [1][14][15]. The manufacturing of PC is material and energy intensive and has high  $\text{CO}_2$  emission. Mehta [2] reported that, approximately 1.5 tons of raw materials is required in the production of every ton of PC, at the same time release about one ton of  $\text{CO}_2$  into the atmosphere. The hydration reactions of cement converts about 75% of the cement paste into calcium silicate hydrate (C-S-H) which binds the aggregates together. The remaining 25% converts into calcium hydroxide (CH) as byproduct. The CH raises the PH and passivation to the embedded steel reinforcement but do not subsidizes to the strength or durability of the concrete. In the presence of reactive aggregates, the CH provoke the alkali silica reaction which considerably affect the integrity of the concrete [3]. The portlandite (CH) reacts with the pozzolan in the presence of water. Either the equilibrium shift allows more solid CH to liquefy until the pozzolan or portlandite is exhausted.



Blended (composite) cement refers to any hydraulic cement made by blending PC and one or more inorganic materials that take part in the hydration reactions and contribute to the strength development [1]. The inorganic materials are collectively termed as supplementary cementing materials (SCMs). They are pozzolanic materials, which possesses either pozzolanic properties or both pozzolanic and latent hydraulic properties. Composite cements are used for various reasons such as improving properties of concrete and mortar, utilizing waste materials, decreasing energy consumption [6], reduce environmental destruction caused by extraction of PC raw materials and CO<sub>2</sub> emission [16]. Latent hydraulic cements/pozzolan has compositions broadly intermediate between those of pozzolanic materials and PC. They act as hydraulic cements when mixed with water and a minimal amount of some other substance that serves as a catalyst or activator. Research shows that, blending of PC with pozzolanic materials improve rheology, strength, permeability and durability of mortar and concrete and lower the total cost of cement and concrete structures [17][5]. Addition of such materials in clinker has added advantages in terms of energy saving, promoting ecological balance, and conservation of natural resources. In addition, all pozzolanic cements reported by Neville and Brooks, [1] are produced either by blending PC clinker with ground GGBFS or by FA. Moreover, research found that, calcined clays have the greatest overall potential as artificial pozzolanic materials owing to the abundant availability of clays, (particularly kaolinite) in large quantities in almost all regions of the world [18].

### **2.1.2 Supplementary Cementitious Materials**

The attempt to identify suitable and affordable alternative material to supplement Portland cement for structural and non-structural building and civil works is crucial. Through series of study, researchers carefully investigated various materials to explore their potentials to substitute cement in mortar and concrete. Pozzolan appears the best supplementary cementing materials [19]. The amount of cement replaced is subject to the amount of reactive silica and

alumina in the pozzolan. Pozzolans are used to replace Portland cement owing to its ability to react with the CH released in the hydration reactions [19]. SCMs are used in cement factories to replace part of Portland cement clinker to achieve reduced cost and enhanced performance of the cement [20]. Besides, they are used as mineral admixture to enrich concrete characteristics such as: increased durability, mechanical strength, chemical resistance (sulfate resistance), workability and reduce the expansion, and heat of hydration [5][21]. It is also used to reduce environmental degradation caused by extraction of PC raw materials, CO<sub>2</sub> emission, and promote economic benefits [16][22]. In some area around the world, the use of pozzolan is must for achieving low permeability and controlling thermal cracks [23].

## **2.2 Pozzolanic materials**

Pozzolan refers to natural volcanic materials and calcined earths composed of aluminosilicate minerals that react with CH at ambient temperature [24]. The pozzolan owns little or no binding properties but in finely ground and in the presence of water react chemically with lime to form cementing compounds [1][16][25]. A true pozzolan have no hydraulic properties of its own but latent hydraulic pozzolan such as GGBFS react very slowly with water [26].

The history of pozzolan dated back to 5000 BC whereby lime was mixed with diatomaceous earth from Persian Gulf to produce a hydraulic binder [27][28]. Next notable applications of natural pozzolans went back to 1600 BC on Thera Island (Santorin) followed by Napels Italy in 79 AD [3][27][28]. The first known pozzolan was a volcanic ash from Pozzuoli from where the material derived its name. In the ancient age, pozzolans were produced from not only volcanic soils but also from crushed pottery, brick and tiles. From early twenty-century pozzolans are produced from diverse materials including calcined clay, fly ash, silica fume, GGBFS, volcanic ashes, volcanic tuff, and diatomaceous earth. They are classified as natural and artificial. Neville and Brooks, [1] and Sabir et al. [16] defined natural pozzolanic materials as volcanic ash (the original pozzolan) and metakaolin. According to

Ramezaniapour [28], natural pozzolans are materials, which need no more treatment apart from grinding to react with CH, here the clay is excluded. They occur naturally on the earth's crust and frequently used as additives to PC to increase the long-term strength and other properties. Artificial pozzolans are materials with low pozzolanic activity that need additional treatment to bring about pozzolanic reactions. These are inorganic for example clay, silica fume, GGBFS, and fly ash. Organic pozzolans are agricultural byproducts for instance RHA, sugarcane bagasse ash (SCBA), coffee hull ash, and coconut shells ash [12][29]. The active component of the pozzolan are amorphous or semi-amorphous siliceous or aluminous which are very unstable and chemically active [17]. Most frequently used pozzolans are fly ash, silica fume, GGBFS and RHA

### 2.2.1 Silica fume

According to ACI [30], silica fume is a non-crystalline byproduct of the manufacture of silicon or silicon alloy. It was at first collected in Kristiansand Norway in 1747. Silica fume has the chemical composition shown in **Table 2.1** [31] and the particles have average diameter 0.1 to 0.2  $\mu\text{m}$ . Silica fume significantly improve many properties of cement and concrete because of its high fineness (20,000  $\text{m}^2/\text{kg}$ ) and pozzolanic activity [32]. Fine particles expose larger areas for the reaction with CH and good parking [32]. The parking effect fill up spaces between cement particles the same way as cement fill the spaces between the aggregates. This refine pores size and pores size distribution within the cement paste-aggregate interface resulting into reduced bleeding, reduced permeability, and increased durability [32]. The parking effects densify the concrete and increase its compressive strength. The high fineness and high amorphous silica content make the silica fume (SF) effective pozzolanic materials [33].

### 2.2.2 Fly ash

Fly ash (FA) results from the combustion of pulverized coal in electrical power plant [34]. These materials are widely used to substitute cement in concrete to modify various properties. FA are of siliceous (class F fly ash) or calcareous (class C fly ash) in nature [24]. The replacement level is limited to 15 - 25% for class F fly ash and 15 - 40% for class C fly ash [34]. For a high volume fly ash concrete, the dosage is usually 50 - 60% [35]. According ASTM C 595 [24], Fly ash class F is of mostly spherical particle fine powder having strong pozzolanic properties. It is composed of reactive silica and alumina. In contrast, fly ash class C have fairly coarser particle composed of oxides of iron and calcium. Generally, fly ash class F has pozzolanic properties whereas fly ash class C has both pozzolanic and latent hydraulicity properties. Reactivity of fly ash depend on fineness, silica content, calcium oxide content, CO<sub>2</sub>, and crystallinity percentages [34][36]. **Table 2.1** shows the chemical composition of fly ash as addressed by Xiuping and Boyd [34], Ghassan et al. [5] and Paya *et al.*, [37].

### 2.2.3 Ground Granulated Blast Furnace Slag

The (GGBFS) is a byproduct of the manufacture of iron, which processes both hydraulic and pozzolanic properties. The slag composed of mostly silica and alumina combined with oxides of iron and limestone [38]. According to Fathollah and Hashim [22] the GGBFS reduces mobility of ions and water in the pore system thereby resulting into: reduced diffusion of chloride ions and therefore improved corrosion resistance of steel reinforcements, lower permeability, and improved resistance against sulphate corrosion of cement-blended materials. In fact, properties and influence of GGBFS depend mainly on chemical composition (**Table 2.1**) and fineness [39]. The GGBFS influence the size and alignment of CH crystals. Beside, modifies the rate of heat evolution significantly. GGBFS blended cement is suitable in the construction of a massive structures like dams and offshore structures due to its low heat of

hydration. The GGBFS blended cement has extremely satisfactory performance under acidic environment exposure [32].

**Table 2.1:** Chemical composition of some pozzolans

Oxide	MK	SF	FA	GGBFS	Scoria	Pumice	RHA
	[%]	[%]	[%]	[%]	[%]	[%]	[%]
<b>Si<sub>2</sub>O<sub>3</sub></b>	54.1	93.55	27.88 – 59.68	31.2	45 – 50	60.82	94.95
<b>Al<sub>2</sub>O<sub>3</sub></b>	16.7	20.65	5.23 – 33.99	12.96	13 – 15	16.71	0.39
<b>Fe<sub>2</sub>O<sub>3</sub></b>	10.1	12.31	1.21 – 29.63	0.87	7 – 8	7.04	0.26
<b>CaO</b>	1.0	10.43	0.37 – 27.68	41.43	5 – 8	4.44	0.54
<b>MgO</b>	2.9	2.13	0.422 – 8.79	4.27	4 – 6	1.94	0.90
<b>K<sub>2</sub>O</b>	1.8	1.50	0.64 – 6.68	0.31	4 – 6	2.25	0.94
<b>Na<sub>2</sub>O</b>	0.5	1.33	0.20 – 6.90	0.11		5.42	0.25
<b>SO<sub>3</sub></b>	0.4	2.53	0.04 – 4.71	0.04	0.01-0.02	0.14	-
<b>TiO<sub>2</sub></b>	2.0	0.52	0.24 – 1.73	0.49	-	-	0.02
<b>LoI</b>	9.88	3.00	0.21 – 28.37	6.00	1.25 – 1.5	1.52	0.85
<b>SG</b>	2.5						

#### 2.2.4 Metakaolin

Metakaolin is a chemical phase formed upon calcining clay (kaolinite) between 600 to 900 °C [40]. Amorphous phase produced is rich in silica (**Table 2.1**) and it is very reactive, such that, they are used as pozzolanic materials to supplement cement in mortar and concrete [16][27][12][41][23]. Metakaolin has a very high pozzolanic activity such that it produces early strength and long-term strength when used to supplement cement. Although it has high heat of hydration [16]. Low proportion of metakaolin is used to control hydration rate and heat

evolution in concrete so as to control shrinkage and cracking [23]. Metakaolin is composed of very fine clay and silt, which are accountable for high shrinkage even though they promote good parking effects [29]. Metakaolin cement has a reduced permeability to fluids and chloride ions and it is best in oil well concrete to enhance flexural and compressive strength.

In the study of Al-rawas and Hago [42] on the potential of metakaolin, five clays from Al-Khod, Soor Al-Haboos, Al-Fulaij, Al-Hamra, and Al-Awabi) in Northern Oman was calcined between 740 to 800 °C for one hour. The reactive phase produced from the calcination of Al-Fulaij clay yield higher compressive strength than the other clays. Moreover, investigation of the activity of clays from four locations in Tunisia, reported that, at calcining temperature of 700 °C kaolinite rich clays has the best pozzolanic activity [43][44]. Abdul et al., [18] in their investigation revealed optimum calcining temperature of clay as 700 °C, beyond that pozzolanic activity decreases significantly due to formation of crystalline phase. This is highly influenced by the percentage of the reactive silica and aluminosilicate. According to ACI 234 R [45], the lower the amount of siliceous and aluminous material the lesser the reactivity of metakaolin which may also diminish as the particles become coarser.

### **2.2.5 Rice Husk Ash**

Rice husks of sufficient purity have many applications in different fields of science. Such applications are the production of high-grade silicon, zeolite, aerogel, pozzolans, fertilizer and bio-fuel [46][47][10][48]. Of course, applications that have direct interest to this work are the use of RHA as pozzolan or alternative cementing materials. RHA is used as SCM in India, Thailand, Indonesia, Malaysia and Sri Lanka and other places around the world [12]. RHA is produced by burning rice husk in a kiln under controlled supply of oxygen to achieve the most reactive silica phase. The amount of reactive silica increases with increasing calcining temperature. Nevertheless, this is not customary a rule since there are other factors such as mineral composition [43], purity and fineness [48][49]. Nair [50] reported that, burning of rice

husk at 500 - 700 °C for more than 12 hours produced RHA with high reactivity. The author also claimed short burning durations between 15 to 360 minutes produces RHA with high amount of carbon even if calcined at high temperature range between 500 - 700 °C. Besides, according to Della et al. [10], RHA calcined at 700 °C has 94.95 percentage of silica, **Table 2.1**. In addition, Abdullahi *et al.*, [48], Wansom et al. [51] and Givi *et al.*, [52], reported that burning of RHA at different temperatures and different conditions of oxygen supply give variations in silica contents.

The percent replacement of PC to achieve the desired characteristics of concrete and mortar depends on the quality of RHA, chemical compositions, calcining conditions and fineness. Different authors suggested different replacement percent depending on the factors associated with production of the RHA and the available CH. Nevertheless, Rajput, *et al.*, [53] and Karim *et al.*, [54] cited replacement of cement with RHA up to 40% is possible without significant loss of strength of mortar or concrete.

#### **2.2.6 Scoria**

Scoria is a pyroclastic rock consisting of fragmented volcanic materials, which have been blown onto the atmosphere by explosive volcanic activity [55]. It is volcanic lava with viscous consistency. It is a pumice of basaltic composition comprising of extremely small amounts of feldspar and pyroxene crystals [56]. Different researchers addressed different chemical compositions of scoria, basing on concentration rather than types of oxide or element. Chemical analysis according to Khandaker [7] indicated that, scoria is comprised of basically silica, alumina, iron oxide, calcium oxide, and alkali ( $\text{Na}_2\text{O}$  &  $\text{K}_2\text{O}$ ), in proportions shown in **Table 2.1**. Worldwide, scoria is applied as lightweight aggregates in making of lightweight concrete [55]. With regard to the chemical compositions, scoria qualifies as pozzolanic material and potential SCM [57]. Furthermore, huge amount of scoria is accessible and readily processed, that could reduce the cost of cement among other benefits.

### 2.2.7 Pumice

Pumice is an extrusive volcanic rock material, produced when lava, which is full of water and gases (volatiles), is ejected or thrown on the earth surface by volcanic action [58]. Pumice is a volcanic rock light-colored that indicate high silica ( $\text{SiO}_2$ ) content and low iron and magnesium content. It is vesicular glass generally composed of 60-70%  $\text{SiO}_2$ , 12-14%  $\text{Al}_2\text{O}_3$ , 1-2%  $\text{Fe}_2\text{O}_3$  and alkali oxides, **Table 2.1** [57][9][59]. This composition is not customary equal for pumice and pumicite from different sources because they depend on the mineralogical characteristics and petrography of the volcanic lava, temperature and rate of cooling. For a pumice to qualify as pozzolans, ASTM C 618 [57] requires the sum of basic oxides ( $\text{SiO}_2$ ,  $\text{Al}_2\text{O}_3$  and  $\text{Fe}_2\text{O}_3$ ) be not less than 70%. Accessibility and easy with which it can be processed for application makes pumice an ideal SCM.

## 2.3 Pozzolanic reactions

Pozzolanic reaction of natural pozzolan is slower relative to all other reactions, taking place during hydration of cement, and thus lowers the early strength of concrete made with pozzolan-blended cement compared to concrete made with PC. According to ACI 232.1R [27], pozzolanic reactions depend upon the dissolution of pozzolans at early stages. High specific surface area exposes more areas for the reactions. Portland Pozzolana cements (PPC) are more sensitive to temperature compared to the hydration reaction of Portland cement because pozzolanic reactions have higher activation energies.

### 2.3.1 Pozzolanic activity index

Once pozzolanic materials are mixed with PC, the silica combine with the free lime released during the hydration of cement to form C-S-H [60]. This reaction is termed as pozzolanic reaction and continue slowly as lime is released form hydration of PC [61]. The rate and extent by which these reactions occur is defined as pozzolanic activity index. The reactions occur as



shown in **Equation 2-1** and **2-2**. Pozzolanic reaction is a complex base-acid reaction expressed in its simple form in **Equation 2-2**.

Hydration of Portland cement



The CH produced combines with silica of the pozzolan



Pozzolanic activity and strength activity indices (PAI and SAI) are used to evaluate the quality of SCM by monitoring the reaction of the amorphous part of pozzolan and calcium hydroxide. Various methods categorized as direct and indirect has been developed for the qualitative and quantitative evaluation of PAI and SAI. Direct methods measure the amount of CH consumed in the lime-pozzolan water system and indirect method measure the relative compressive strength [7]. The direct methods involve chemical titration, electrical conductivity measurement, X-ray diffraction (XRD), and thermo-gravimetric analysis (TGA) [62]. Luxan *et al.*, McCarter and Tran methods are the direct methods based on conductivity. [26][51][63]. Luxan's method is accurate for early age determination of PAI but McCarter and Tran method is more accurate for the later ages.

Luxan *et al.*, [63] studied the PAI using 16.00 g of natural rock pozzolan in 300 mL of saturated calcium hydroxide solution and measure conductivity over 2 min, 20 min and 4 h periods at  $40 \pm 1$  °C and at constant stirring, 2min was found sufficient for stabilization. The same study was done by observing the variation in conductivity during the first 2 min of a reaction between 5 g of pozzolan and 200 mL of saturated  $\text{Ca}(\text{OH})_2$  solution at  $40 \pm 1$  °C and 2 min were also found sufficient for the stabilization of the reaction. McCarter and Tran [26] measured conductivity of various pozzolans mixed with  $\text{Ca}(\text{OH})_2$  powder and water for 48 h.

Stiffening of the paste was observed between 24 to 48 h, Figure 2.1. The rate of change of conductivity corresponded to the rate of consumption of lime in the pozzolanic reactions.

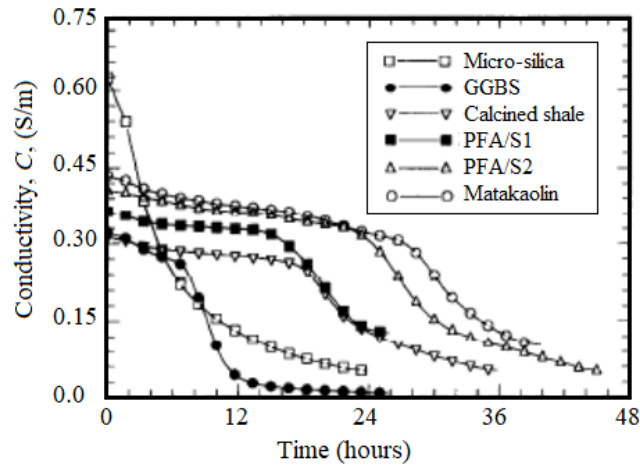


**Figure 2.1:** Conductivity-time relationship (McCarter *et al.*, [26])

Donatello *et al.* [64] study on PAI using Frantini method revealed improved PAI as fineness increases due to more exposed surface for the reaction. Furthermore, observation on the solubility curve revealed that 8 days at 40 °C was sufficient time for cement to create saturated solution of CH. In the same study, the author compared the test methods of assessing PAI, such as SAI, Frantini, and saturated lime tests. There was significant relationship between the SAI test results and the Frantini test results ( $R^2 = 0.86$ ). Contrary, no relationship between saturated lime test results and the SAI or Frantini test results. The specified time for SAI was 7 days and 28 days at 23 °C but Frantini was 8 days at 40 °C. The author cited that, necessary factor in such comparison is the CH-pozzolan mass ratio. The observation showed for SAI that, 2000mg of pozzolan is required in 8000mg of cement containing only 25% of CH, making a mass ratio of 1:1. Also observed that a 75 ml of saturated lime solution containing 0.15 g CH required 1 g of pozzolan resulting to a lower CH-pozzolan ratio of 0.15:1 hence showing a positive PAI compared to the other tests.

Wansom et al. [51] studied and compare various electrical methods of measuring PAI of RHA for 10 and 60 minutes in a saturated Ca(OH)<sub>2</sub>-pozzolan-water system. The study revealed that, conductivity of lime-pozzolan-water system reduced with time as the reaction proceeds. The author observed further decrease of conductivity beyond 60 minutes. The authors measured the PAI and SAI and find the conductivity change at 2 minutes had correlation coefficients of 0.91, 0.77, and 0.49 with the SAI at 3, 7, 28 days. The conductivity change at 5 minutes and 60 minutes show approximately the same correlation coefficients signifying that no improvement of the method by taking measurement in longer time. This attributes amorphous silica of the RHA, which react very fast with the CH that, in 3 days' time there could be no more CH left for further pozzolanic reaction. Therefore, beyond 3 days no more strength improvement resulted from pozzolanic reactions.

Paya *et al.*, [37] modified the Luxan's method by using 800 mg of Ca(OH)<sub>2</sub> powder in 1000 mL of deionized water instead of saturated solution of Ca(OH)<sub>2</sub>. In their study, FA, RHA, silica fume, and natural pozzolan were tested. The results exposed FA contained soluble salts almost 10 times greater compared to natural pozzolan and silica fume, and 3 times more than rice husk ash. The results insisted the need to consider the influence of soluble ions attached to the surfaces of pozzolan particles such as sulphate compounds of Na, K, and Ca. The author found astonished high pH for fly ash comparative to other pozzolans attributed to the leaching of the metallic alkalis of Na, K, and Ca from vitreous aluminosilicates of fly ash particles. Taking into consideration this factor and temperature effect, Paya *et al.*, used **Equation 2-5** to evaluate pozzolanic activity index.

$$\% \text{ LC} = \frac{[C_0 - (C_t - C_{p,t})]}{C_0} \times 100 \quad \text{Equation 2-6}$$

Where: % LC = Relative loss in conductivity

$C_0$  = Conductivity of limewater system

$C_t$  = Conductivity of lime-pozzolan-water system at time (t)

$C_{p,t}$  = Conductivity of pozzolan-water system at time (t)

$(C_t - C_{p,t})$  = Absolute conductivity of lime-pozzolan-water system at time (t)

## 2.4 Properties of Pozzolan Blended Cement

### 2.4.1 Setting Times

Setting times and soundness are both consistency tests used to evaluate cement quality. The tests are conducted on standard consistence paste. Setting time describe the stiffening from fluid to rigid state of cement paste resulting from initial hydration of  $C_3S$  and  $C_2S$  [1]. According to SS-EN 196-3 [65], setting times are categorized as initial and final setting time. Initial setting time describe the time laps from zero time to the time when the Vicat needle penetrate to a depth of  $6\pm 3$ mm from the base plate in 30 seconds. It estimates the time when cement has stiffened and lost its workability. Final setting time express the time laps measured from zero time when water is added to the cement to that at which the needle first penetrates only 0.5 mm into the specimen. A ring attachment fails to mark the specimen and is reported to the nearest 15 minutes at the time. Initial setting time should not be less than 30 minutes, however SS-EN 197-1 [66] specified  $\geq 45, 60,$  and  $75$  minutes for strength classes 32.5, 42.5, and 52.5 respectively. A final setting time shall not exceed 10 hours. Certainly, no standard limit for final setting time, but Neville and Brooks, [1] cited as equals  $90 + 1.2 \times$  initial setting time. Comprehensive literatures regarding the influence of SCM on setting time of pozzolan-blended cement is scarce; however, the available few, talk on specific SCM at a time. It was found that, cement blended with very fine RHA exhibit superior setting time [52]. In the same study, initial setting time of RHA increased with increasing replacement level in the blended

cement over PC. Furthermore, in the study of El-Dakroury *et al.*, [67], initial and final setting times of rice husk ash blended cement increased with increasing percent of RHA in the mixture. The authors established that could be attributed to the slower rate of heat-induced evaporation of water from the RHA-PC mixture. Also, Mary et al [68] reported increased setting time of the fly ash and GGBFS blended cements. They also reported on the impact of curing temperature and composition to the setting time of blended cement. No threshold set above which, the slag will not delay the setting times. It was also cited that, increased setting times with added amount of natural pozzolan is the effect of increased water-cement ratio and increased SCM replacement level [6][69].

#### 2.4.2 Soundness

Soundness is a consistence test used to assess conformity of cement with its specification. It is the measure of volume stability or volume consistence of cement [70]. It is the ability of cement paste to retain its volume after setting and hardening. Unsound cement is associated with volume changes caused by expansion after setting due to delayed hydration or other reactions [71]. It is the attribute of the reaction of free lime, calcium sulphate and magnesia. Free lime hydrates slowly occupying a larger volume than the original calcium oxide. There is difficult to determine and distinguish free lime between the reacted and unreacted calcium oxide and calcium hydroxide produced by the hydration reactions when cement is exposed to the atmosphere [1]. The reactions of calcium sulphate cause expansion through the formation of calcium sulfoaluminate (ettringite/Mikaelian salt) which occupy larger volume than the CaO and Ca(OH). On the other hand, magnesia reacts with water the same way as calcium oxide forming deleterious crystals. Soundness is measured using Le Chartelier apparatus according to Neville and Brooks and SS-EN 196-3 procedures and **Equation 2-7** [1][65].

$$\delta L = L_2 - L_1 < 10 \text{ mm}$$

Equation 2-8

$\delta L$  = soundness/expansion (mm)

$L_2$  = final distance between the tips (mm)

$L_1$  = initial distance between the tips (mm)

### 2.4.3 Effect of Alkali

Alkalis contained in cement and SCM have serious impact on the properties and performance of cement, mortar and concrete. There are various kinds of alkalis but that of Sodium ( $\text{Na}_2\text{O}$ ) and Potassium ( $\text{K}_2\text{O}$ ) is of interest. These alkalis ( $\text{Na}_2\text{O}$  and  $\text{K}_2\text{O}$ ) are expressed as sodium equivalent,  $\text{Na}_2\text{O}_{\text{eq}}$  ( $= \text{Na}_2\text{O} + 0.658\text{K}_2\text{O}$ ) is the most common alkali involved in alkali silica reaction. PC has approximately 0.3 to 1.2%, but in the pozzolan blended PC these values vary depending on the type of pozzolanic materials and the alkali content [72]. Alkali affect rate of setting and strength gain of cement, mortar, and concrete. Alkalis in cement react with silica in the aggregates and cause undesirable effects to the cement paste, mortar, and concrete. These effects include early hydration and setting, strength growth and ultimate strength, drying shrinkage, cracking, and microstructure pattern of the hydrated cements, permeability and durability. As alkali content increases, it lowers the ultimate compressive strength of cement and concrete, but intermediate improves the modulus of rupture.

When alkali-containing cement is mixed with water, the alkali metal ions readily go into the liquid phase of the hydrating system and influence the rate of cement hydration and the morphology of the hydration products [72]. These affect the properties of concrete for instance mechanical strength and durability. The C-S-H becomes coarser and heterogeneous in alkali solutions and the lower strength development at later age is due to this heterogeneous structure. Under high alkali contents the hydration products becomes gelatinous rather than crystalline and the microstructure of the cement paste become less dense contrast to a low alkali paste.

## **2.5 Properties of mortar and concrete**

### **2.5.1 Workability**

Workability is essential property of mortar and concrete. It embraces the rheological properties such as bleeding, segregation, flow, cohesion, and compactability. Workable mortar or concrete allows easy application or placing, compaction, and finishing with less bleeding or segregation. It is also the determinant of pumpability and constructability of the mixture. Workability is influenced by particle size and particle size distribution (PSD) of the binder, aggregates size and shape, aggregate grading, water demand, binder content, admixture, temperature of concrete and the surrounding, and SCM content [52]. Beside, workability of fresh mortar and concrete also depend on mix proportioning. Smooth grading curve increases workability and final compressive strength. It is common in construction industry to opt for admixture to bring about desired workability. Yet beyond admixtures, many other factors affect concrete workability. However changing one or more of these factors changes both workability and other characteristics of concrete, like strength and durability. In addition, optimum particle size and particle size distribution of the binder and the aggregates account for undesirable water required to achieve projected workability.

Out of more than 61 workability test methods, none of them is perfect over the range of factors involved in workability. One or more of the available test methods determine workability of mortar and concrete for a range of specific factors. In fact, the applicability of each method has led the user to opt for the simplest and that which are easily applicable in both laboratory and sites. Therefore, the slump test, compaction factor and flow test methods are the most preferred among others. In this research, slump and mortar flow tests are considered.

## **2.6 Properties of blended cement**

### **2.6.1 Density, Porosity and water absorption**

Density of blended cement increases relative to specific gravity of SCM's and replacement level. The density does not depend only on specific gravity of SCM but also the particle size, particle size distribution and admixture like high range water reducer (HRWR) [73]. The HRWR increases the dispersion of solids in the binder system whereby increasing the packing density and reduce porosity of the blended cement. Optimum proportion of PC and SCM's has more significant effect on packing density compared to HRWR [73]. Optimum proportioning of PC and SCM purge the effect of inclusion of more particles of the same size, which could otherwise spoil the packing density of cement and concrete. Porous microstructure increases absorption and permeability of the concrete but reduced strength and durability. Permeability controls the access of harmful substances (for instance moisture, ions and gaseous) into the concrete. However, sufficient optimization of the binder ingredients (PC and SCM), low water binder ratio, and HRWR increases packing density, reduce porosity and its impact to cement, cement mortar matrix and concrete. Optimum PC/SCM ratio in binary or ternary mix increases gel space ratio that results into reduced porosity and improved mechanical strength and durability [35].

The interfacial transition zone linking the aggregate and cement paste is composed of high water-binder ratio and more spaces that allow formation of porous hydration products having larger crystal of CH and ettringite [35]. These zones are the weaker area compared to the bulk of cement paste which have lower water-binder ratio and are prone to micro-cracks that results from stress. The micro-cracks in the cement paste-aggregate interface determine the mechanical strength, permeability, and durability properties of hardened concrete when exposed into external stress or aggressive environment. Fluid flow rate in concrete depend on percolation through networks of interconnected cracks than capillary or diffusion.



Addition of porous SCM to PC and concrete may result into a porous and absorptive microstructure, but fine ground SCM and optimum blending reduce porosity. Proper preparation of SCM yield high amount of the reactive silica (for instance RHA) necessary for pozzolanic reaction. This increases hydration products and packing density, and reduced both porosity and absorption [14]. Less porous cement or concrete has less carbonation, low diffusion of chloride and sulfate ions, resistance to ASR, resistance to freeze and thaw, low leaching of CH to the concrete surface, and increased strength and durability [14][62].

### **2.6.2 Mechanical Strength**

Hardened cement paste, mortar, or concrete are micro-porous materials. Compressive strength, flexural strength and durability of cement mortar and concrete relates to porosity, micro-cracks in the cement paste-aggregates interface, and the thickness of the interface. According to Mehta [35], the size of interface increase with water-cement ratio become porous and weak, and lowers mechanical strength, and durability of cement concrete. The micro-cracks propagate as hardening continue due to shrinkage. The different coefficients of thermal expansion of the paste and the aggregates set the concrete into a state of stress even under no external stress [60]. Furthermore, the author explained the formation of large CH crystals and ettringite in this zone. These zones become weaker with many micro-cracks and are less resistant to stresses. The flexural strength and splitting tensile strength decreased as the interfacial transition zone becomes weaker. Usually cement paste in the transition zone deforms under small loads. The weakest points are undetected in uniaxial compression but decisive in tensile failure [74].

Incorporation of very fine SCM, which reacts with the CH from hydrating cement, reduces its concentration in the interfacial zone, refines the pores and pore size distribution, and increases the packing density. SCM increase long-term strength because the pozzolanic reaction start later and continue for long time. Generally, mechanical strength increases as the

gel-space ratio increases in the interfacial zone. For example, Givi *et al.*, [52] reported increased of 28 and 90 days compressive strength of concrete when cement was replaced by 10% RHA and then it decreases, although specimen with 15% RHA have strength higher than that of control. Replacement up to 20% by RHA decreased compressive strength to a value below control concrete. This was attributed to the higher amount of RHA in the mix than the amount required for the reaction with the available CH. The un-reacted fine portion of the SCM fills the available pores but the excess silica in the microstructure contributes no strength. In fact Givi *et al.*, [52] reported lower 7 days compressive strength for all mixes replaced by RHA contrast to the control mix which increases towards 90 days. This occurred due to low fineness of RHA, if the particles were 90% less than 45  $\mu\text{m}$  the 7 days compressive strength could be quiet higher above that of control concrete as pozzolanic activity of very fine RHA occurs at early age [51].

GGBFS is a byproduct of iron manufacturing produced by rapid cooling of molten slag in water. The slag is a latent hydraulic cement as it shows both hydraulic and pozzolanic properties [22][75][76]. The slag rich in silica and alumina must be, finely ground to increase the specific surface area needed for the reaction with lime. Replacement of cement by GGBFS has the advantage of reduced heat of hydration, high resistance to sulphate and acid attack, improved workability, improved ultimate strength and durability [22]. Optimum slag replacement is essential since high replacement level lead to loss of workability and dilution of cement that results into lower mechanical strength.

The use of silica fume (SF) and fly ash (FA) to replace cement densify the concrete due to their micro-filling effect [76]. Increasing SF replacement level reduces early strength of cement paste and concrete since high content of mineral admixture reduce the available lime [76]. Because of its high fineness (20,000  $\text{m}^2/\text{kg}$ ), more area is exposed for the reaction with CH [32]. High PAI of silica promote more C-S-H gel that improve mechanical and durability

properties of cement and concrete. In addition, high fineness offer good parking that densify the concrete by refining pores and pore size distribution, increasing compressive strength, increasing durability, reducing permeability, rate of carbonation, and diffusion of chlorine and sulphate ions [32]. ACI 234R - 06 [33] and Obada [32] suggested the optimum SF-cement replacement level as 10%. Moreover, the study conducted by Bhanja *et al.*, [77] show improved compressive strength between 10 to 20% replacement level and split tensile strength at replacement level between 5 to 15%. Such significant improvements are the advantage of reduced water-cement ratio offered by silica fume. Fly ash replacement level has the same effects to cement paste and concrete as that of silica fume. According to ASTM C 311 and ASTM C 618 [78][57] specifications, fly ash mortar and concrete should have a minimum strength activity index (SAI) of 75% of the standard mortar at 7 and 28 days curing period when PC is replaced by 20% fly ash.

The optimum calcination temperature for clay is 700 °C beyond which the PAI decreases as more amorphous phase convert into crystalline phase. It highly influences the percentage of the reactive silica and aluminosilicate, [12][16][23][27][41]. Metakaolin improves the strength of the aggregate-paste interface as well as increasing the density of the paste which in turn improves the mechanical strength of the concrete significantly [41]. Typical cement replacement level ranges from 5 to 20% by mass. Metakaolin has a very high pozzolanic activity compared to GGBS which reflect to high early strength, long-term strength, and durability although it has high heat of hydration [16][26]. Besides, factors such as parking effects, dilution effects and the reactions with CH affects the mechanical strength of concrete [41]. Therefore low proportion of metakaolin is used to control hydration rate and heat evolution in concrete to control shrinkage and cracking [23]. Metakaolin cement has a reduced permeability to fluids and chloride ions and it is ideal in oil well concrete to improve flexural and compressive strength.

## **2.7 Durability of concrete containing diverse Pozzolanic materials**

Resistance in aggressive environments like in chemical industries and marine environment is very essential for any concrete structure. Durable concrete usually requires high cement content. Although high cement content improves workability through lubrication it can result into high heat of hydration and drying cracking [35]. According to Holm and Bremner [74], the aggregate-cement interface contain not only pores but also extensive microcracks occurring from differential response to stress, temperature gradient, and volume change related to chemical reaction of the hydrating cement within the concrete. In such case the interface, become prone to permeability, ions diffusion, and site for alkali silica reaction to initiate [41]. The cracks open the way to aggressive influence to enter the concrete and cause more problems. Pure PC deteriorates easily and become unstable in aggressive environmental exposure. Also pure PC is composed of sulphate, free calcium oxide, and the CH from hydration reactions, which reacts with the reactive aggregates and cause a destructive expansion that lead to more cracks and damage to the concrete [41]. There is conservative believe that high strength concrete is always durable, though it is not always the case. This misconception has resulted into many cases of cracking and premature deterioration of many concrete structures associated with the use of high cement content and neat cement [35]. High performance concrete (HPC) and high strength high performance concrete (HSHPC) known for several decades refers to a concrete with desired strength ( $> 40$  MPa) that can withstand aggressive environment for longer time [41][79]. Durable of cement concrete show no significant microcracks at the aggregate-cement paste interface. The hydration products is inferior at the aggregate-cement paste interface, weaken the cement mortar matrix and the concrete as a whole [74].

### 2.7.1 Shrinkage

Shrinkage and expansion are deformations in concrete, which are of extreme importance especially in large concrete structure. Deformations in cement mortar matrix and concrete often occur as results of chemical processes within the microstructure and materials responses to external stress and environment [23]. Drying and carbonation shrinkage are distinct and has different formation mechanisms. The magnitude and rate of drying and carbonation shrinkage depend on the prevailing relative humidity, temperature, conditions of curing and concrete size [80]. Carbonation shrinkage may occur due to chemical reaction with the CO<sub>2</sub> in the atmosphere [80]. The responses of concrete to temperature and humidity effects always set the concrete in a state of dynamic disequilibrium with its environment [81]. Freshly hardened concrete exposed to ambient temperature and humidity undergoes thermal shrinkage associated with cooling, and drying shrinkage related to loss of moisture. Factors such as size of the structure, characteristics of concrete ingredients, mix proportions, and admixtures determine which of the two-shrinkage strain will dominate. The magnitude is determined by the coefficient of thermal expansion of aggregate, type and quantity of cement, and the temperature of concrete ingredients [23]. The microcracks in the paste-aggregates interface continue to propagate as the shrinkage factors persist. The microcracks propagate as hardening continue due to shrinkage and difference between the coefficients of thermal expansion of the paste and the aggregates which set the concrete into a state of stress even under no external stress [60]. In normal concrete, aggregates occupy between 60 - 70% by volume of concrete thus it play a very important role in controlling shrinkage and expansion. Beside, concrete containing pozzolan has lower elastic modulus contrast to concrete made of plain cement; hence the cracking trend ascending from drying shrinkage of concrete comprising pozzolan is less compared to that in similar concrete made of plain cement [27].

### 2.7.2 Expansion and Alkali silica reactions

Expansion and alkali-silica reaction are both concrete deterioration caused by chemical reaction taking place within the concrete. Expansion occurs in cement paste and concrete when cement rich in magnesium sulphate is exposed into moisture and temperature gradient [82]. Magnesium react directly with CH and destabilizes C-S-H gel resulting in the formation of gypsum which undergo an expansion with ettringite resulting into more expansive effects [82]. In the same way sodium sulfate react with CH to form gypsum. Furthermore, autoclave expansion associated to the delayed hydration of calcium and magnesium oxide contribute to the total expansion of a concrete [7]. The  $C_3A$  reaction with water in the presence of excess calcium sulphate lead to the formation of calcium sulfoaluminate hydrates (ettringite). The ettringite may form before or after the paste has hardened. When ettringite forms before hardening contributes to early strength because the needle like crystals work as reinforcement for the C-S-H and expansion is not significant. For the case when the ettringite formed after the paste has hardened where the free space have been occupied by other hydration products; due to its large volume it will force the space by breaking the hardened paste, creating cracks, and volume instability [82]. Formation of ettringite and gypsum is responsible for the expansion of concrete; therefore, magnesium sulfate attack has the most aggressive effect on concrete.

Alkali silica reaction is the chemical reaction between the reactive silica in the coarse aggregates and the alkali produced during hydration reactions of high alkali PC of over 0.6% in the presence of adequate moisture [15][83]. The sulphate, free calcium oxide, and the CH from hydration reactions of PC react with the reactive silicates of the aggregates and cause a volume expansion that lead to cracks and damage to the concrete [23][84]. It is the source of distress of concrete located in humid environments [23]. Alkali in cement is restricted to 0.6% expressed as sodium oxide equivalent ( $Na_2O_{eq}$ ) [14]. The reaction produces alkali-silica gel,

which exhibit an uneven ability for swelling caused by the absorption of more moisture. These phenomena cause undesirable damage to the concrete aesthetics and durability behaviour. Alkali-silica reaction is undesirable to concrete it should be suppressed by using pozzolanic materials. Alkali-silica reactions cause expansions that create stresses within the concrete and cracking that affects the durability of embedded steels. The same is catastrophic in pre-stressed concrete structures. Alkali-silica reaction is mitigated by using none reactive aggregates and low alkali cement [81]

Pozzolanic materials, for instance GGBFS, fly ash, silica fume, natural and artificial pozzolans potentially inhibit expansion and alkali-silica reaction. Similarly, pozzolan elevate the ratio  $\text{SiO}_2/(\text{Al}_2\text{O}_3+\text{Fe}_2\text{O}_3)$  of blended cement and therefore culminating increased resistance to sulfate and sea water attack. The effectiveness of each pozzolanic materials to conquer expansion and alkali-silica reaction is ascribed to the reactive silica content, fineness and packing effects, which contributes to pore refinement of the microstructure and reduced ions mobility [83]. The use of pozzolan reduce alkalinity in the pore solution by consuming the CH in the pozzolanic reaction thereby reducing expansion and alkali-silica reaction while producing additional C-S-H responsible for strength and pore refinement [83]. Contrary, removal of alkalinity from the pore solution lowers pH and passivation to the steel reinforcements. However, dense microstructure, low ions mobility and low gaseous diffusion prevent corrosion of reinforcements. According to ACI 232, using natural pozzolan between 20 to 30% is satisfactory to control alkali-silica reaction [21].

### 2.7.3 Carbonation

Carbonation is one of the core factors causing deterioration of the concrete structure. Carbonation is a chemical reaction between  $\text{CO}_2$  in the presence of moisture and CH present in the pores of hydrated concrete to form  $\text{CaCO}_3$ , [85]. It occurs at the surface of concrete some few millimeters deep including the cracked areas but the depth increases with decreasing rate.

Carbonation is influenced by diffusion of gases with sufficient concentration of CO<sub>2</sub> into the pore system of the hardened concrete [80]. It reduces alkalinity of the concrete and causes de-passivation around steel reinforcement. Contrary, alkalinity increases in the pore solution as hydration of cement proceed increases carbonation rate and depth of cement and concrete, [80][86]. These result into carbonation shrinkage, loss of strength, and formation of more microcracks leading further spoil to the performance of concrete.

#### **2.7.4 Chloride ion diffusion**

Pozzolan such as metakaolin at 10% replacement level significantly increase chloride binding capacity of cement paste and reduces chloride diffusion [21][27][40]. This reduces deterioration of the embedded steel elements and increase durability of reinforced concrete structures. It reduces alkali silica reaction and efflorescence where concretes are made of reactive aggregates, hence improving the aesthetics of bare faced concrete.

#### **2.7.5 Sulphate resistance**

Pores of concrete exposed to sulphate increases due to aggressive reactions of sulphates with concrete resulting into a destruction of the concrete structures, [87]. The use of blended cements and SCM decreased permeability, while increasing resistance of concrete to damage by aggressive media.



**Chapter 3 : MEASUREMENT OF POZZOLANIC ACTIVITY INDEX OF SCORIA,  
PUMICE AND RICE HUSK ASH AS POTENTIAL SUPPLEMENTARY  
CEMENTITIOUS MATERIALS FOR PORTLAND CEMENT<sup>1</sup>**

**Abstract**

This work investigated the properties of scoria and pumice as supplementary cementitious materials (SCMs) for Portland cement and compared to those of rice husk ash (RHA). X-ray fluorescence, X-ray diffraction, and pozzolanic activity index (PAI) tests confirmed the suitability of these two materials as potential SCMs. Scoria and RHA samples achieved over 75% PAI at 7 days whereas pumice did this after 28 days. Initial and final mean setting times observed for the composite cement blended with these materials were 166 and 285 min respectively. These setting times are longer than that of Ordinary Portland cement but shorter compared to that of common Portland pozzolana cement. The ultimate mean compressive strengths achieved at 28 days of curing were 42.5, 44.8, and 43.0 MPa for scoria, pumice, and RHA respectively signifying that these materials are good SCMs. Higher fineness yielded higher ultimate mean strengths. For instance, a scoria sample with a fineness of 575 m<sup>2</sup>/kg achieved the strength of 52.2 MPa after 28 days.

**Keywords:** pozzolanic activity index, strength activity index, blended cement, scoria, pumice, rice husk ash

---

<sup>1</sup> **This chapter is based on the published paper:**

Hieronimi A. Mboya, Cecil K. King'onde, Karoli N. Njau, Alex L. Mrema, (2017). "Measurement of Pozzolanic Activity Index of Scoria, Pumice and Rice Husk Ash as Potential Supplementary Cementitious Materials for Portland Cement". *Advances in Civil Engineering* Volume 2017, Article ID 6952645, 13 pages <https://doi.org/10.1155/2017/6952645> - Hindawi.

### 3.1 Introduction

Mortar is a workable paste prepared by adding water to a mixture of sand and binding materials like cement or lime. Cement sand mortar is used for binding building materials such as clay bricks, concrete blocks, stones, coarse aggregates in concrete, and for plastering. The strength and durability of a mortar or a concrete is a function of the volume and quality of the binder and the water/binder ratio used. Hydration of cement gives the strength of mortar and concrete; the hydration products fill the pores between the aggregates. Addition of supplementary cementitious materials (SCMs) reduce the amount of cement and improves the properties of mortar and concrete such as mechanical strengths, resistance to chemical attack, reduced permeability and shrinkage [70][20]. SCMs are pozzolans with high amount of silica ( $\text{SiO}_2$ ) and alumina ( $\text{Al}_2\text{O}_3$ ). As such, they react, in the presence of water, with calcium hydroxide (CH) at ordinary temperature to form calcium silicate hydrates (C-S-H) and calcium aluminosilicate hydrates (C-A-H). Both the C-S-H and C-A-H bind the aggregates and give additional strength to mortar and concrete. Fly ash, silica fume, ground granulated blast furnace slag (GGBFS), diatomaceous earth, calcined shale, volcanic tuff, and metakaolin (MK) are frequently used SCMs. Sugar cane bagasse ash and rice husk ash (RHA) obtained from agricultural byproducts are also used as SCMs. Incinerator bottom ash and slug ash are under investigation hopefully they will also emerge as good pozzolana. The use of SCMs is driven by reasons of their abundance, economic, environmental benefits, and today's advances in cement technology. The influence of SCMs on the properties of blended cement in mortar and concrete such as setting times and early strength depend on the quantity and quality of the reactive  $\text{SiO}_2$  and  $\text{Al}_2\text{O}_3$  present, particle size distribution (PSD), and the specific surface area. These three dictate the amounts of CH consumed by SCMs and the degree of C-S-H and C-A-H formation. In contrast, PSD, and specific surface area, influence the water/binder ratio, rheology of mortar and concrete, and the rate at which C-S-H and C-A-H are formed [62]. The

quality of SCMs is evaluated by pozzolanic activity index (PAI) and strength activity index (SAI), which measure the reaction between the amorphous part of pozzolana and calcium hydroxide. The PAI embraces all the reactions between CH and the reactive silica and aluminates in the pozzolans in the presence of water, that lead to the formation of the same products as that of the hydration of cement, [61][14]. It is an indirect indicator of the reaction between pozzolana and calcium hydroxide. PAI is the relative conductivity (in percentage) of the initial conductivity. It depends on the physical form, chemical composition, amount of reactive silica and alumina present, the limiting amount of lime a given pozzolana can react with, specific surface area of pozzolana and hence the rate of reaction [14][87] A number of methods, categorized as direct and indirect, have been developed for the qualitative and quantitative determination of these indices. Direct and indirect methods measure the amount of CH consumed and the relative compressive strength respectively [7]. The direct methods involve chemical titration, electrical conductivity measurement, and thermo-gravimetric analysis and so forth [62]. The indirect method compares the relative compressive strength of pozzolana blended cement mortar to that of Portland cement mortar. The reliability of each method is an important factor. For instance, Luxan et al.'s method (direct method) is accurate for early age determination of PAI but McCarter and Tran's method (also a direct method) is more accurate for the later ages [26]. Both of these methods are based on conductivity [51]. Luxan et al. [63] studied PAI of natural rock pozzolan by monitoring the change in conductivity during the first 2 min of a reaction between 5 g of pozzolan and 200 mL of saturated  $\text{Ca}(\text{OH})_2$  solution at  $40 \pm 1^\circ\text{C}$ . Two min were found sufficient for the stabilization of the reaction. Also, McCarter and Tran [26] measured conductivity of various pozzolans mixed with  $\text{Ca}(\text{OH})_2$  powder and water for 48 h. Stiffening of the paste was observed between 24 to 48 h. On the other hand, Wansom et al., [51] studied and compared various electrical methods of measuring PAI of RHA for 1 h in a saturated  $\text{Ca}(\text{OH})_2$ -pozzolan-water system. Paya et al., [37] modified

the Luxan et al.'s method by using 800 mg of  $\text{Ca}(\text{OH})_2$  powder in 1000 mL of deionized water instead of saturated solution of  $\text{Ca}(\text{OH})_2$ . In their study, the proposed observation time was 120 min but the actual time used was ~17 min. The above studies limited the time for PAI determination to 48 h. In this study, the time was prolonged to 28 days to reflect the required curing period of cement to achieve ultimate compressive strength. Furthermore, time for taking the readings was tailored to 2, 7, and 28 days to match the curing period for measuring compressive strength of cement-sand mortar. Concentrations of  $\text{Ca}^{2+}$  ions were also measured to investigate the fixation pattern. This work aimed at exploring new SCMs (scoria and pumice), comparing their pozzolanic activity index and performance in mortar with that made with RHA.

Scoria and pumice are pyroclastic ejecta which are found in many areas around the world [7]. Scoria is composed of red colored fragments indicating the presence of iron. It is highly vesicular and composed of crystalline structure. Pumice is an extrusive volcanic rock material, produced when lava, which is full of water and gases is ejected on the earth surface by volcanic action [88]. It is light-colored extremely vesicular and composed of high silica and alumina, and low in iron and magnesium. The chemical compositions of scoria and pumice from different sources vary depending on the mineralogical composition, formation temperature, and rate of cooling. The chemical composition of scoria and pumice are show in **Table 3.1**. Although scoria and pumice possess pozzolanic properties they have not yet been used as SCMs to the best of our knowledge.

Rice husk ash is produced when rice husk is incinerated at low temperature ( $< 800\text{ }^\circ\text{C}$ ) with controlled supply of air to achieve the reactive silica phase [51]. When incinerated above  $800\text{ }^\circ\text{C}$  amorphous silica convert into crystalline silica phase. The properties of the ash depend on chemical composition, purity, fineness and the amount of amorphous silica which decreases with calcination [89][90]. According to Della et al. [10], RHA burned at  $700\text{ }^\circ\text{C}$  has 94.95% of

reactive silica (**Table 3.1**). Wansom et al. [51] and Givi et al. [52], state that burning of RHA at different temperatures and supply of oxygen result into different amounts of reactive silica.

**Table 3.1:** Chemical Compositions of Scoria, pumice, and RHA from different literatures

Sample	SiO <sub>2</sub>	Fe <sub>2</sub> O <sub>3</sub>	Al <sub>2</sub> O <sub>3</sub>	CaO	Alkali	MgO	TiO <sub>2</sub>	L.o.I
	[%]	[%]	[%]	[%]	[%]	[%]	[%]	[%]
(a) SCORIA								
Khandaker and Hossain [7]	45-50	7-10	13-15	5-8	4-6	4-6		1.25-1.50
Taha et al. [56] Yemen scoria	47-50		28-30	7-10	3-6			
Taha et al. [56] Italy scoria	51.4		25.7	6.5	6.4			
Taha et al. [56] Australian scoria	47.7		25.4	6.8	6.2			
Njau et al. [91]	35.4		31.9	12.7	5.6			
(b) PUMICE								
Ismail et al. [92]	70.97	1.88	14.24	1.37	8.48	0.35	0.14	2.41
(c) RHA								
Wansom et al. [51]	93.59	0.31	0.89	2.28	1.30		0.61	
Della et al. [10] (at 700°C)	94.95	0.26	0.39	0.54	1.19	0.9	0.2	0.85

## 3.2 Materials and Methods

### 3.2.1 Materials

This study was carried out using scoria obtained from Uchira-Kilimanjaro, Tanzania, and pumice and rice husk from Mbeya, Tanzania. Analytical grade calcium hydroxide ( $\text{Ca}(\text{OH})_2$ ) and Portland Limestone Cement (PLC) CEM II/A-L class 42.5 N conforming to BS 197-1 was used. Standard sand prepared according to SS- EN 196-1 was also used.

### 3.2.2 Experimental Procedures

Samples of scoria, pumice, and rice husk were calcined at different temperatures ranging from 600 to 900 °C in a muffle furnace at a rate of 7 °C/min. The samples were kept at the respective temperature for 1 h and then cooled to room temperature. Natural samples of scoria and pumice, and a sample of rice husk ash incinerated in uncontrolled condition were included in for comparison purposes. The incineration in uncontrolled condition was set in a small room of 2 m<sup>2</sup> and the rice husks were sprayed to 0.5 m depth. The ash obtained from this condition was designated as RHA-uc. All samples were milled using disc mill model 4A100L6T1 SN 535277 (**Figure 3.1**) at a rate of 2 kg/h and sieved through 75 μ BS standard sieve mounted on automatic sieve shaker [93]. 95% of the weight of each sample passed this sieve. The samples designations and notation are shown in **Table 3.2**.

**Table 3.2:** Sample Designation of notation.

Calcination Temperature (°C)	Sample Designation		
	Scoria	Pumice	Rice husk ash (RHA)
900	S 900	P 900	RHA 900
800	S 800	P 800	RHA 800
700	S 700	P 700	RHA 700
600	S 600	P 600	RHA 600
Uncontrolled condition			RHA-uc#
Natural	S-N*	P-N*	

\*Natural scoria and pumice                      # combustion in an uncontrolled condition

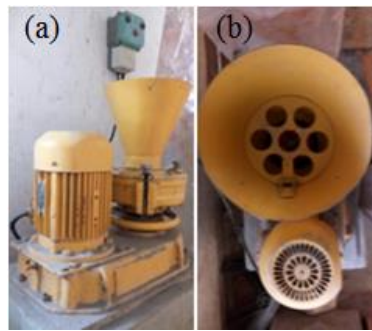


**Figure 3.1:** Disc milling machine, (a) Front view (b) Top View

### 3.2.3 Determination of chemical and phase composition

Chemical and phase compositions of the samples in **Table 3.2** were analyzed by X-ray fluorescence (XRF) and X-ray Diffraction (XRD) techniques [94] [28]. XRF analysis was performed using Bruker XRF-S8 Tiger spectrometer, while XRD analysis was done using Bruker S8 diffractometer with Cu  $K_{\alpha}$  radiation. Scanning was performed between  $2^{\circ} \leq 2\theta \leq 60^{\circ}$  for the XRF samples and  $5^{\circ} \leq 2\theta \leq 70^{\circ}$  for the XRD samples. The scanning rate for both XRF and XRD was 0.02 degrees/sec. The analyses were done according to ASTM C 618 [57] which requires the sum of the basic oxides, silica, alumina, and ferrous to be higher than 70% for pozzolana.

### **3.2.4 Determination of specific gravity, specific surface area, particle size distribution (PSD), and pozzolanic activity index (PAI)**

The specific gravity (SG) of cement and powder materials were determined according to SS-EN 197-1, ASTM D 854 and B8E1-1 [66][95][96]. Specific surface area was measured using Automatic Blaine Apparatus (AIM-391-3) SN 2001 from Aimil Ltd, India [97]. Particle size distribution (PSD) was analyzed using isopropanol procedure and Laser Mastersizer [23][25]. Pozzolanic activity index was measured using 200 mg of  $\text{Ca(OH)}_2$  in 250 mL distilled water [63][37].

### **3.2.5 Determination of setting times and soundness**

#### **a) Standard consistency test**

Standard consistence tests were determined for cement paste replaced with 10, 20, 30, and 40% of scoria and pumice treated at different temperatures (**Table 3.2**). Standard consistency paste contains enough water for the desired plasticity state required for setting times and soundness tests. The paste were prepared according to SS EN 196-3 [65] by 500 g of dry cement and 125 g of distilled water. Similarly ASTM C 187 [101] recommended 300 g of cement powder and 80 mL of distilled water. Standard consistence is achieved when the Vicat plunger penetrate to a depth of  $6 \pm 2$  mm from the base in 30 s [65]. Also ASTM C 187 [101] demand penetration of 10 mm from the surface in 30 sec. Neville and Brooks [1] cited the standard consistence paste as one having water requirement between 26 to 33 percent of cement powder.

#### **b) Setting time test:**

Initial and final setting time were determined according to SS-EN 196-3 [65] to study the influence of scoria and pumice in PC replaced with 10, 20, 30, and 40% of scoria and pumice treated at different temperatures. Setting times describe the stiffening from fluid to rigid state of cement paste caused by initial hydration of  $\text{C}_3\text{S}$  and  $\text{C}_2\text{S}$ . Initial setting time is defined as the



time laps from zero time to the time when the Vicat needle penetrate to a depth of  $6 \pm 3$  mm from the base plate [65]. It estimates the time when cement has stiffened and lost its workability. Final setting time is the time laps measured from zero time to that at which the needle first penetrates only 0.5 mm into the specimen [65]. It is the time at which the ring attachment fails to mark the specimen and it is reported to the nearest 15 minutes. Initial setting time should not be less than 30 minutes. SS-EN 197-1 [66], however, specifies an initial setting time of 60 min and a final setting time no more than 10 h for cement strength class 42.5. There is no standard limit which is given for the final setting time. Neville and Brooks, [1] suggested  $90+1.2 \times$  the initial setting time as the final setting time. Initial and final setting times results are shown in **Figure 3.6(a)** and **(b)**.

### c) Soundness test

Soundness is the ability of a hardened cement paste to preserve its volume after setting without late destructive expansion, cracking, volume expansion and unwanted stresses. Cement paste is considered unsound if it undergoes excessive volume change after setting. Unsound cement may contain impurities like CaO, MgO and sulfates which resulted from poor burning of clinker due to inadequate grinding and mixing of raw materials. MgO and CaO react slowly in **Equations 3-1 and 3-2**, causing damage to hardened cement and concrete [82].



Calcium sulfate from excess gypsum react slowly causing expansion through the formation of calcium sulfoaluminate (ettringite) [1][82] which is aggressive to cement and concrete. The tests evaluate the potentials for volumetric change of cement paste. Soundness tests of cement replaced with 10, 20, 30, and 40% of scoria and pumice treated at different temperatures were measured using Le Chartelier apparatus according to SS-EN 196-3[65] procedures and results

are shown in **Figure 3.7(b)**. For acceptable cement quality the values of **Equation 2-4** are recommended [65].

### **3.2.6 Determination of compressive strength**

Compressive strength of cement mortar made of PLC blended with 10, 20, 30, and 40% of scoria, pumice, or RHA treated at different temperatures was measured according to SS-EN 196-1 [102]. Normally, this test uses cement mortar prism of  $40 \times 40 \times 160$  mm, or 70.7 mm cubes. Compression test of cement mortar is also measured on cubes of 50 mm with cement/sand ratio 1:2.75 and water/cement ratio 0.485 [1][82][103]. In this research, SS-EN 196-1 [102] was adopted using 40 mm cubes. Three test and reference cubes were cast and crushed after 2, 7, 28, 56, and 90 days curing periods using compression machines conforming to SS-EN 196-1 [102]. The loading rate was adjusted to 12 to 24 kN/min. The results are as shown on **Figure 3.9** and **Figure 3.11**.

## **3.3 Results and discussion**

### **3.3.1 Materials chemical composition and physical properties**

**Table 3.3** shows results for the chemical composition of scoria, pumice, and RHA materials treated at different temperatures. The mean value for silica ( $\text{SiO}_2$ ) content was found to be 42.9, 57.5, and 92.7 %; basic oxide 71.1, 78.4, and 93.3%; calcium oxide (CaO) 10.1, 1.1 and 0.66%; alkali 3.2, 9.1, and 1.6% and loss on ignition 5.2, 7.4, and 1.9% for scoria, pumice and RHA samples, respectively. Scoria, pumice and RHA samples indicated significant difference with the degree of marginal difference of  $P < 0.05$  for the basic oxides and loss on ignition.

Observation on the chemical composition revealed that significant influence was caused more by the type of materials than on the calcination temperature. Scoria samples showed high CaO content indicating high latent hydraulic properties. Pumice on the other hand had low calcium content indicative of non-hydraulic properties. The chemical composition of

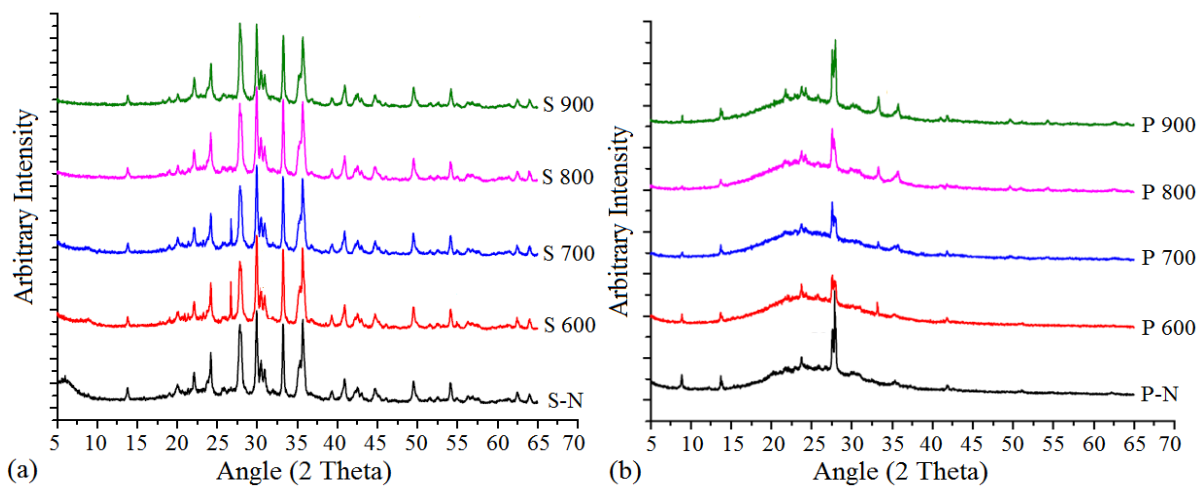
scoria and pumice were comparable with those reported in literature **Table 3.3**. The sum of the basic oxides observed were over 70% as required by ASTM C 618 [57] for a material to qualify as a pozzolan.

**Table 3.3:** Temperature effects on chemical composition and physical properties of the Scoria, Pumice and RHA.

<b>Sample</b>	<b>SiO<sub>2</sub></b>	<b>Fe<sub>2</sub>O<sub>3</sub></b>	<b>Al<sub>2</sub>O<sub>3</sub></b>	<b>Basic oxide</b>	<b>CaO</b>	<b>Alkali</b>	<b>MgO</b>	<b>L.o.I</b>	<b>Specific Gravity</b>	<b>Specific surface area</b>
	[%]	[%]	[%]	[%]	[%]	[%]	[%]	[%]		m <sup>2</sup> /kg
S 900	41.6	15.1	13.4	70.1	10.1	4.2	5.43	5.01	2.95	325
S 800	43.4	14.8	15.6	73.8	10.5	3.64	5.43	1.47	2.96	314
S 700	45.3	14.6	12.9	72.8	10.2	3.16	5.46	3.52	2.97	333
S 600	44.5	15.2	12	71.7	10.3	3.3	5.04	5.05	3.04	456
S-N	40	13.9	13	66.9	9.6	3.15	4.62	10.76	2.93	575
P 900	63.1	4.48	15.9	83.48	0.62	10.25	0.27	4.18	2.50	369
P 800	57.3	4.56	16.6	78.46	1.24	11.23	0.26	7.45	2.41	479
P 700	55	4.42	15.6	75.02	0.8	10.82	0.24	10.32	2.43	447
P 600	56.6	4.56	17.5	78.66	1.27	11.7	0.31	6.2	2.43	573
P-N	55.4	4.64	16.4	76.44	1.7	10.79	0.62	8.78	2.39	506

<b>Sample</b>	<b>SiO<sub>2</sub></b>	<b>Fe<sub>2</sub>O<sub>3</sub></b>	<b>Al<sub>2</sub>O<sub>3</sub></b>	<b>Basic oxide</b>	<b>CaO</b>	<b>Alkali</b>	<b>MgO</b>	<b>L.o.I</b>	<b>Specific Gravity</b>	<b>Specific surface area</b>
	[%]	[%]	[%]	[%]	[%]	[%]	[%]	[%]		m <sup>2</sup> /kg
RHA 900	88.8	0.44	0.32	89.56	0.65	2.02	0.24	6.07	2.28	282
RHA 800	92.4	0.49	0.38	93.27	0.8	2.42	0.3	2.13	2.21	300
RHA 700	94.7	0.24	0.29	95.23	0.55	2.35	0.35	0.21	2.15	309
RHA 600	94.25	0.26	0.33	94.84	0.63	2.51	0.28	0.56	2.14	462
RHA-uc	93.5	0.53	0	94.03	0.67	2.65	0.38	0.86	2.17	611

**Table 3.3** shows the specific gravity (SG) and specific surface area of scoria, pumice, and RHA. The specific gravity increased with calcination temperature for both the pumice and RHA samples. The natural pumice sample (P-N) showed an SG of 2.39. Upon calcination at 900 °C, the specific gravity increased to 2.50. Similarly, SG increased from 2.17 for RHA-uc sample to 2.28 for RHA sample calcined at 900 °C (RHA 900) (**Table 3.3**). There was no obvious trend between specific gravity and calcination temperature was observed for the scoria samples. The increase in specific gravity with temperature for pumice and RHA samples was probably due to the reduction of porosity and increased crystallinity as the materials sintered at higher temperatures. Similarly, specific surface area of scoria and RHA decreased with calcination temperatures from 575 (for S-N) to 325 m<sup>2</sup>/kg (for S 900) and from 611 (for RHA-uc) to 282 m<sup>2</sup>/kg (for RHA 900), respectively. This was probably due to the strengthening of the microstructure via neck growth and agglomeration, densification, and coarsening of the microstructure, that occurred as the materials sintered at elevated temperatures. The low specific gravities of scoria, pumice, and RHA as compared to Portland cement (3.15) are attributed to the porous microstructure. No obvious trend between surface area and calcination temperature was observed for pumice samples.



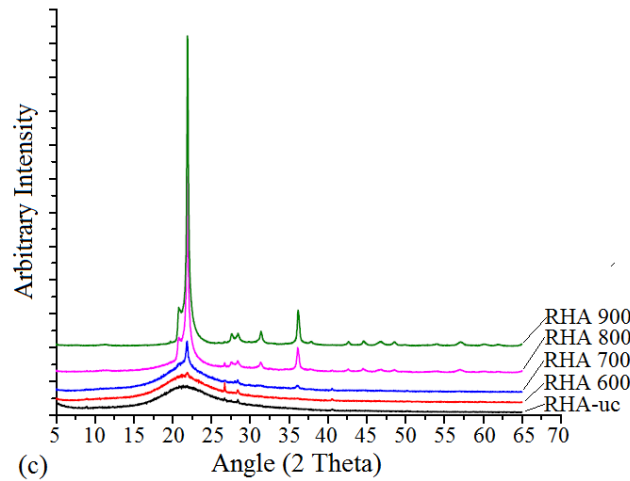


**Figure 3.2:** XRD patterns for (a) Scoria, (b) Pumice, and (c) RHA.

**Figure 3.2** shows the XRD pattern of materials at different calcination temperatures. **Figure 3.2(a)** shows multiple sharp peaks indicative of polycrystalline nature of scoria. There was no observable change in crystallinity of scoria with calcination temperature as peak intensities and widths remained almost the same except for a peak around  $6^\circ$  2-theta which disappeared at higher temperatures. The main phases observed were pyroxene (augite/diopside) and hematite. Similar to scoria materials, no changes in crystallinity with calcination temperature were observed for pumice samples (**Figure 3.2(b)**). The peak at  $33^\circ$  2-theta for P 600 – 900 could be due to preferred orientation. The main phases observed were feldspar (anorthoclase /anorthite) and mica. On the contrary, RHA samples showed dramatic changes in peak intensities and widths with calcination temperature (**Figure 3.2 (c)**). The XRD pattern for RHA-uc and RHA 600 showed one broad peak at around  $22^\circ$  2-theta attributed to amorphous silica [90][104]. This peak becomes narrow and intense at temperatures beyond  $600^\circ\text{C}$ . At  $800 - 900^\circ\text{C}$ , more sharp peaks evolved corresponding to crystalline phase (cristabalite).

### 3.3.2 Particle size distribution (PSD)

**Figure 3.3**, shows the PSD profiles of scoria, pumice, and RHA. The PSD profiles indicated well-graded particles where all particles from coarse to fine were present. Fine particles are more reactive and have good parking effect. The specific surface area and PSD are not only critical to pozzolanic reactions but also translates to reduced setting times, enhanced final strength and packing density of mortar and concrete. This also implies reduced cracking, shrinkage, permeability, and chemical attack of a mortar or concrete. These factors culminate improved durability of the mortar and concrete structures.

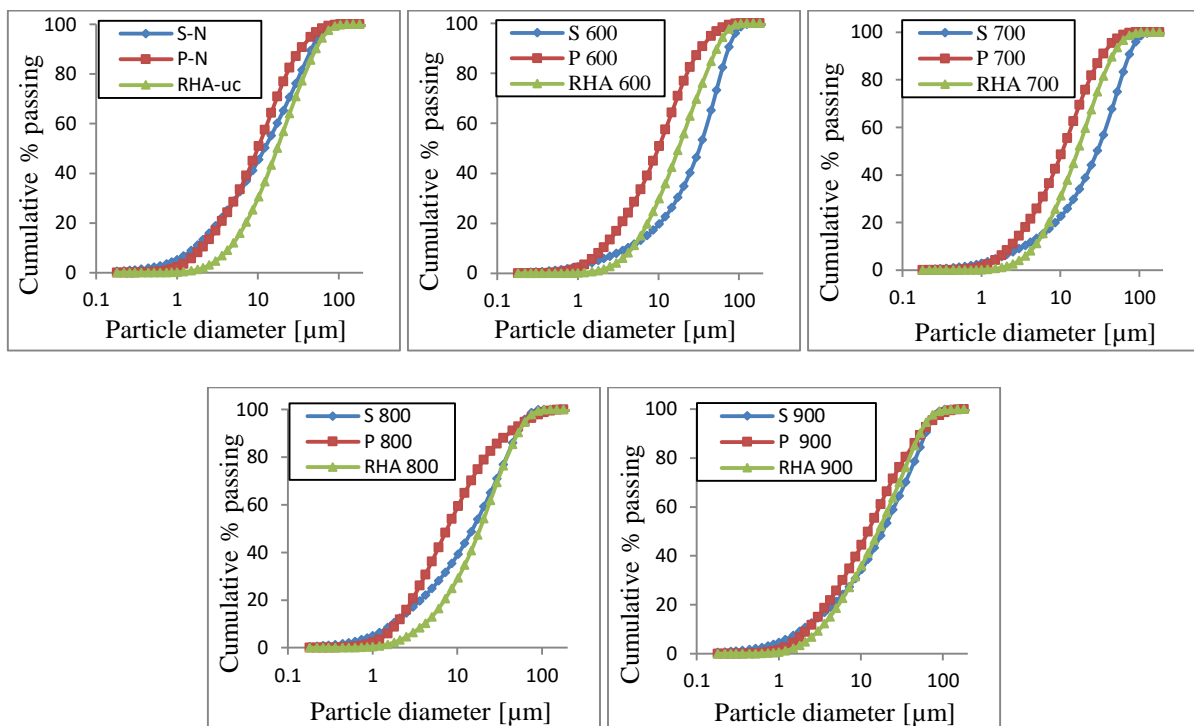


**Figure 3.3:** PSD profiles for scoria, pumice, and RHA at different calcination temperatures.

### 3.3.3 Pozzolanic activity index (PAI)

**Figure 3.4** shows pozzolanic activity index (PAI) patterns of scoria, pumice, and RHA. Pozzolanic activity index increased rapidly within the first 48 h after which the rate decreased and stabilized for scoria and RHA samples (**Figure 3.4(a), (c)**). This was indicative of rapid depletion of the calcium ions ( $\text{Ca}^{2+}$ ) associated with pozzolanic reactions. As the concentrations



of  $\text{Ca}^{2+}$  ions reduced with time, the rates of PAI decreased and stabilized when all the  $\text{Ca}^{2+}$  ions were all consumed. High PAI of RHA samples correlate well with the XRF and the XRD results on **Table 3.3** and **Figure 3.2(c)** which show high amorphous silica content in RHA samples compared to scoria and pumice. Calcination temperature and hence the degree of crystallinity were found to have a strong influence on PAI. This was attributed to the fact that at low temperatures, less crystalline silica is obtained, which is more reactive than the highly crystalline silica obtained at high temperatures. The increase in the degree of crystallinity with temperature is clearly exhibited by XRD patterns on **Figure 3.2(c)**, which show evolution of narrow and intense peaks with increase in temperature. The RHA-uc, and RHA 600, and RHA 700 samples were rather amorphous compared to their scoria and pumice counterparts, **Figure 3.2(a)** and **(b)**. This explains why the PAI of RHA-uc, RHA 600, and RHA 700 samples were higher at 88, 86, and 87% compared to 82, 75, and 75; and 70, 52, 49% for S-N, S 600, and S 700 and P-N, P 600, and P 700, respectively at 7 days. In contrast, pumice attained 86, 75, 75% for P-N, P 600, and P 700 at 28 days. The failures of pumice samples to achieve the minimum PAI of 75% stipulated by ASTM C 618 within 7 days indicated their inability to attain sufficient strength within 7 days. The PAI results show, however, that composite cement made of these materials would achieve the ultimate compressive strength within 28 days.

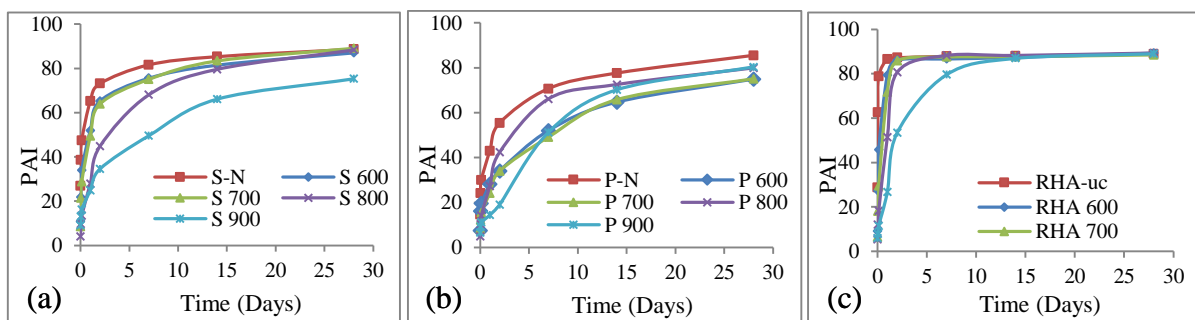


**Figure 3.4:** PAI versus reaction time: (a) Scoria, (b) Pumice, and (c) RHA.

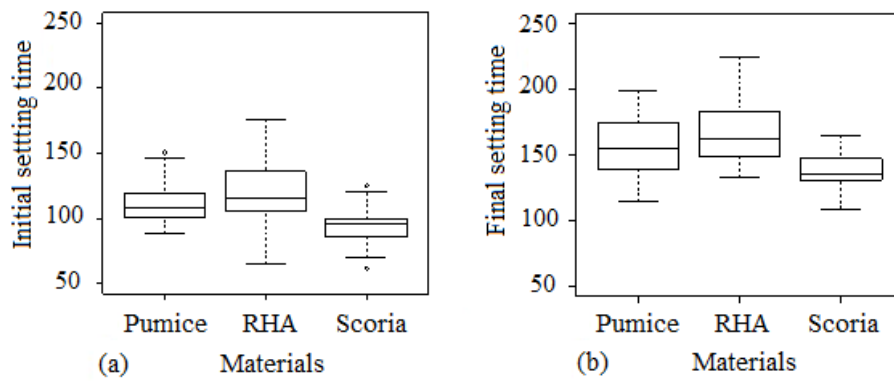
### 3.3.4 Setting times

Prior to setting times and soundness tests, standard consistency paste was prepared from cement blended with scoria, pumice or RHA at 10, 20, 30 and 40% replacement levels. The standard consistency paste indicated water cement ratio requirement of between 0.26 to 0.33 except for RHA-uc, RHA 600, and 700, which showed water cement ratio of 0.38 at 40% replacement level. **Table 3.4** shows the significant influence of materials and fineness on setting times of blended cement. The analysis of experimental data indicated that materials and fineness affected the setting times significantly. The level of marginal significance observed for initial setting time and final setting times was  $P < 0.05$  for fineness and materials, correspondingly (**Table 3.4**), **Figure 3.5**, and **Figure 3.6**). The difference was due to variation in mineralogy, chemical composition and fineness, which dictate the rate and type of chemical reactions to take place. S-N was found to react very fast, as such; it gave the least mean initial setting time of 80 min, (**Figure 3.6(a)**). This was the attribute of low crystallinity and high fineness of 575 m<sup>2</sup>/kg. Nevertheless, P-N reacted slowly despite of its high fineness of 506 m<sup>2</sup>/kg because of delayed pozzolanic reaction. Although RHA 600 was amorphous and had a fineness of 462 m<sup>2</sup>/kg, it showed significantly delayed setting times (154 min initial setting time and 190 min final setting time) owing to the high water content, (**Figure 3.6(c)**). The highest mean initial setting times observed were 103, 146, and 154 min for S 800, P 900, and RHA 600, respectively. Likewise, the highest final setting times (FST) were 156, 182, and 190 min for S 900, P 900, and RHA 600, respectively, **Figure 3.5** and **Figure 3.6**. Initial and final mean setting times observed were shorter compared to that of Portland pozzolana cement, which was 166 and 285 min, respectively.

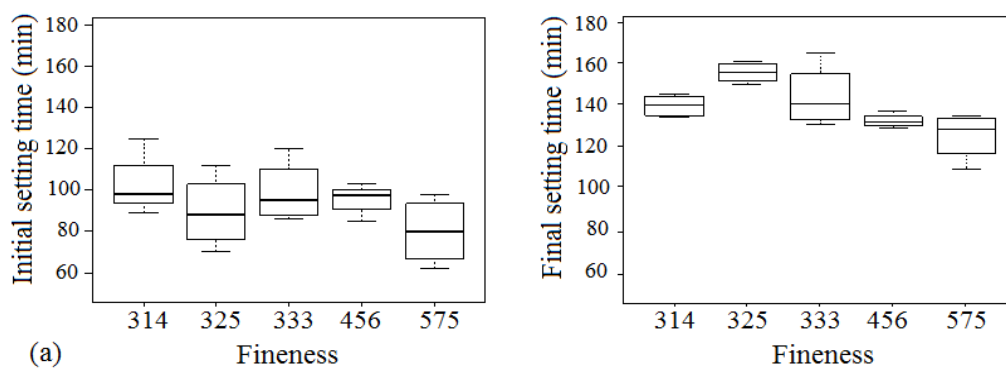
**Table 3.4:** The influence of materials, temperature and chemical composition on initial setting times, final setting times, shrinkage, and soundness.

Independent variable	Pillai trace	Approx. F	Num DF	Den DF	P-value
Materials	0.33431	6.4029	4	51	0.0002967 ***
Temperature	0.13917	2.0613	4	51	0.0996102
Fineness	0.26691	4.6422	4	51	0.0028440 **
Basic oxides	0.13841	2.0483	4	51	0.1014302
Replacement	0.11097	1.5915	4	51	0.1907633

\*\*  $P < 0.01$ , \*\*\*  $P < 0.001$



**Figure 3.5:** Influence of materials on (a) Initial setting time, and (b) Final setting time.



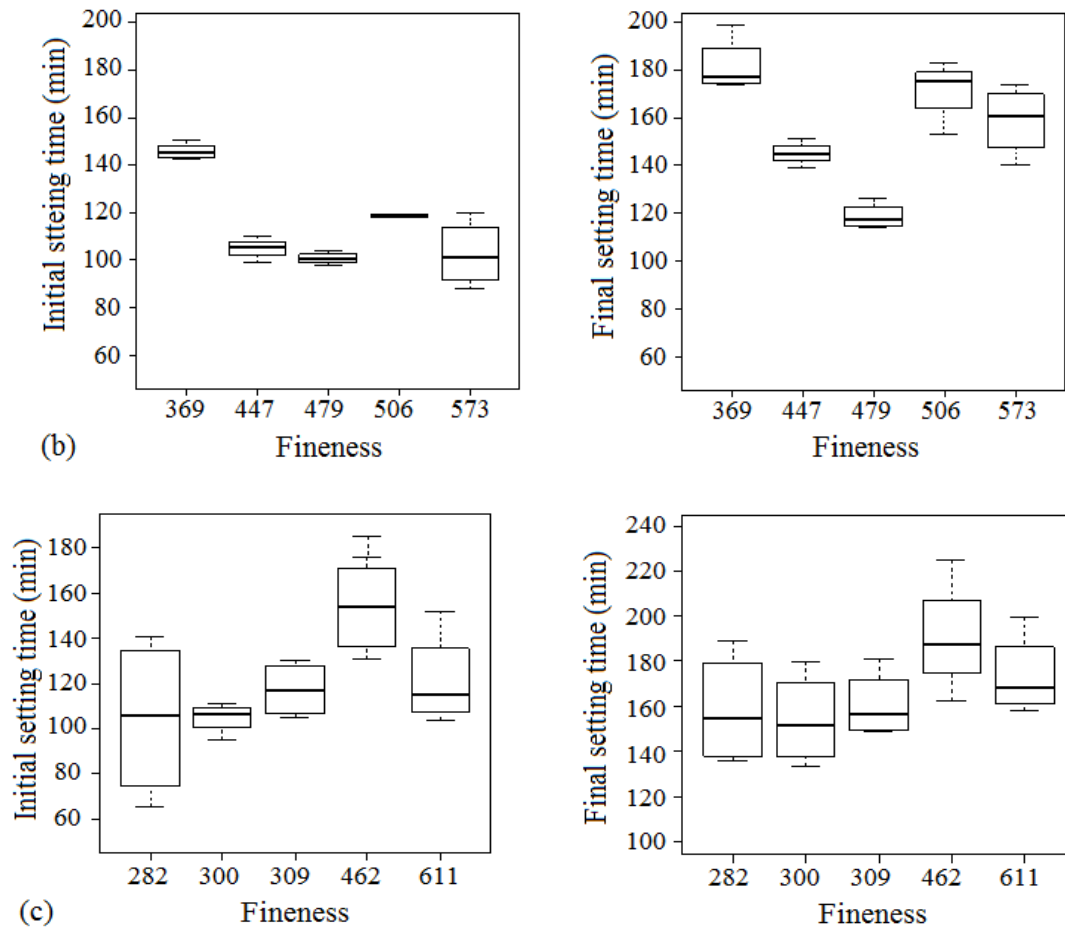


**Figure 3.6:** Influence of fineness on setting times: (a) Scoria, (b) Pumice, and (c) Rice husk ash.

### 3.3.5 Shrinkage and Soundness

**Figure 3.7** and **Figure 3.8**, show shrinkage and soundness test results. The statistical analysis indicated that the type of material and fineness had major influence on soundness and shrinkage. Marginal significance for type of material and fineness  $P < 0.05$  (**Table 3.4**) were observed between pumice-RHA and pumice-scoria **Figure 3.7** correspondingly. The maximum values observed for the materials were 2 and 1.5 mm for shrinkage and soundness, respectively. The minimum and maximum mean values for shrinkage and soundness observed were 0.5 and 1.0 mm, respectively. These results imply that MgO and alkali had no effect on the blended cement and hence the MgO and alkali contents in our SCMs are within the acceptable levels.

The values obtained for soundness and shrinkage in our study are acceptable according to SS-EN 196-3[65].

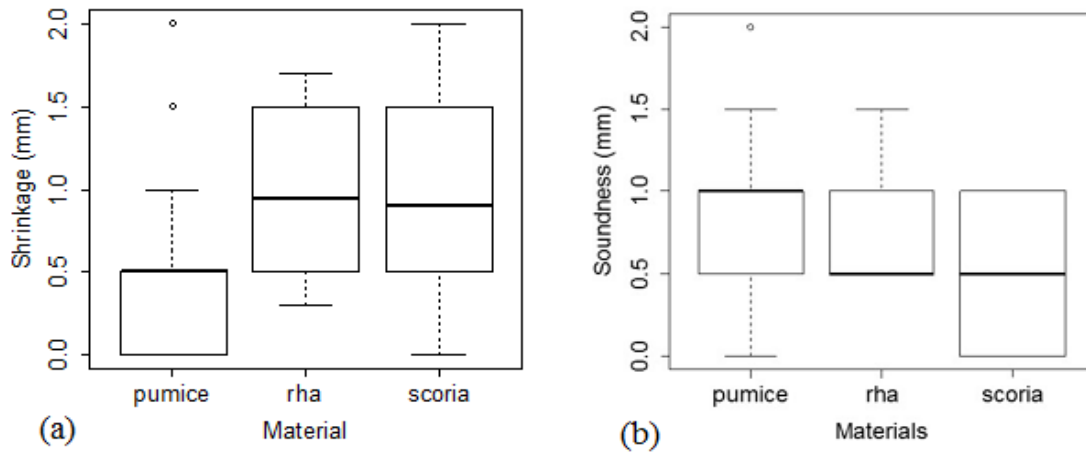


**Figure 3.7:** Effect of materials (a) Shrinkage, and (b) Soundness.

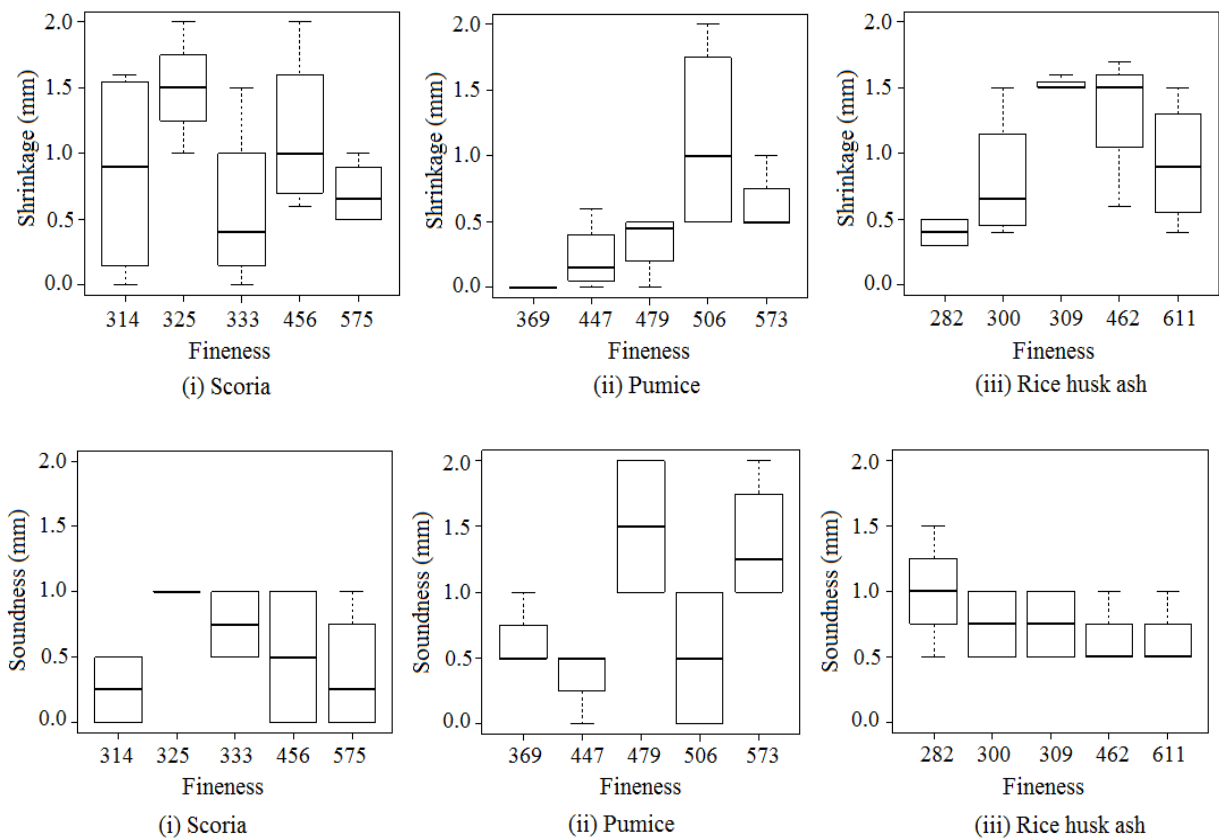


**Figure 3.8:** Effect of fineness on (a) Shrinkage, and (b) Soundness

### 3.3.6 Compressive strength of scoria and pumice blended cement

**Table 3.5** shows statistical analysis of compressive strength test results of scoria, pumice and RHA blended cement. The level of cement replacement, fineness, and type of material were found to have huge influence on the compressive strength development. The level of marginal significances observed for the level of cement replacement, fineness and type of materials was  $P < 0.05$ . Compressive strengths of all samples increased with curing age but decreased with percent of cement replaced, (**Figure 3.9**). Compressive strength increased fast up to 28 days beyond which the growth rate decreased gradually with curing period as the pozzolanic reaction depleted both the CH and silica content.

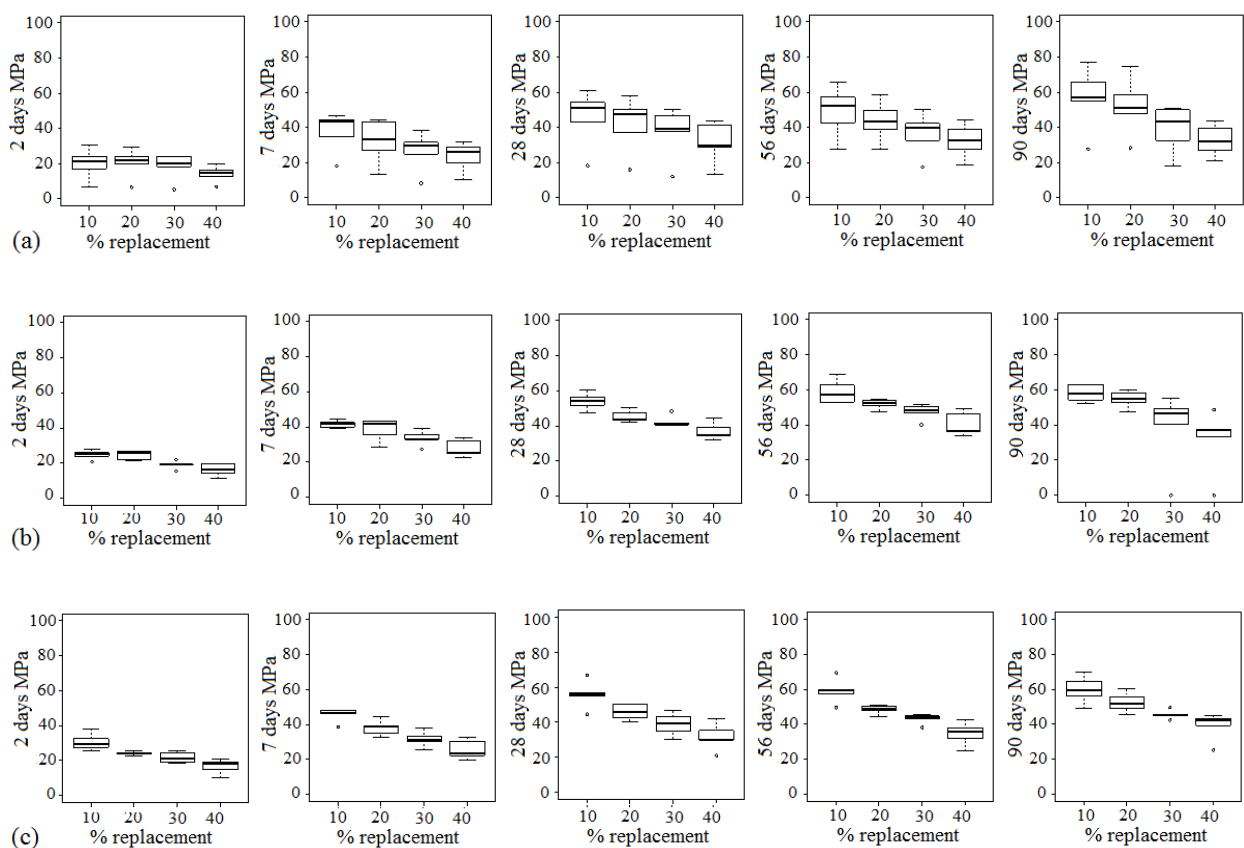


**Figure 3.9:** Compressive strength of blended cement versus percent replacement (a) Scoria, (b) Pumice, and (c) RHA.

**Table 3.5:** Factors influencing compressive strength (MPa)

Independent variable	Pillai trace	Approx. F	Num DF	Den DF	p-value
Materials	0.29584	4.2854	5	51	0.002492 **
Temperature	0.18776	2.3579	5	51	0.053215 <sup>ns</sup>
Fineness	0.28073	3.9811	5	51	0.003997 **
Replacement	0.58722	14.5108	5	51	7.733e-09 ***

\*\*  $P < 0.01$ , \*\*\*  $P < 0.001$ , ns = non-significant ( $P > 0.05$ )

Mean compressive strength of all samples after 2, 7, and 28 days curing period indicated that pumice and RHA samples performed better compared to scoria samples (**Figure 3.10(a)** and **(c)**). Scoria samples treated at high temperature reacted poorly due to low amorphous silica content hence contributing to low mean compressive strength. This was probably due to the decrease in the amount of reactive amorphous silica content and evolution of more non-reactive crystalline silica content with temperature. Pumice reacted slowly with CH from hydrating cement and gained the mean ultimate compressive strength of over 42.5 MPa at 28 days. The mean ultimate compressive strengths at 28 days curing period for scoria, pumice, and RHA blended cements were rather similar since over 95 percent of the pozzolanic reaction was over. The ultimate mean compressive strengths achieved at 28 days curing period were 44.8, 43.0, and 42.5 MPa for pumice, RHA, and scoria, respectively (**Figure 3.10c**). With regards to fineness, the ultimate mean strength at 28 days for scoria samples with fineness of 575 m<sup>2</sup>/kg was 52.2 MPa compared to 43.1 and 44.6 MPa for pumice and RHA with fineness of 506 and 611 m<sup>2</sup>/kg, respectively (**Figure 3.11**). Natural scoria achieved high compressive strength possibly due to latent hydraulicity, high reactive silica content and good packing effects.

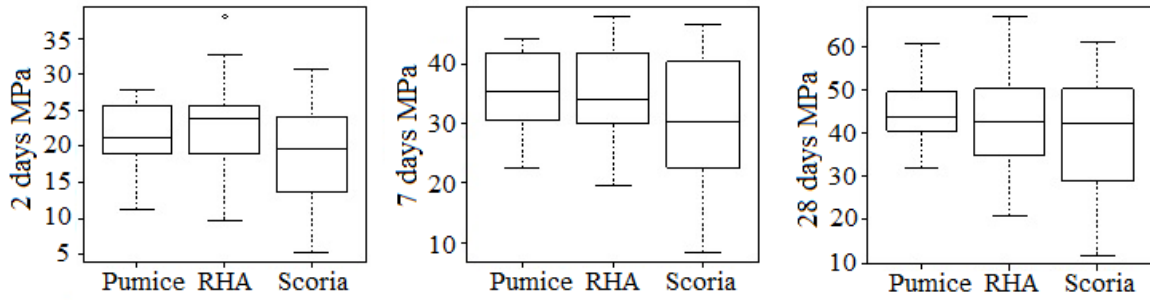


**Figure 3.10:** Effect of materials on compressive strength of blended cement

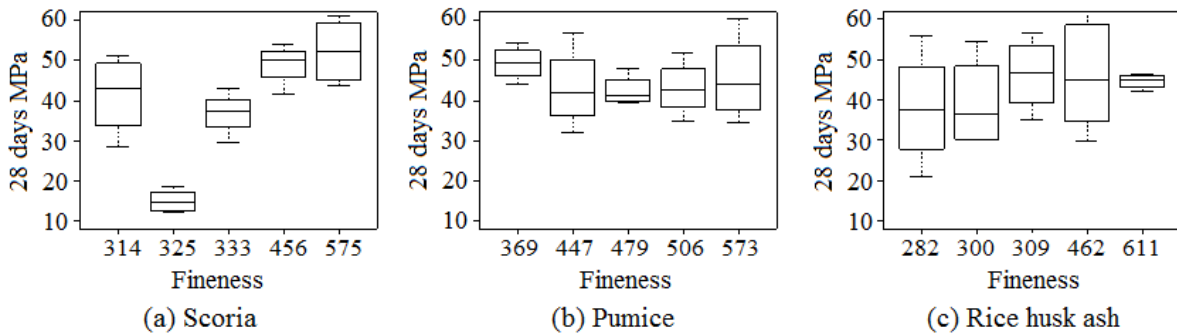


**Figure 3.11:** Effect of fineness on 28-days compressive strength.

### 3.4 Conclusion

Scoria, pumice, and RHA materials were successfully characterized according to ASTM C 618 criteria and were tested to establish their potential as SCMs. Finely milled un-calcined samples of scoria and pumices, and rice husk ash calcined in uncontrolled condition has specific surface area of 575, 506, and 611 m<sup>2</sup>/kg, respectively. These materials showed high PAI of 82, 70.7, and 87.8% at 7 days: 89.0, 85.5, and 88.9% at 28 days in that order. These values meet the criteria for SCMs. Pozzolanic activity indices achieved by all scoria samples at 7 days were above the specified minimum of 75%. In comparison, rice husk ash achieved over 80% PAI after 7 days. Contrary, all pumice samples achieved minimum pozzolanic activity index after 28 days. Scoria and rice husk ash blended cement reached the ultimate compressive strength in 7 days while pumice blended cement achieved in 28 days. The ultimate mean compressive strengths achieved were 44.8, 43.0, and 42.5 MPa for pumice, RHA, and scoria respectively, after 28 days curing period. In addition, setting time observed for all samples ranged from a



minimum mean initial setting time of 80 min for S-N to maximum mean initial setting time of 154 min for RHA 600. Likewise, the final setting time ranged from a minimum mean final setting time of 156 min for S 900 to maximum final setting time of 190 min for RHA 600. Initial and final setting times for scoria, pumice, RHA were lower compared to those of Portland pozzolana cement (PPC), which were 166 and 285 min initial setting time and final setting times in that order. On the other hand, soundness and shrinkage determined for all samples had a maximum mean value of 1.5 mm. The combination of all the above parameters demonstrated the suitability of natural scoria and pumice as SCMs.

## **Chapter 4 : INFLUENCE OF SCORIA AND PUMICE ON KEY PERFORMANCE**

### **INDICATORS OF PORTLAND CEMENT CONCRETE<sup>2</sup>**

#### **Abstract**

Cement industries have a huge CO<sub>2</sub> signature that can be reduced in an effort to mitigate climate change via precise cement substitution with supplementary cementing materials (SCMs). The substituting materials and their amounts ought not to degrade the key performance indicators of concrete such as slump, flow, permeability, shrinkage, modulus of rupture, compressive and tensile splitting strength. In addition to cutting the CO<sub>2</sub> emissions, SCMs reduce energy bills and confer extra strength and resistance to mortar and concrete. In this chapter, the influence of natural scoria (S-N) and natural pumice (P-N) binders on the key performance indicators of the fresh and hardened Portland cement concrete was successfully examined. The performance indicators were tested at Portland limestone cement (PLC) substitution (with S-N or P-N) levels 10, 20, 30, and 40% and the results compared to the control (CTRL) made of PLC only. The characteristic and target mean strength of 30 and 38.2 MPa were considered. The 28-days maximum compressive strength achieved by the blended cement concrete were 44.2 and 43.1 MPa for S-N 10 and P-N 10, respectively. The minimum compressive strength obtained was 35.6 MPa while the ultimate mean 28-days compressive strength was 39.9 MPa. The modulus of rupture decreased with the amount of S-N from 6.0 MPa to 4.1 MPa at 10 and

---

<sup>2</sup> **This chapter is based on the published paper:**

Hieronimi A. Mboya, Cecil K. King'onde, Karoli N. Njau, Alex L. Mrema, (2018). "Influence of Scoria and Pumice on Key Performance Indicators of Portland Cement Concrete". *Construction and Building Materials* 197 (2019) 444–453 - Elsevier.

40% replacement levels. Contrary, that of its P-N counterpart increased to a maximum of 8.0 MP at 20% replacement then dropped to minimum 6.4 MPa at 40% replacement level. The residual compressive strength of P-N blended cement concrete samples, after subsection to high temperatures of 600 °C, was higher than that of its S-N equivalents. All the concrete specimens showed residual compressive strength of over 50% except S-N 40 mix which afforded 45.5%. S-N 10 – 30 deliver coefficients of permeability ( $K$ ) of 5.2526E-08, 5.20833E-08, and 4.9741E-08 m/s, in that order, that are remarkable close (even better at 30% replacement level) than that of Portland cement concrete, 5.35714E-08 m/s. This low permeability attested by their low porosity microstructure as shown by the micrographs implies reduced chemical attack, less carbonation, improved protection of steel reinforcement against corrosion, and hence improved durability of the concrete. The micrographs of the concrete mixes: CTRL, S-N 10 – 30, and natural pumice (P-N) P-N 20 - 30 were denser and less porous reflecting to low permeability. The specimens; S-N 40, P-N 10, and P-N 40 showed porous microstructure that translated to high permeability.

**Keywords:** Modulus of rupture, Scoria, Pumice, Compressive strength, Slump, Residual strength

## 4.1 Introduction

Concrete is a composite construction material made of Portland cement and other cementitious materials (such as fly ash, ground granulated blast furnace slag, silica fume, and metakaolin); coarse and fine aggregates; and water which develops its strength by hydration of cement [82]. It is a manmade material produced by mixing Portland cement, sand, gravel or crushed stone and water [23]. Neville et al., [1], define concrete as any product made by using cementing medium. Cement paste forms a matrix, which embeds and glue the aggregate particles to form a hard stony like mass with sufficient strength to bear the loads while retaining its structural integrity.

Hardening of concrete results from hydration of cement and continues for a long time after the concrete has gain sufficient strength. The quantity and quality of cement, and water/cement ratio dictates the quality of concrete such as strength and durability. High strength concretes need more cement than normal strength concrete to enhance workability, the rate of the heat of hydration, strength, durability, and volume stability of hardened concrete [82]. Beside, durable concrete depends on permeability, which is influenced by porosity and pore size distribution. Porous concrete is permeable to harmful influences such as chloride and it is prone to carbonation and efflorescence. Hydration products make the concrete dense by filling the pores between aggregates interface. High cement content has a negative impact to the concrete such as high heat of hydration, shrinkage, and cracking. In addition, cement component does not promise well with the environment due to the high energy consumption and CO<sub>2</sub> emission involved during its production [105]. Therefore, the need to reduce cement content in concrete by use of supplementary cementitious materials (SCMs).

SCMs are used to improve properties of fresh and hardened concrete and reduce cement content [1][103]. Specifically, the SCMs improve workability and cohesion, and reduce segregation, and bleeding of concrete, increase compressive and flexural strengths, increase

resistance to chemical attack, reduce permeability, reduce effects of alkali-silica reaction (ASR), reduce shrinkage due to particle packing, produce denser concrete, reduce potential for efflorescence, and increases accessibility of cement [106][107]. Impermeable concrete is resistant to penetration of harmful ingredients such as chloride ions and CO<sub>2</sub>.

Pozzolanic reactions of SCMs reduce passivation of concrete by utilizing the calcium hydroxide (CH). On the other hand, produces calcium silicate and calcium aluminosilicate hydrates, which give additional strength to the cement and concrete. Although the above advantages are vital, high volume replacement result into low strength forcing researchers into suitable optimum that balances replacement and performance. Natural materials like scoria and pumice have pozzolanic properties yet they are not utilized as SCMs. Scoria and pumice are sustainable eco-friendly materials that can reduce extraction of ordinary materials used to produce Portland cement, energy consumption, CO<sub>2</sub> emission, and increase accessibility of cement. In Tanzania, there are huge deposits of scoria in Kilimanjaro and Arusha regions and vast deposits of pumice in Mbeya and Iringa regions. Moreover, information indicated deposits of scoria and pumice of approximately one hundred billion tons each are accessible in the country [58].

#### **4.1.1 Classes of Concrete**

Concrete is classified with reference to the type of materials used, strength, performance, application and method of construction [82][1]. Classes of concrete includes lightweight concrete having a density ranging from 800 to 2000 kg/m<sup>3</sup> [1][108]; High strength concretes with 28 days compressive strength greater than 40 MPa [109]; High performance concretes defined as the concrete that meets performance and uniformity that conventional concrete could not meet (such as strength and durability are mandatory) [79]; Self-consolidating concrete (SCC) that can flow through intricate geometrical configurations under its own weight without segregation; Special concrete (that contain non-routinely materials and not proportioned in

normal procedures); Normal weight concretes with density between 2200 - 2600 kg/m<sup>3</sup> and 28 days compressive strength  $\leq$  40 MPa, used for general concrete works [1]; High-density concrete (density  $>$  2600 kg/m<sup>3</sup> and 28 days strength  $\geq$  79 MPa) used in radiation shields [110]. In these classes, finished concrete products find its application with various aspects.

#### **4.1.2 Economical application of Scoria and Pumice**

Currently in Tanzania, scoria rocks are cut into dimension blocks and the remaining fragments are used as coarse aggregates for small concrete works and concrete blocks, as well as wearing course in gravel roads. No evidence of any identified economical use of pumice in Tanzania.

#### **4.2 Objectives,**

The objective of this section is to explore comprehensively the effects of replacing scoria or pumice at various levels on performance of cement concrete. Emphasis was given on workability, compression strength, modulus of rupture, shrinkage, expansion, permeability, as well as residual compression strength upon exposure to high temperature.

#### **4.3 Materials and Methods**

##### **4.3.1 Materials**

Materials used in this work were Portland limestone cement (PLC), scoria, pumice, fine aggregates and coarse aggregates. Portland limestone cement conforms to SS-EN 197-1 CEM II/A-L class 42.5 N [66]. Scoria sample composed of red colored fragments was collected from Uchira Moshi-Kilimanjaro. Likewise, pumice sample composed of white colored particles was collected from Ikuti Mbeya. Fine aggregate was river sand from Mpigi and coarse aggregate was crushed granites from Lugoba collected from roadside (local) dealers.

### 4.3.2 Methods and laboratory experiments

S-N and P-N samples were milled using disc mill model 4A100L6T1 SN 535277 at a rate of 2 kg/h and sieved through 75  $\mu$  conforming to BS 410 [93] and analyzed to determine chemical and physical properties. The PSD profiles are shown in **Figure 4.1**. The chemical and physical properties of PLC, scoria (labelled S-N) and pumice (labelled P-N) are shown in **Table 4.1**. The chemical composition of S-N and P-N translate these materials as good pozzolan. Indeed, the specific gravities of P-N are significantly lower than that of Portland cement (SG = 3.15). This is significant when replacing Portland cement with equal weight of pumice the volume of non-hydraulic powder will be increased as such it may exceed the amount necessary for pozzolanic reaction and filler thus resulting in adverse effects. The physical characteristics of fine and coarse aggregates are shown **Table 4.2**. The fine and coarse aggregates were graded and blended to conform to the specification of the PD 6682-1 and BS 12620 [111][112].

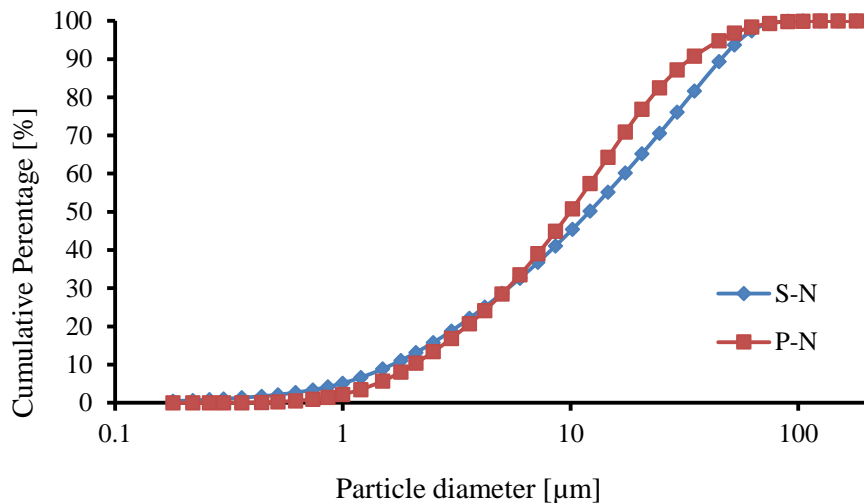


**Figure 4.1:** Particle size distribution of scoria and pumice powder

**Table 4.1:** Chemical and Physical properties of natural scoria (S-N) and pumice (P-N)

Material	SiO <sub>2</sub>	Fe <sub>2</sub> O <sub>3</sub>	Al <sub>2</sub> O <sub>3</sub>	CaO	K <sub>2</sub> O	Na <sub>2</sub> O	MgO	TiO <sub>2</sub>	L.o.I	Blain Fineness	Density
	[%]	[%]	[%]	[%]	[%]	[%]	[%]	[%]	[%]	[m <sup>2</sup> /kg]	[kg/m <sup>3</sup> ]
S-N	40.00	13.90	13.00	9.60	1.22	2.13	4.62	3.08	10.76	575	2930
P-N	55.40	4.64	16.40	1.70	5.46	5.33	0.62	0.68	8.78	506	2390
PLC	17.3	2.7	5.5	60.4		0.22*	0.5	-	11.9	465	3030

$$*Na_2O_{eq} = Na_2O + 0.685K_2O$$

**Table 4.2:** Physical properties of aggregates

Property	Coarse aggregate	Fine aggregate
Maximum size [mm]	19.0	4.75
Bulk density [kg/m <sup>3</sup> ]	1465	1483
Specific gravity	2.7	2.5
Absorption [%]	0	1.3
Fineness Modulus	6.6	2.2

### 4.3.3 Aggregate grading and blending

Fine and coarse aggregate were graded and blended to determine the suitable proportions to achieve the desired properties of fresh and hardened concrete [111], [112]. The fine and coarse aggregates were combined according to BS EN 12620 [111]. The combined fine and coarse aggregates gave the proportion of 33 % to 67 % fine to coarse aggregates and combined fineness modulus (FM) 5.1. Maximum size of coarse aggregate was 19 mm. The combined specific gravity (SG) was 2.6.



#### 4.3.4 Concrete Mix Design

Cement and SCM (S-N or P-N) were combined in the ratio of 90/10, 80/20, 70/30, and 60/40 cement/SCM powder. The concrete mixes were designed and produced according to BS EN 206-1 [113], BS EN 12390-2 [114] and BRE [115]. Target mean strength ( $f_m$ ) was determined basing on the characteristic strength ( $f_{cu}$ ), standard deviation ( $S_n$ ) and confidence limit factor ( $\lambda$ ) using Neville and BRE procedures [1][115]. Reference characteristic strength of 30 MPa was adopted and  $S_n = 5$  MPa for a number of samples less than 20, and  $\lambda = 1.64$ . With reference to BRE [115], the target mean strength of 38.2 MPa is acceptable for the cement class 42.5. Nine different concrete mixes were designed and produced with water cementitious ratio of 0.45 [115]. The mixes consisted of one control mix proportion with zero cement replacement and eight test mix proportions with cement replaced by 10, 20, 30, and 40% of S-N or P-N respectively, **Table 4.3**. The concrete mix proportions were designed to have free water content 190 kg/m<sup>3</sup> for FM 5.1, the medium slump of 30 to 60 mm and air content 2.5%, BS EN 12350-2 [93]. Concretes production, casting and testing of fresh and hardened concrete was carried out in accordance to Neville [1], BS EN 12350-6-7 [116][117], BS EN 12390-2 [114], BS 1881-116[118], BS EN 206 [119] and CSI [120]. Prior to casting, concrete mortar was extracted from each fresh concrete mix by sieving through 5.0 mm sieve for mortar flow testing. Then concrete beams 100×100×500 mm and cubes 100×100×100 mm were cast from each mix, for determination of flexural modulus, compression strength, fire resistance and permeability. Alongside, prisms of 100×100×300 mm and mortar bars 25×25×285 mm were cast for shrinkage and alkali silica reaction (accelerated mortar bar test (AMBT)) tests. Compaction, curing and testing equipment used conformed to BS EN 12390-2 [114] and BS 1881-116 [118].

**Table 4.3:** Mix proportions (kg/m<sup>3</sup>) of an unblended and blended cement concrete.

Material description	Control	Scoria blended cement				Pumice blended cement			
	M0	S-N 10	S-N 20	S-N 30	S-N 40	P-N 10	P-N 20	P-N 30	P-N 40
Cement	427	384	341	299	256	384	341	299	256
Fine aggregate	591	591	591	591	591	591	591	591	591
Coarse aggregate	1200	1200	1200	1200	1200	1200	1200	1200	1200
S-N/P-N	0.0	43	86	128	171	31	62	91	122
Water	205	205	205	205	205	205	205	205	205
Fresh concrete density	2423	2423	2423	2423	2423	2411	2399	2386	2374
Water-cement ratio	0.45	0.45	0.45	0.45	0.45	0.45	0.45	0.45	0.45
Cement replaced [%]	0	10	20	30	40	10	20	30	40

## 4.4 Results and Discussion

### 4.4.1 Properties of fresh concretes

**Figure 4.2(a)** shows the relationship between a slump and the percent of cement replaced. The slump determines the homogeneity and easy with which concrete can be manipulated to the final finishing. **Figure 4.2(a)** indicated loss of slump with increasing replacement levels. Scoria show less loss of slump than its counterpart pumice. Observation indicated fast significant loss of slump at 10 % cement replacement level for both materials (from 75 mm to 57 mm for S-N) and (from 75 to 38 mm when cement was replaced by 10% S-N or P-N powder and continue with a small rate to 48 and 34 mm for P-N). At 20% replacement, the slump loss reached minima values of 48 and 34 mm for S-N and P-N, in that order. Remarkably it marginally

increased at 30% cement replacement level for both materials to a maximum of 50 and 36 mm for S-N and P-N respectively, and decreased at 40% cement replacement level although drastically for P-N. The apparent observed slump loss was attributed slightly to the hydration of cement and pozzolanic reactions but mostly to the dramatic fall for P-N was due to the high water absorption caused by the larger fraction of the porous P-N at 40% replacement level. Observation indicated that air content and flow decreased with cementitious content (**Table 4.4**). At 10% replacement, both S-N and P-N showed the same flow (21 cm), which was slightly lower than that of CTRL (23 cm). At 20% replacement level, the flow reduced to 19 and 18 cm for S-N and P-N, respectively, **Figure 4.2(b)**. When replacement level was increased to 30% the flow showed no change but remain constant at 19 cm for S-N while for P-N, it increased to 20 cm. At 40 % cement replacement level, the flow decreased to 18 cm for both S-N and P-N.

In blended cement heat of hydration of cement decreases and rate of water absorption increases with increase in replacement level. Hence, the general decrease in flow observed as amount of both S-N and P-N increases was due to reduction in lubrication and stiffening of mortar aroused from reduced heat of hydration and increased water absorption. The equilibrium between the heats of hydration of cement and water absorption and hence no change in flow was obtained at 30% replacement level for S-N. However, since P-N is less hydraulic and less reactive than S-N due to its low CaO content, **Table 3.1**, the heat of hydration evolved and the amount of water consumed during the pozzolanic reaction were relatively low compared to S-N. Conversely, the lubrication was higher and stiffness lower at 30% replacement level due to the presence of higher amount of water for lubrication and lower heat of hydration and thus the higher flow for P-N than S-N, **Figure 4.2(b)**. In addition, at 40% replacement level, the heat of hydration was low owing to limited pozzolanic reactions and the water absorption was high due to the presence of large proportion of porous materials. This, drastically reduced the

lubrication and increased the stiffness of the concrete thus reducing the flow for both S-N and P-N cement concrete.

Furthermore, air content in fresh concrete decreased with cement replacement level for both S-N and P-N. This was attributed to the increased packing density and elimination of pores by the pozzolanic reactions. On the other hand, there was no significant change in the density of the fresh concrete with cement replacement level for S-N, **Table 4.4**. This was because the densities of S-N and PLC are comparable, **Table 4.1**. Contrary to S-N, the density of fresh concrete with cement replaced by P-N decreased slightly from 2463 kg/m<sup>3</sup> at 0% replacement to 2420 kg/m<sup>3</sup> at 40% replacement level, **Table 4.4**, due to increasing proportions of P-N which is less dense than S-N and PLC, **Table 4.1**. Additionally, explains the incomplete compaction due to lack of lubrication of the particles resulted from absorption of water by the porous pumice particles which occur as replacement level increases. Furthermore, during concrete mix design, the density of fresh concrete is calculated from the total mass per cubic meter of the ingredients which depends on the mass of individual ingredient materials. However, the density of the actual fresh concrete depend on the degree of compaction in addition to the total mass per cubic meter of the measured ingredients and hence difference in densities presented in **Table 4.1, 4.3, and 4.4**.

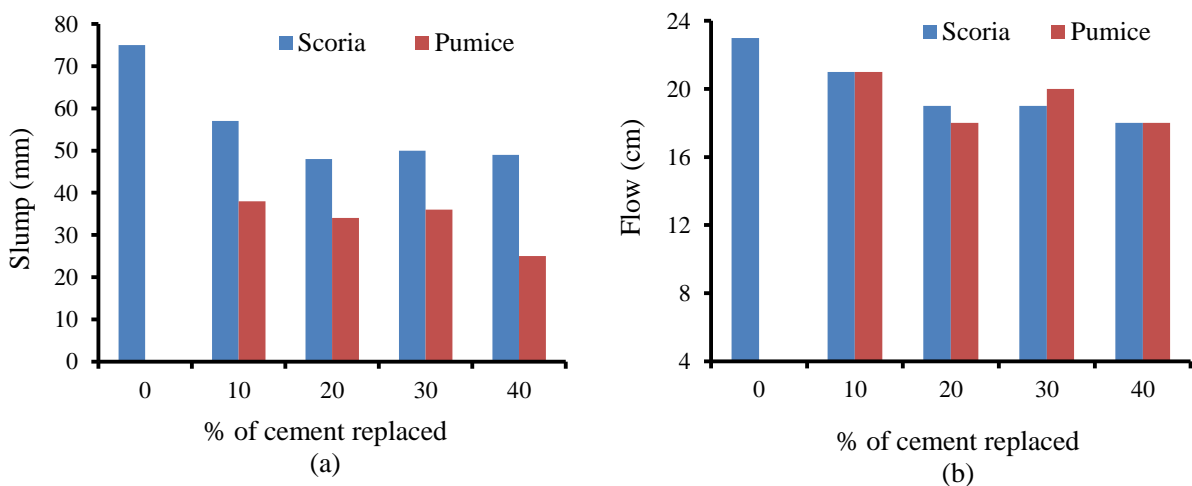


**Figure 4.2:** Slump versus (a) cement replacement (b) flow versus % replacement

**Table 4.4:** Flow, density and entrapped air test results

Cement replacement level	Scoria			Pumice		
	Air	Flow	Density	Air	Flow	Density
	content			content		
[%]	[%]	[%]	[kg/m <sup>3</sup> ]	[%]	[%]	[kg/m <sup>3</sup> ]
0	3.0	56.5	2463	3.0	56.5	2463
10	2.5	52.4	2465	1.2	52.4	2460
20	1.0	47.4	2465	1.2	44.4	2451
30	1.1	47.4	2465	1.2	50.0	2434
40	1.0	44.4	2465	1.1	44.4	2420

#### 4.4.2 Properties of hardened concretes

##### 4.4.2.1 Expansion and Shrinkage

**Table 4.5** summarizes the results of 14 days accelerated mortar bar test (AMBT) for expansion and 28 days drying shrinkage tests. Unblended cement mortar showed higher expansion (0.02 mm) compared to 0.01 mm for S-N and P-N blended cement mortar at all replacement levels (10, 20, 30, and 40%) except for S-N at 40% replacement which showed 0.02 mm expansion similar to that of unblended cement mortar. It is worth noting that all the blended cement mortars showed expansion less than 0.01%. This partly suggests that the coarse and fine aggregates used are not reactive and partly that PLC, S-N and P-N contain very low amount of free MgO and CaO and thus low expansion upon their hydration. In addition, S-N and P-N can be regarded as effective mineral admixture in mitigating alkali-silica reactions. The chemical content of alkali, magnesium, and sulphate did not affect shrinkage or expansion as they were

within the acceptable limits, [72]. No significant influence of cement content, water content, and the water to binder ratio on the expansion was observed.

The shrinkage test results, **Table 4.5**, show that unblended cement concrete shrink to the same extent (0.01 mm) as the cement concrete blended at 30 and 40% for S-N and 10 and 40% for P-N. On the other hand, blending cement concrete at 10 and 20% for S-N and 20 and 30% for P-N afforded slightly higher shrinkage (0.02 mm). Most importantly, all the blended cement concretes showed shrinkage of less than 0.04% specified as the limit for good concretes/mortar [121][122]. Generally, the observed low shrinkage values for both S-N and P-N concretes are attributed to evolution of microstructures with improved pore size and pore size distribution caused by the consumption of the CH and water in the pores by S-N and P-N via pozzolanic reactions. The products of these pozzolanic reaction gets deposited in the pores originally occupied the CH and water thereby creating a relatively dense microstructure capable of resisting volume change.

With regards to shrinkage differences among the S-N and P-N specimens at different cement substitution levels, we suggest that these differences stem from chemical and autogenous shrinkage. Chemical shrinkage arises from the fact that water is one of the reactants in cement hydration. Therefore, as water transformed from free water to being part of the hydration products (C-S-H and C-A,F-H), the volume of the concrete decreased [123]. Autogenous shrinkage on the other hand is caused by the self-desiccation occurring at the additional capillary pores formed by cement hydration. The self-desiccation caused by the consumption of water in the pores as cement hydration process progresses leads to decrease of pressure in the capillary pores. In response to the pressure drop, the volume of the concrete matrix decreases resulting to shrinkage [123].

At 10 and 20% replacement levels for S-N, there was higher consumption of pore water and higher self-desiccation driven by heightened pozzolanic reactions than at 30 and 40% and

hence higher shrinkage. Pozzolanic reactions in all S-N mortar samples (**Table 4.5**) were driven by CH generated from hydration of quicklime (CaO) in S-N (**Table 4.1**) and the CH from cement hydration. However, at 30 and 40% substitution levels, the amount of Fe<sub>2</sub>O<sub>3</sub> (**Table 4.1**) might have increased high enough to hamper the dissolution of reactive silica in S-N and hence the pozzolanic reaction. As a result, low amount of pore water was consumed and low self-desiccation occurred leading to their low shrinkage. Fe<sub>2</sub>O<sub>3</sub> has been linked to slow dissolution of reactive silica in SCMs including coal fly ash [124].

P-N 10 showed lower shrinkage than S-N 10 probably due to the lower content of CaO in P-N compared to S-N. The heat of hydration of CaO and the CH generated thereof is thought to have enhanced the pozzolanic reaction of less reactive fraction of silica in S-N. Consequently, both the chemical and autogenous shrinkage was higher in S-N 10 than P-N 10. As the substitution level for P-N was increase to 20 and 30%, the fraction of reactive silica also increased leading to increased pozzolanic cement hydration and thus higher shrinkage. At 40 % substitution level, the amount of CH was not enough for significant pozzolanic driven cement hydration and thus lower shrinkage than 20 and 30%. Moreover, the shrinkage results in **Table 4.5** show the tremendous volume stability of concretes made from S-N and P-N blended cements and therefore the effectiveness and potential of S-N and P-N in preventing cracking in mortar and concrete. In regards to concrete durability from the sulfate attack standpoint, the ability of S-N and P-N to prevent shrinkage induced cracking means durable concrete since the entry points for sulfate ions into concrete are open pore and cracks.

**Table 4.5:** 14 days accelerated mortar bar test (AMBT) for expansion and 28 days shrinkage tests results.

Sample ID	Cement replacement %	14 days AMBT (Expansion) [mm]	28 days Shrinkage [mm]
CTRL	0	0.02	0.01
S-N 10	10	0.01	0.02
S-N 20	20	0.01	0.02
S-N 30	30	0.01	0.01
S-N 40	40	0.02	0.01
P-N 10	10	0.01	0.01
P-N 20	20	0.01	0.02
P-N 30	30	0.01	0.02
P-N 40	40	0.01	0.01

#### 4.4.2.2 Modulus of rupture

Moduli of rupture for concrete made of cement blended with scoria and pumice powder are shown in **Figure 4.3**. Generally, modulus of rupture for S-N blended cement concrete decreased with increase in cement replacement in all the three categories of curing period (3, 7, 28 days). However, it increased with curing period from 3.8 MPa at 3 days to 6.3 MPa at 28 days for CTRL and from 2.8 MPa at 3 days to 6.0 MPa at 28 days for S-N at 10% replacement level, **Figure 4.3(a)**. Over 3 days curing period, S-N showed a significant drop in modulus of rupture, from 3.8 MPa at 0% replacement to 2.8 MPa at 10 and 20% replacement level, **Figure 4.3(a)**. Above 20% replacement level, it continued to drop slowly to 2.1 MPa at 40%



replacement level. Unlike 3 days curing period, 10% replacement afforded little or no drop in modulus of rupture over 7 days curing period for S-N, **Figure 4.3(a)**. It is suggested that, over the 7 days curing period, CH generated from hydration of quicklime (CaO) in S-N (**Table 4.1**) and the CH from cement hydration was present at optimum concentration for adequate pozzolanic reactions to occur. This generated more hydration products which further reduced porosity while at the same time producing additional strength to the concrete and hence no drop in modulus of rupture.

Beyond 10% replacement level at 7 days curing period, modulus of rupture dropped unceasingly to 3.2 MPa at 40% replacement level. In contrast to 3 and 7 days curing periods, 28 days curing period afforded a monotonic decrease in modulus of rupture from 6.3 MPa at 0% replacement to 4.1 MPa at 40% replacement level. Above 10% substitution level, CH is suggested to be the limiting reactant, therefore, appreciable amount of unreacted S-N remained in the concrete. The presence of unreacted non-hydraulic materials (S-N) increased the interfacial distances between the aggregate particles and the cement hydration products leading to the formation of weak sites where cracks could initiate easily. This explain the observed decline in the moduli of rupture beyond 10% replacement (**Figure 4.3(a)**) for all the three curing periods (3, 7, and 28 days). Moreover, since S-N contains high amount of  $\text{Fe}_2\text{O}_3$ , **Table 4.1** which obviously increased as the level of substitution increased, the dissolution of reactive silica in S-N and thus pozzolanic reactions were progressively hindered. The concrete strength therefore reduced with substitution and so does the modulus of rupture.  $\text{Fe}_2\text{O}_3$  has been linked to slow dissolution of reactive silica in SCMs including coal fly ash [124].

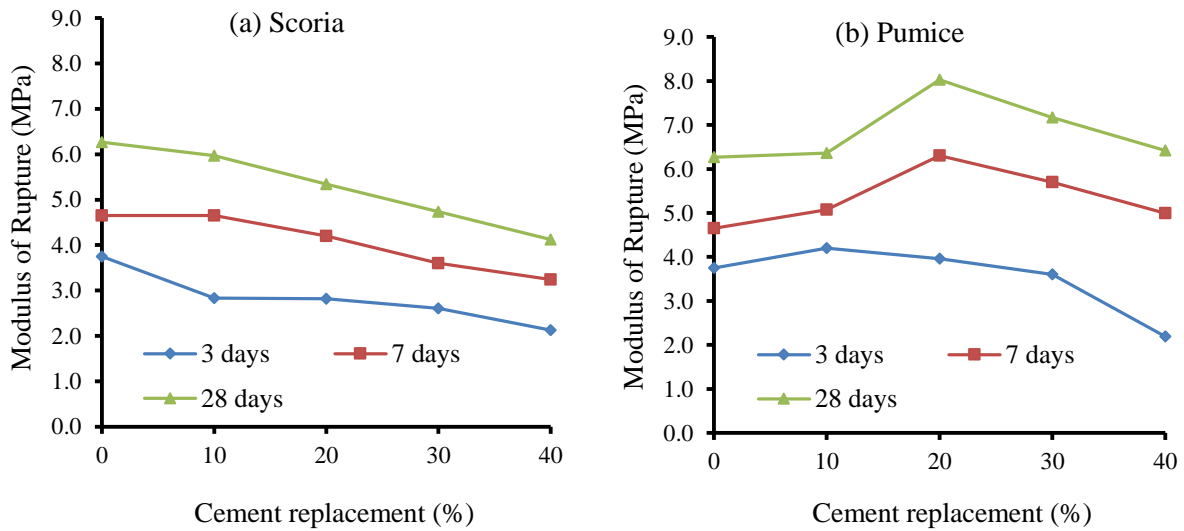


**Figure 4.3:** Modulus of rupture versus percent of cement replaced

Unlike S-N, the moduli of rupture of P-N-blended cement concrete at 10% replacement level were higher than that of CTRL, over all the curing periods (3, 7 and 28 days). At 20% replacement level, the modulus of rupture increased dramatically from 4.0 MPa at 3 day to 8.0 MPa at 28 days, **Figure 4.3(b)**. The dramatic increase in moduli of rupture at 20% cement replacement level over 7 and 28 day was attributed to the increased strength due to high amounts of C-S-H and C-A-H in the microstructure resulting from good progression of pozzolanic reactions favored by the low amount of  $\text{Fe}_2\text{O}_3$ . The microstructure obtained at this replacement level could absorb more stress than at the other replacement levels. On the other hand, the drop in modulus of rupture beyond 20% replacement level for all curing regimes (3, 7, and 28 days) was due to increasing existence of non-hydraulic materials (P-N) in the microstructure. The non-hydraulic materials decreased binder volume ratio and increased interfacial distances between the aggregate particles and the cement hydration products thereby decreasing the strength.

#### 4.4.2.3 Compressive strength

**Figure 4.4** shows compressive strength growth versus curing period. Compressive strength for both S-N and P-N blended cement concrete at all the four replacement levels (10, 20, 30, and 40%) developed rapidly from 3 to 7 days and continued to develop although gradually until the 28 curing days, **Figure 4.4**. The development of compressive strength for P-N blended concretes was more rapid between the 3<sup>rd</sup> and the 7<sup>th</sup> day than that of its S-N counterparts. This is illustrated by the steeper/high gradient curves for P-N within 3 to 7 days period, **Figure 4.4(b)**.

The more rapid growth of compressive strength for P-N blended concretes between 3<sup>rd</sup> and 7<sup>th</sup> days compared S-N was due to the fact that the heat of hydration was higher in P-N concrete than in its S-N counterpart. This was probably because of the higher contents of SiO<sub>2</sub> and Al<sub>2</sub>O<sub>3</sub> and lower amount of Fe<sub>2</sub>O<sub>3</sub> in P-N than in S-N **Table 4.1** all of which favored pozzolanic reactions. Furthermore, P-N has a high amounts of K<sub>2</sub>O and Na<sub>2</sub>O, see **Table 4.1** which influence the hydration of cement phases differently at different hydration stages thereby affecting the strength gain. K<sub>2</sub>O has been shown to promote rapid early strength and slow later strength [1][22]. On the other hand, the slow compressive strength growth after the 7<sup>th</sup> day was due to reduced heat evolution from hydration.

Interestingly, the control (CTRL) and the concrete blended with S-N and P-N at 10%, replacement level attained comparable compressive strengths of 43.5, 44.2, and 43.5 MPa, respectively, after 28 days curing period, **Figure 4.4**. Moreover, S-N and P-N blended cement at all the replacement levels (10, 20, 30, and 40%) achieved compressive strengths higher than the characteristic strength of 35 MPa after 28 days, **Figure 4.5**. This implies the great potential both S-N and P-N materials have in their utility as SCMs. Generally, for both S-N and P-N, the compressive strength decreased with the increase in percent of cement replaced. This was linked to the amount of unreacted S-N or P-N in the microstructure which increased with the

increase in substitution level. As a result, discontinuous bond and thus the interfacial distances between the aggregate particles and the hydrated cement increased within the microstructure leading to the decrease in strength.

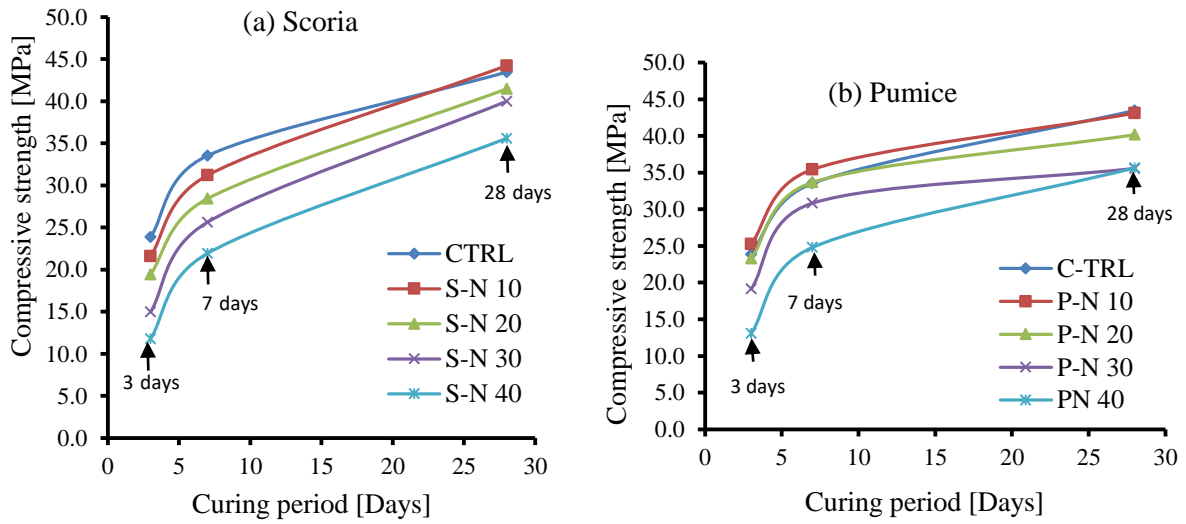


**Figure 4.4:** Compressive strength growth versus curing period

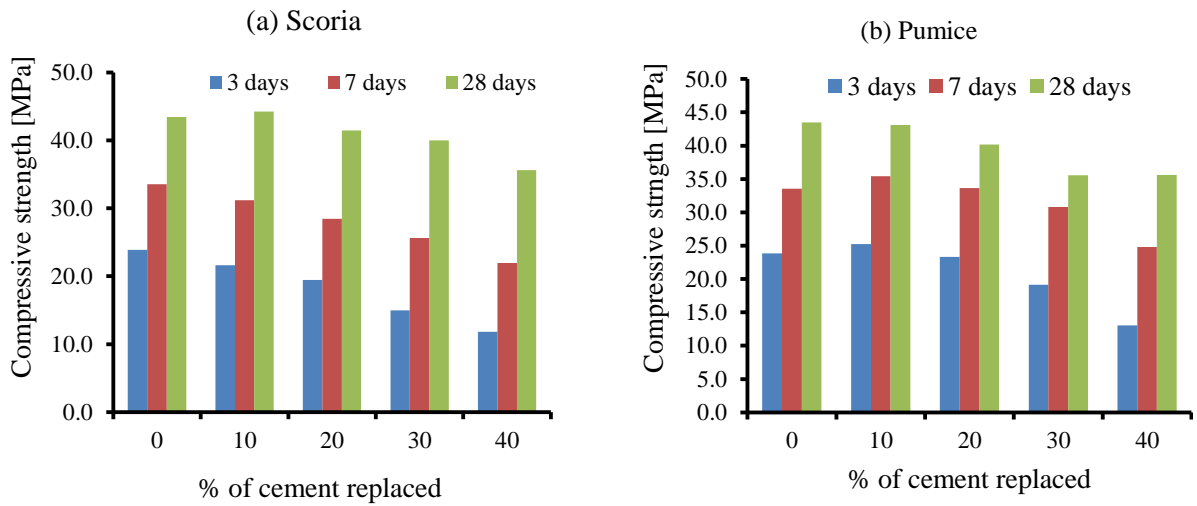


**Figure 4.5:** Compressive strength versus percent cement replacement

#### 4.4.2.4 Modulus of rupture and splitting tensile strength versus 28 days compressive strength

The influence of compressive strength on the modulus of rupture and splitting tensile strength is shown in **Figure 4.6**. Modulus of rupture of S-N blended cement concrete increased from 4.1 to 6.3 MPa when the 28 days compressive strength increased from 35.6 to 44.2 MPa, **Figure 4.6(a)**. The correlation coefficient ( $R^2$ ) of 0.9106 for S-N is indicative of a good relationship between the modulus of rupture and compressive strength for S-N blended concretes. The correlation also suggests that compressive strength, modulus of rupture and stiffness increased with decreasing percent replacement. The behavior was attributed to the binder volume ratio which increased with decreasing proportion of non-hydraulic materials.

Likewise, modulus of rupture of pumice blended cement concretes increased from 6.4 to 8.3 MPa when the 28 days compressive strength increased from 35.6 to 43.1 MPa, **Figure 4.6(a)**. This gave correlation coefficient ( $R^2$ ) of 0.8229 that points to the good relationship between modulus of rupture and compressive strength for P-N. The high modulus of rupture for P-N concrete at each cement replacement level compared to S-N, **Figure 4.6(a)**, is indicative of superior ability to endure more sustained stresses such as those caused by tremors and earthquakes and also the ability to tolerate impact related stress. Therefore blending of cement with P-N could be a breakthrough in solving the problem of brittleness in concrete materials.

The splitting tensile strength of both the S-N and P-N blended cement concretes increased with compressive strength, however, the increase was more heightened for S-N concretes than for P-N concrete, **Figure 4.6(b)**. The correlation coefficients ( $R^2$ ) of 0.9822 and 0.8073 for S-N and P-N, respectively, suggest a good relation between the splitting tensile strength and compressive strength. This was due to pozzolanic reactions proceeding effectively

and to a large extent and good parking effect, of both the aggregates and C-S-H gel, which translated to high density concrete and thus increased strength.

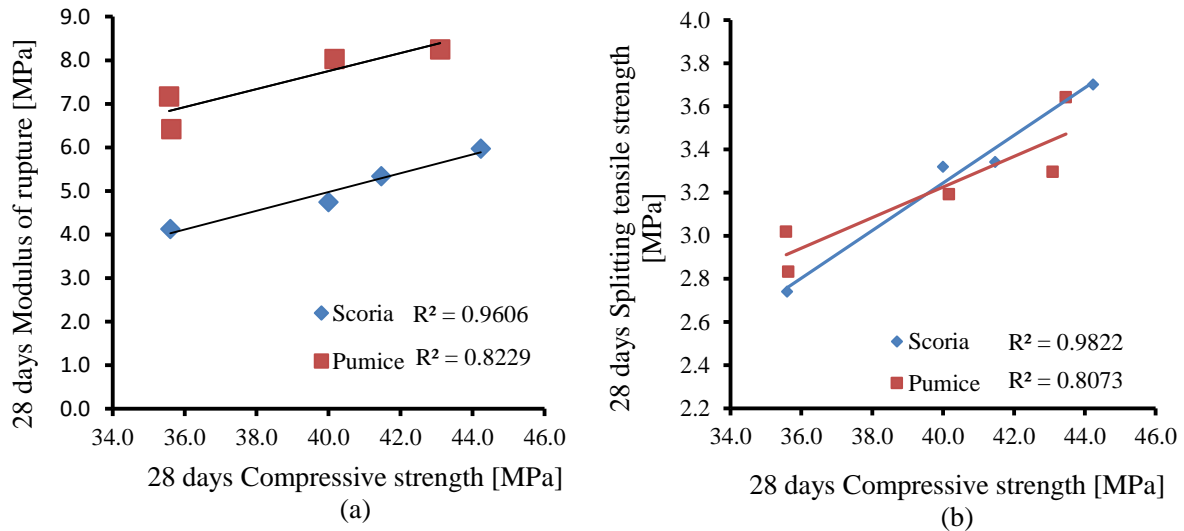


**Figure 4.6:** 28 days (a) modulus of rupture (b) splitting tensile strength versus 28 days compressive strength for scoria and pumice blended cement concretes

#### 4.4.2.5 Microstructure of the PLC and S-N/P-N blended cement concretes

The results for the microstructure of the PLC, S-N, and P-N concrete studied by fluorescence microscope (Optika B-350) are shown by the micrographs in **Figure 4.7**. The micrographs show that the concrete specimens, S-N 10, 20, and 30 were denser and less porous than CTRL, P-N 10, and 20 and hence their high compressive strengths (**Figure 4.5**) and low permeability, **Figure 4.8**. The denser and less porous microstructure of S-N 10, 20, and 30 is not related to the density of S-N materials used but to the hydration of cement and the pozzolanic reactions between CH and S-N that produced C-S-H and C-A-H gel. This gel fills the voids within the concrete matrix thereby creating a dense microstructure. Additionally, S-N contains appreciable amount of CaO, **Table 4.1**, which upon hydration generates heat and CH both of which further promotes pozzolanic reactions and hence densification of the microstructure. Both the S-N 40 and P-N 40 show highly porous microstructure, **Figure 4.7**, that is in harmony

with their high permeability (**Figure 4.8**) compared to the PLC and other concrete samples of lower cement substitution. At high substitution levels, in this case 40%, the excess non-hydraulic S-N and P-N materials prevented the formation of continuous C-S-H gel bond. Consequently, interfacial gaps were created between hydrated cement, aggregate particles, and unreacted S-N/P-N particles and hence the porous microstructure.

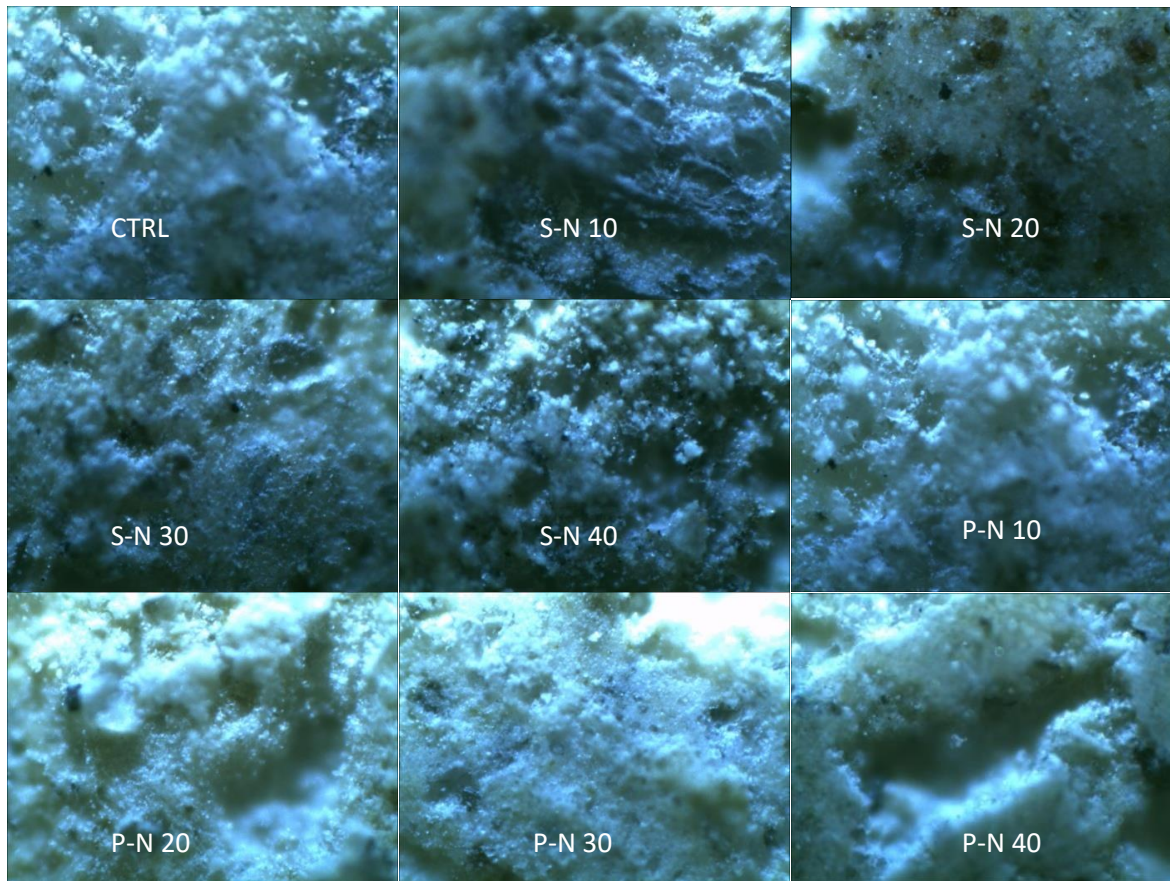


**Figure 4.7:** Fluorescence microscope images of Portland cement, scoria and pumice blended

#### 4.4.2.6 Permeability of hardened concrete

The permeability results for PLC, S-N, and P-N blended concretes are shown in **Figure 4.8**. The results reveal that the coefficients of permeability ( $K$ ) of  $5.2526E-08$ ,  $5.20833E-08$ , and  $4.9741E-08$  m/s for S-N blended concretes at 10, 20, and 30% replacement levels, respectively, were very close to that of Portland cement concrete,  $5.35714E-08$  m/s. However, at 40% cement replacement, the coefficient of permeability was very high,  $7.71605E-08$  m/s, **Figure**

**4.8.** This was due to increased porosity of the concrete caused by the low amount of the hydration products (C-S-H and C-A-H) caused by limited pozzolanic reactions and high amount of non-hydraulic materials in the microstructure.

Contrary, the coefficients of permeability for P-N blended concretes were significantly higher than that of CTRL except for P-N 30. Similar to S-N, blending with P-N at 40% replacement level afforded a very high coefficients of permeability, **Figure 4.8**. At 10% replacement level, the amount of P-N powder could not consume all the available CH generated by cement hydration thus limited pozzolanic reactions occurred. These resulted to inadequate filling of the pores in the microstructure by the pozzolanic reaction products (C-S-H and C-A-H) and hence significant permeability. The decrease in permeability upon increasing the replacement levels to 20 and 30% was attributed to the significant pozzolanic reactions by the sufficient consumption of the CH by reactive silica and alumina in P-N. Consequently, the reaction products were deposited into the pores thereby substantially reducing the porosity of the concrete mortar matrix and hence the permeability. At 40% replacement level, the amount of CH was exhausted, leaving a large portion of the non-hydraulic, unreacted P-N materials within the concrete matrix. This translated to discontinuous bonds between hydrated cement and aggregates and thus resulting to formation of pores. Coupling this to the inter-particle spaces between the particles of the unreacted P-N leads to high porosity and permeability. The concretes samples with low coefficient of permeability (S-N 10 to 30 and P-N 30) are expected to be less prone to chemical attack and carbonation. This in turn leads to better protection of steels reinforcements against corrosion, and hence improved durability of the concrete.



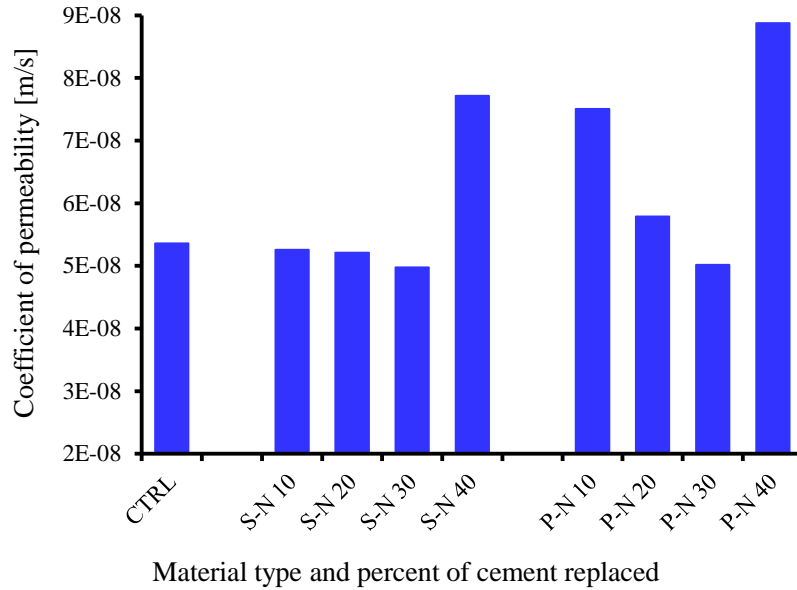


**Figure 4.8:** Permeability versus materials and percent cement replacement

#### 4.4.2.7 Effect of temperature on compressive strength of hardened concrete

Compressive strength loss upon subsection of 100 mm hardened concrete cubes, cured for 28 days, to high temperature of 600 °C for 2 h followed by cooling to room temperature is displayed in **Table 4.6**. Although, all the concrete samples lost compressive strength upon exposure to high temperature, the residual compressive strength was more than 50% except for S-N 40 which attained 45.5%. It worth mentioning that the residual strength for S-N 10 and P-N 10 (59.8% and 57.8, respectively) was higher than that of CTRL, **Table 4.6** The loss of compressive strength at 600 °C was attributed to the loss of gel pore water and thus the dehydration of the C-S-H gel at high temperatures. Once the C-S-H gel got dehydrated, its volume decreased leading to the debonding of the hydrated cement and the aggregates and hence the loss of compressive strength. In addition, at 600 °C the vapor pressure within the capillaries in the microstructure might exceeded the tensile strength leading to further weakening of the interfacial bond between aggregates and cement paste thereby creating regions where microcracks could start and propagate within the microstructure. The cracks

severity decreases with replacement level, the indication of increasing thermal resistance of the blended cement concrete with increasing proportions of S-N and P-N.

Noticeably, P-N blended cement concrete showed superior performance with regard to high temperature resistance compared to S-N blended cement concrete generally. This is exemplified by their higher residual compressive strength, particularly the 69.1 and 63.2% at high cement replacement levels of 30 and 40%, correspondingly. At these two replacement levels, S-N showed low residual compressive strength of 51.3 and 45.5% in that order. The superior performance of the P-N blended concretes could be due to the low thermal conductivity stemming from the excellent insulating characteristics of the porous P-N materials compared to the less porous S-N materials. High residual strengths resulted from internal autoclaving formed in the cement paste and pozzolanic reactions that occurred as temperature increases. During heating the chemical compositions within the microstructure changed through dehydration of cement, which starts at 400 °C and continue as temperature increases to 600 °C which weaken the interfacial bond between aggregate and cement paste. Strong heating destroyed the bond in the aggregate-paste interface, instigate sparkling, and micro cracks within the microstructure.

**Table 4.6:** 28 days ultimate and residual compressive strength after 600 °C temperature exposure.

<b>Specimen ID</b>	<b>CTRL</b>	<b>S-N 10</b>	<b>S-N 20</b>	<b>S-N 30</b>	<b>S-N 40</b>	<b>P-N 10</b>	<b>P-N 20</b>	<b>P-N 30</b>	<b>P-N 40</b>
28 days Ultimate Compressive Strength (MPa)	43.5	44.2	41.5	40	35.6	43.1	40.2	35.6	35.6
Residual Strength(MPa)	22.9	26.2	21.8	20.5	16.2	24.9	24.5	24.6	22.5
% Residual Compressive Strength	52.6	59.3	52.5	51.3	45.5	57.8	60.9	69.1	63.2

## 4.5 Conclusions

Investigation on the influence of S-N and P-N pozzolanic binders on the key performance indicators of Portland cement concrete was successfully carried out. It was found that Portland cement could be blended with S-N and P-N binders at 10% substitution level without compromising the compressive strength, modulus of rupture, flow, slump, permeability, thermal and volume stability and hence durability of the concrete. The optimum replacement level was therefore found to be 10% for both S-N and P-N. Contrary to the expectations, S-N and P-N blended cement concrete at 10% substitution level showed slightly superior residual compressive strength after 600 °C temperature exposure compared to unblended PLC concrete. This implies that S-N and P-N could be used to blend cement in the construction of structures in areas that are more prone to fire accidents. Moreover, the results show that S-N and P-N have greater potential in reducing the amount of cement used in construction, the energy consumed during clinkering process, and the CO<sub>2</sub> emitted by the cement industries. Therefore, these materials could be used for climate change mitigation.

Although the replacement of S-N and P-N at level higher than 10% negatively affected more than once concrete performance attributes, the slump, flow, and air content of fresh concrete were all within the acceptable ranges. Also the fire resistance of P-N blended cement concrete was even superior at 20 and 30% replacement level. On the other hand, no significant change in the density of fresh S-N and P-N blended concrete was observed despite the fact that air content decreased with the increase in the substitution level. The density of all the concrete sample examined was within the range for normal weight concrete indicating that even at high substitution level of 40 %, the density of the ordinary concrete is not adversely affected.

The shrinkage and expansion of 0.01% observed at all the substitution levels was within the acceptable limits of the standards. The coefficients of permeability decreased with the increase in the amount of S-N, reaching 4.9741 m/s at 30% replacement level compared to

5.35714E-08 m/s for the control (unblended PLC concrete). S-N could therefore be used to make dense (less porous) concrete with reduced susceptibility to chemical attack, carbonation, improved protection of steel against corrosion, and hence durability. Contrary to the expectation, P-N delivered inferior coefficients of permeability compared to the PLC concrete except P-N 30 concrete.

The correlation between modulus of rupture and compressive strength at all the substitution levels was much better for S-N concrete ( $R^2 = 0.9606$ ) than P-N ( $R^2 = 0.8229$ ). However, P-N concrete showed substantially higher modulus of rupture versus compressive strength at each cement replacement level compared to S-N. This is indicative of the superior ability of the P-N concrete to endure more sustained stress such as those caused by tremors and earthquakes and also the ability to tolerate impact-related stress. Therefore blending cement with P-N could be a breakthrough in solving the problem of brittleness in concrete materials. The reason for the dramatic increase in modulus of rupture over 7 and 28 days curing periods and at 20% substitution level for P-N was not fully understood. Therefore, there is need for further studies to unravel why this increase occurred for P-N and not for S-N materials.

**Chapter 5 EFFECTS OF CEMENT BLENDED WITH SCORIA AND RHA OR  
PUMICE AND RHA TO THE PROPERTIES OF MORTAR AND CONCRETE:  
OPTIMIZATION OF THE BLENDING PROPORTIONS<sup>3</sup>**

**Abstract**

The strength activity index (SAI) of mortar and pastes containing natural scoria (S-N) and natural pumice (P-N) mixed with rice husk ash (RHA) have been investigated and compared. The rice husk ash was calcined by heating at 600 °C and soaking for one hour in order to increase the pozzolanic reactivity. The investigation involved a combination of the three materials, the cement which has binding properties and the pozzolans S-N and RHA or P-N and RHA which have no binding properties of their own. In this investigation, the cement was kept constant at 70% and the pozzolans were varied from 0 to 30% alternatively. The pozzolan were investigated to establish their influence on strength activity index when mixed with Portland cement. Two blended mixes were produced by mixing Portland cement, S-N and RHA in the first mix and Portland cement, P-N and RHA in the second mix. The third mix was the control made of plain Portland cement. The properties investigated for such cement blended with diverse pozzolanic materials were the setting times, soundness, flow, compressive strength and SAI. The water required for standard consistency paste reduced from 27.4% for plain cement to 27.2% when 30% of cement was replaced by S-N and then increased constantly 38.6% at cement replacement of 10/20% S-N/RHA. Further increase of RHA slightly increased the water demand at slower rate to 41.4 at cement replacement of 0/30% S-N/RHA. Contrary to S-N, water required for standard consistency paste increased from 27.4% for plain cement to 36 % when 30 % of cement was replaced by P-N and then increased slowly 42.2% at cement

---

<sup>3</sup> This Chapter is based on unpublished Paper

replacement of 10/20% P-N/RHA. No more significant change was observed as the percent of RHA increased to 30%.

Initial setting time (IST) of 99 and 188 minutes was attained when Portland cement was replaced by 30% of both S-N and P-N. The maximum IST of 151 was reached at 15/15% for S-N/RHA blended cement. The final setting time (FST) reduced from 184 minutes for plain cement to 167 minutes at 30% S-N contrary to P-N which increased to a maximum of 222 minutes at 20/10% P-N/RHA. In both cases the maximum FST was found at 20/10% S-N/RHA and P-N/RHA respectively. The flow reduced faster from 39 mm for plain cement to 24 to 14 mm when 30/0 and 25/5 % S-N/RHA respectively was added. Upon increasing percent of RHA up to 30 the flow decreased slowly to zero. Addition of 30% pumice reduced the flow from 39 mm for plain cement to 9 mm and continue to fall slowly to zero as percent of RHA was increasing. The maximum 28 days compressive strength of S-N/RHA blended cement were 46.6 and 46.3 MPa achieved at 30/0 and 0/30% S-N/RHA replacement level respectively. Contrary, the maximum 28 days compressive strength achieved for P-N/RHA blended cement was 53.8 MPa attained at 10/20% P-N/RHA replacement level. The 28 days SAI reflected the compressive strength development pattern. In addition, cumulative SAI of P-N/RHA was quiet high compared to that of S-N/RHA. Generally, no need of mixing S-N and RHA in ternary materials, rather use it separately with Portland cement in binary materials. It is advantageous to use P-N/RHA 10/20% optimum with Portland cement in ternary materials.

Keywords: Ternary material

## 5.1 Introduction

Cement is intensively used all over the world as binding materials for mortar and concrete production. However, during cement manufacturing high energy is needed and gives intensive emission during its production. For example, in producing a ton of cement it requires 4.7 million BTU ( $\approx 5$  MJ) of energy, equivalent to about 200 kilogram of coal and generates nearly a ton of CO<sub>2</sub>. According to World Bank Report it is estimated that every tone of cement produced consume around 66 kWh [125]. Given its high emission and critical importance to the society, cement production is an obvious place to look to reduce greenhouse gas emissions. Researcher have discovered several materials that can be used as partial replacement of Portland cement; but there is still a need to establish the optimum proportion of these materials as they differ from place to place due to chemical composition and geological formation.

Ternary binding material is achieved by mixing of two or more non-cementing materials with hydraulic cement to achieve beneficial advantage of both materials. These materials have improved properties over Portland cement, reduced CO<sub>2</sub> emission, reduced energy and depletion of ordinary cementing materials, resistance to freezing and thawing, chemicals resistance, resistance to alkali silica reaction (ASR) and other aggressive media or environments. To achieve the optimum performance of the blended cement, the optimum proportions of the ternary materials is very essential and it depend on the chemical composition and fineness of the binder composition (S-N, P-N, RHA and Portland cement clinker). These can be achieved by investigating the behavior of mortar and concrete made by partial replacement of Portland cement with SCMs (such as S-N, P-N and RHA). In this instance, S-N and P-N were used in combination with RHA to replace part of cement. S-N and P-N has great potentials in construction when used as binder to replace partly the cement which is expensive and has adverse impact to the environment as from extraction of raw materials to the manufacturing stage. Owing to the new effort towards environmental sustainability, the



mitigation to reduce cement content of concrete mixtures has been a global topic to scientists and researchers. In this regard, the amount of Portland cement in concrete mixtures has been reduced with addition of supplementary cementing materials such as limestone powder, fly ash, silica fume, GGBFS, S-N, P-N and RHA, [126][127]. The compounds present in ordinary Portland cement, such as  $C_3S$  and  $C_2S$ , are known to react with water [2] to form approximately 70% C-S-H, 20% CH, 7% sulfoaluminate, and 3% secondary phases [3]. The 20% CH react with pozzolan to form cementing compounds resembling that of cement in the pozzolanic reactions as  $Ca(OH)_2 + H_4SiO_4 \rightarrow CaH_2SiO_4 \cdot 2 H_2O$  (C-S-H). The reaction products such as  $CaH_2SiO_4 \cdot 2H_2O$  (calcium silicate hydrate gel) is of high cementitious properties such as compressive strength, bonding strength and abrasion resistance, [128].

The assessment of Natural Pozzolan in this chapter is based on the strength activity index, which is described in ASTM C311 [4] and specified by ASTM C618 [5]. From ASTM C311 test method [4], the 7 days and 28 days compressive strengths specimens of mortar was prepared with a 30 % SCM substitution of cement by weight basis, the values achieved were compared to those of a control mortar. According to ASTM C618 specification [5], the SCM mixture should have 75 % strength of the control at 7 or 28 days. In addition, the pozzolans showing pozzolanic activity greater than 5.4 MPa and have alumina content of 11.6-14.7% are considered as highly resistant to sulphate attack, [6].

## **5.2 Materials and Methods**

### **5.2.1 Materials**

Materials used in this work were Portland limestone cement (PLC) conforming to SS-EN 197-1 CEM II/A-L class 42.5 N [66], the cement used in this investigation has chemical composition as shown in Table 4.1. S-N collected from Uchira Moshi-Kilimanjaro region, P-N collected from Ikuti and rice husk (RH) collected from Wellar Rice Mill Mbeya City. Fine

aggregate was river sand collected from Mbarali and distilled water was prepared from chemistry laboratory. S-N are pyroclastic ejecta which are found in many areas of the world. It is composed of red colored fragments which is the indicator of presence of iron [129]. The particles are highly vesicular and composed of most crystalline structure. Its chemical composition vary depending on mineralogical composition, formation temperature and rate of cooling. Pumice are white fragment composed of mainly silica and alumina, [129]. The P-N aggregates are highly vesicular materials and are classified as acidic pumice, [130]. RHA are the protective coverings of rice grains which is mostly indigestible by humans. Its chemical composition when burnt under controlled temperature is as high as 95% [129]. The RHA is a potential source of amorphous silica which has a variety application in material science and construction industry in the production of blended cement. These materials were tested to investigate their chemical and physical properties and the results are as presented earlier in **Table 4.1**.

### **5.2.2 Methods**

Samples of grounded S-N, P-N, and RHA passing 75  $\mu$  standard sieve were mixed with cement in the ratios shown in **Table 5.1** and **Table 5.2**, and tested to investigate the influence of diverse pozzolans on the properties of Portland cement. The properties investigated embrace fineness and specific surface area according to SS-EN 196-6 [97], setting time and soundness according to Neville and Brook, and SS-EN 196-3:2005+A1:2008 (E) [1][65], strength and strength activity index according to SS-EN 196-1 and BS-EN 196 – 1 [102] [131]. The setting time and soundness test procedures involved determination of standard consistency paste which is necessary for ensuring uniformity of the test specimens conferring to SS-EN 196-3, [65]. The compressive strength were determined from cement sand mortar made from standard sand, plain as well as blended cement. The test was conducted in accordance to SS-EN 196-1 [102].

The standard sand was prepared from selected clean fine aggregates conforming to SS-EN 196-1 and PD 6682-1:2003 [102] [132]. The control and test mortar were prepared with a water-to-cement ratio (w/c) by mass of 0.484. The strength activity index (SAI) was determined according to ASTM C [57][78]. The reference specimen with 100% Portland cement and the test specimens were mould according to a set specific recipes where part of Portland cement were replaced by pozzolan. The effect of S-N, P-N, RHA, S-N/RHA and P-N/RHA materials were expressed as the ratio of the compressive strength of the test specimen to the compressive strength of reference specimen [133].

**Table 5.1:** Mix proportion of S-N, RHA and Portland cement

Sample Designation	CTRL	30/0	25/5	20/10	15/15	10/20	5/25	0/30
Cement (%)	100	70	70	70	70	70	70	70
S-N (%)	0	30	25	20	15	10	5	0
RHA (%)	0	0	5	10	15	20	25	30
Total (%)	100	100	100	100	100	100	100	100

**Table 5.2:** Mix proportion of P-N, RHA and Portland cement

Sample Designation	CTRL	30/0	25/5	20/10	15/15	10/20	5/25	0/30
Cement (%)	100	70	70	70	70	70	70	70
P-N (%)	0	30	25	20	15	10	5	0
RHA (%)	0	0	5	10	15	20	25	30
Total (%)	100	100	100	100	100	100	100	100

## 5.3 Results and Discussion

### 5.3.1 Standard consistence of cement blended with S-N, P-N and RHA

The standard consistency paste were determined for 14 specimens of blended cement paste and one plain cement as a control paste. Analyses of test results are shown in **Figure 5.1**. It was observed that replacing cement with 30% S-N reduced water required for standard paste from 27.4 to 27.2% indicating that cement is more reactive and absorptive than S-N. These results show a constant increase of water required for the standard consistence paste for cement blended with S-N/RHA from 27.2% (at 30% S-N and 0% RHA replacement) to 38.6% (at 10% S-N and 20% RHA replacement). Further increase at lower rate was observed from 38.6% to 41.4% (at 0% S-N and 30% RHA replacement). The increased water demand indicated increased water absorption as the percent of RHA which is porous than S-N increases. In contrary the replacement of cement with 30% P-N increased water required for standard paste from 27.4 to 36 indicating the high absorption characteristics of P-N. From 36% (at 30% P-N and 0% RHA replacement) the water demand for the standard consistence paste of cement blended with P-N/RHA increased gradually to 42.2% maximum (at 10% P-N and 20% RHA replacement). The water demand then reduces from 42.2 % maximum to 41.4% (at 0% P-N and 30% RHA replacement). In general it shows that water demand increases with increasing percent of RHA. This is obvious but in both cases of S-N and P-N plus RHA, since the RHA is very reactive the heat of hydration and the hydration reactions demanded more water as the addition of RHA was increased.

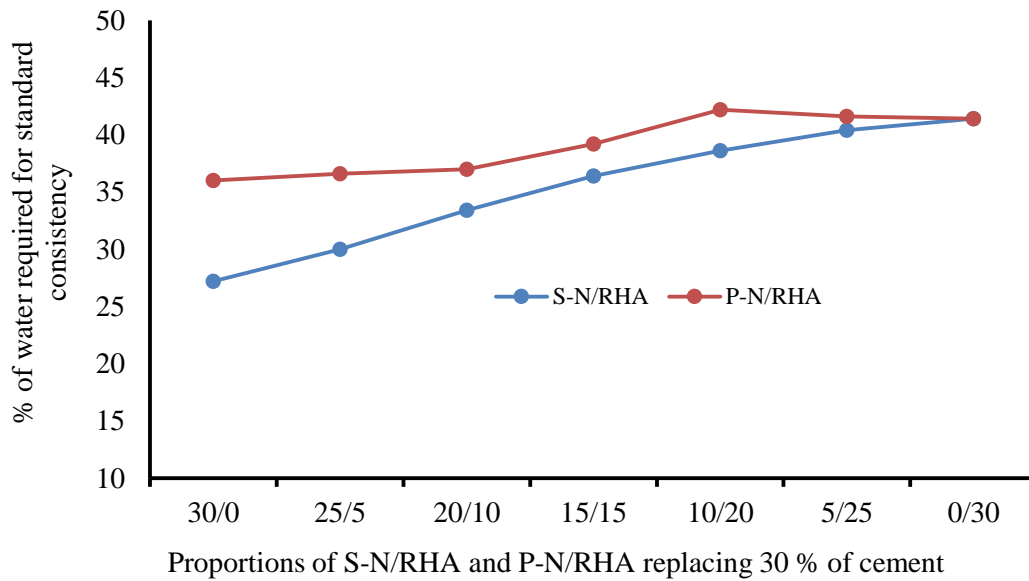


**Figure 5.1:** Water required for the standard paste of S-N, P-N and RHA blended cement

### 5.3.2 Setting times and Soundness of Cement blended with S-N, P-N and RHA

**Figure 5.2** show the setting times of the S-N, P-N and RHA blended cement. Observation indicated both initial setting times (IST) and final setting times (FST) reduced from 139 and 184 minutes to 99 and 167 minutes respectively for the cement blended with 30% S-N, **Figure 5.2 (a)**. This uniqueness was attributed with the absorption and reactivity characteristic of S-N powder. As the percent of S-N decreases and percent of RHA increases, both IST and FST increases to a maximum of 151 and 185 minutes at addition of 15/15% S-N/RHA and 20/10% S-N/RHA respectively. These results from increased water for the standard paste and increased percent of RHA which lowers the heat of hydration and delayed pozzolanic reaction. Beyond 15% S-N and 15% RHA, IST reduced faster to 86 minutes but FST reduced slowly down to 154 minutes indicating the effect of absorption of porous RHA powder.

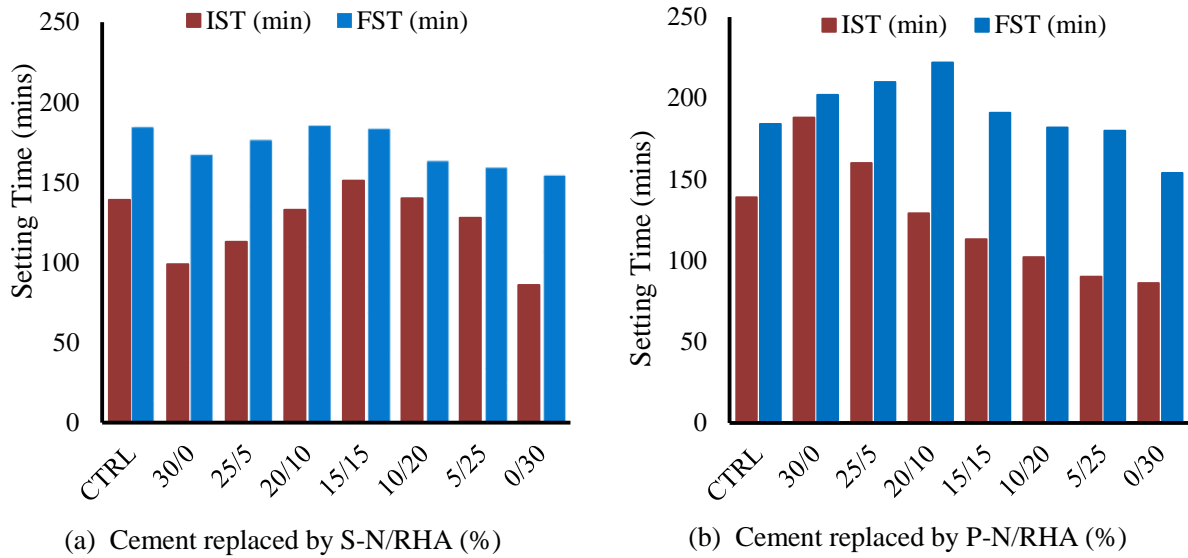


**Figure 5.2:** Setting times of Portland cement blended with (a) S-N/RHA and (b) P-N/RHA.

Contrary to S-N/RHA, the P-N/RHA **Figure 5.2 (b)** indicated increased IST and FST from 139 and 184 minutes to 188 and 202 minutes respectively for the cement blended with 30% P-N. IST was then reduced with diminishing rate as the percent of P-N decreases while increasing that of RHA to 86 minutes at 30% RHA. On the other hand the FST increased to 222 minutes at addition of 20% P-N and 10% RHA and the reduced constantly to 154 minutes at 30 percent of cement replaced by RHA. In this case the FST were delayed by P-N by interfering the pozzolanic reactions of RHA which is known to have early pozzolanic reaction. Further observation indicated higher FST of the blended cement than that of Portland cement when the two pozzolan were added in the order of 30/0, 25/5, 20/10 and 15/15 % P-N/RHA.

The soundness of the blended cement were found to range within 1 to 2 mm maximum **Table 5.3**. This results indicated no expansion due excess lime and/or magnesium. Therefore the proportions of pozzolan/Portland cement conform to the requirements of the SS EN 197-1 [66]. In this view the blended cement have the advantage of reduced heat of hydration, reduced expansion and associated cracks and hence increased durability.

**Table 5.3:** Soundness of S-N/RHA and P-N/RHA blended cement.

Sample Designation	CTRL	30/0	25/5	20/10	15/15	10/20	5/25	0/30
S-N/RHA	2	1	1	1	1	0	1	2
P-N/RHA	2	1	0	1	2	1	1	2

### 5.3.3 Flow of the blended cement mortar

**Figure 5.3** shows the trend of flow of hydraulic cement mortar for both blended and unblended cement determined using ASTM C 1437–07 procedures. The flow of plain cement mortar was found to be 39 mm. This flow fall to 24 and 9 mm following the addition of 30% S-N and P-N respectively due to fineness and absorption characteristics of S-N and P-N. On addition of 25% S-N and 5% RHA, the flow drop further to 14 mm. As the percent of S-N decreased while increasing the percent of RHA the flow of the blended cement mortar decreased to zero at 0% S-N and 30% RHA respectively. This attributes to increased percent of high reactive RHA which is also more porous and absorptive than cement and scoria. The increased RHA, also reduces lubrication of fine aggregates as part of water was absorbed and part bound to hydrating cement **Figure 5.3**. This means that at constant water cement ratio, the amount of water available for hydration was less than the required amount that can lead into incomplete hydration resulting into low strength.

On the other hand, the addition 5% RHA the flow of P-N/RHA blended cement mortar decreased slightly from 9 to 8 mm and continue to fall gradually upon further addition RHA to zero at 10% P-N and 20% RHA respectively and remain unchanged up to 0% and 30% P-N and RHA respectively. For the case of Portland cement blended with P-N and RHA, beyond 15% of RHA the flow drop to zero and remained constant. This trend was associated with absorptive nature of both P-N and RHA and fast reactivity of RHA. All these contributed to

the seizure of flow and incomplete hydration of Portland cement, low pozzolanic reaction thus culminating low strength. The loss of flow of mortar in both cases explain the excess water required for standard cement sand mortar (**Figure 5.1**) and that must be added during concrete production. This suggested that partial replacement of Portland cement with RHA and other pozzolans could raise the water demand in concrete manufacturing to keep the amount of water required for full hydration of Portland cement and pozzolanic reaction.

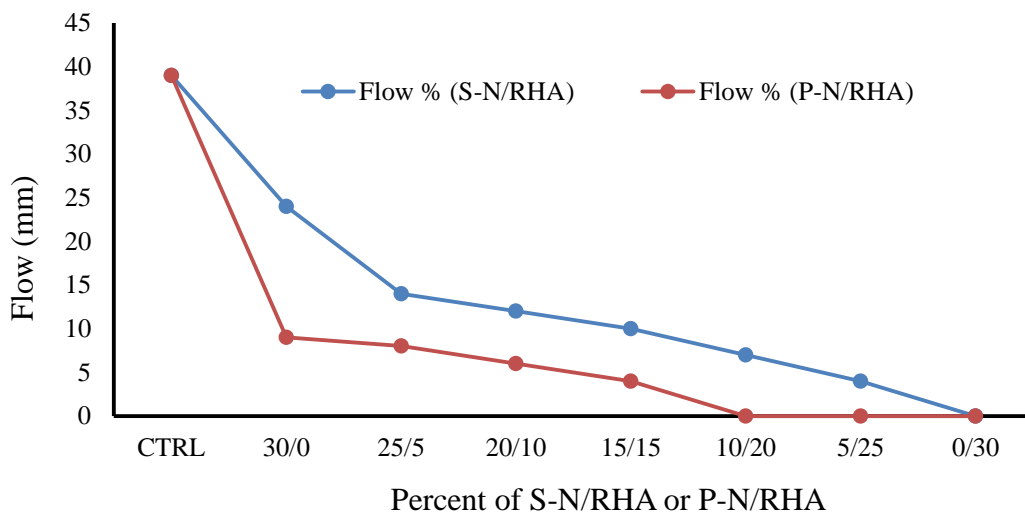


**Figure 5.3:** Flow of blended cement mortar

### 5.3.4 Compressive strength

In the study of the effects of cement blended with S-N and RHA or P-N and RHA to the properties of mortar and concrete, the cubical moulds of size 40 mm × 40 mm × 40 mm were used. The blended cement sand mortar were prepared and casted according to SS EN 196-1:2005 (E) [102] After 24 hours the moulds were removed and test specimens were kept in water for curing. The level of cement replacement and type of materials showed a huge influence on the compressive strength of the blended cement, **Figure 5.4** and **Figure 5.5**. Compressive strength increased of plain cement increased usually with curing period as was expected in both cases.



From **Figure 5.4**, at two days curing period, the compressive strength of blended cement increased from 22.1 MPa to 24.3 MPa when Portland cement was replaced by 30% S-N. But when Portland cement was replaced with 25% S-N and 5% RHA the compressive strength drop slightly to 23.5 MPa. The compressive strength reduced more to 18.5 MPa at replacement with 15/15% of S-N to RHA respectively. This could be a results of disturbed or contradicted hydration and pozzolanic reactions resulted from different chemical energies the S-N and RHA have. Beyond 15/15% of S-N to RHA replacement, the compressive strength increased gently to 25.5 MPa at 0/30% S-N to RHA replacement. The same trend was experienced at 7 days curing period. At 28 days curing period the compressive strength fall from 53.9 MPa to 46.6 MPa upon cement replacement by 30% S-N due to increased non-reactive S-N and less CH required for pozzolanic reaction. Further strength reduction was observed up to 20/10% S-N to RHA replacement level. Beyond these replacement, the compressive strength increased rapidly to 39.2 MPa at 15/15% S-N to RHA replacement. Then increased gradually to 46.3 MPa at 0/30% S-N to RHA replacement level. The increased strength was associated to increased amount of reactive RHA and subtraction of controverting S-N reactant. The general observation on **Figure 5.4** showed that, compressive strength at all curing periods were higher when these pozzolan work alone. Thus it suggested that it is better to choose for S-N or RHA but not both albeit both materials are available.

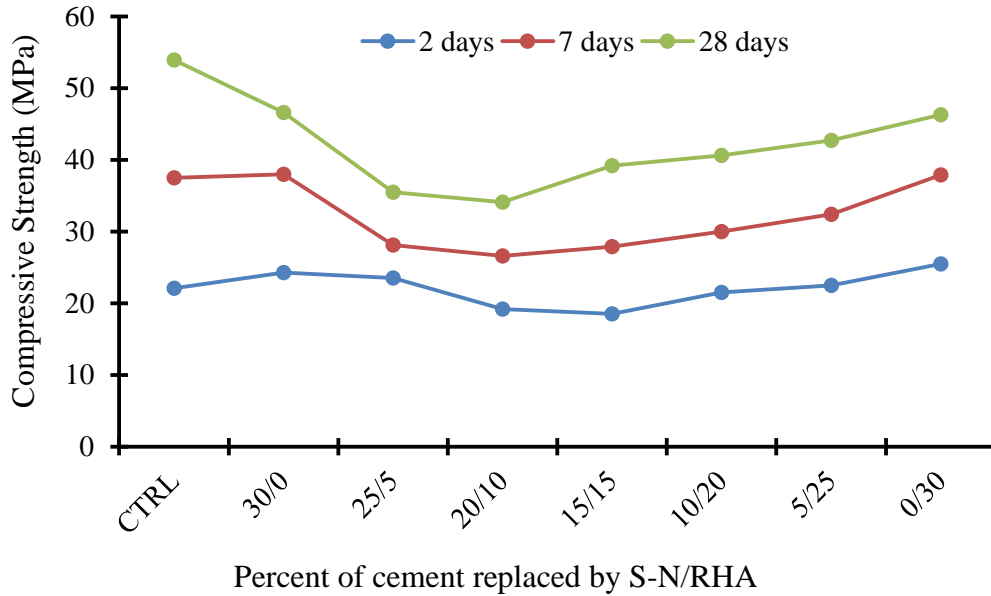


**Figure 5.4:** Compressive Strength versus percent of cement replaced by S-N/RHA

**Figure 5.5**, showed that at two days curing period, the compressive strength decreased slowly from 22.1 MPa for Portland cement to 14.9 MPa when cement was replaced with 20/10% P-N/RHA. This reduction in compressive strength was influenced by delayed pozzolanic reaction of P-N. It was also attributed to incomplete hydration caused by absorption of both P-N and RHA. From 14.9 MPa, the compressive strength increased gently to 27.1 MPa when Portland cement was replaced by 5/25% P-N to RHA. This trend was ascribed to the increased percent of amorphous RHA in the microstructure which partake high pozzolanic reaction. The strength dropped to 25.5 MPa due to increased non-hydraulic RHA in the microstructure and insufficient amount of CH needed for pozzolanic reaction. Comparable trend as for S-N/RHA blended cement was observed for S-N/RHA blended cement at 7 days curing period.

The 28 days compressive strength drop from 53.9 MPa for plain cement to 41.9 MPa at 30 % replacement by P-N, **Figure 5.5**. The decrease of compressive strength could be caused by increased non-hydraulic materials (P-N) in the microstructure and delayed pozzolanic reaction. The compressive strength then increased gently with slight kink at 25/5% P-N/RHA

cement replacement to 53.8 MPa at 10/20% P-N/RHA cement replacement level. This trend was attributed to the increasing amount of amorphous RHA which improved pozzolanic reaction. The same was attributed to the reactions between the excess amorphous silica and alkali from P-N in the microstructure resulting into increased compressive strength. It could also be associated to the decreasing of P-N which have delayed pozzolanic reaction. Beyond 10/20% P-N/RHA cement replacement level, the compressive strength decreased to 47.3 MPa at 5/25% P-N/RHA cement replacement level. Then reduced to 46.3 MPa when cement was replaced by 30% RHA. The reduced compressive strength was associated to increasing amount of RHA in the microstructure and exhaustion of CH needed for pozzolanic reaction. The general observation on **Figure 5.5** show that, 28 days compressive strength at all replacement level were above the minimum compressive strength for the type of cement used (i.e. 42.5 MPa) except at 30% S-N. Thus, it suggested that P-N and RHA can be thought as binary materials for cement replacement to improve performance of common Portland cement. It also suggested that, blending of 70/10/20% Portland cement to P-N to RHA could be the optimum combination of these ternary materials.

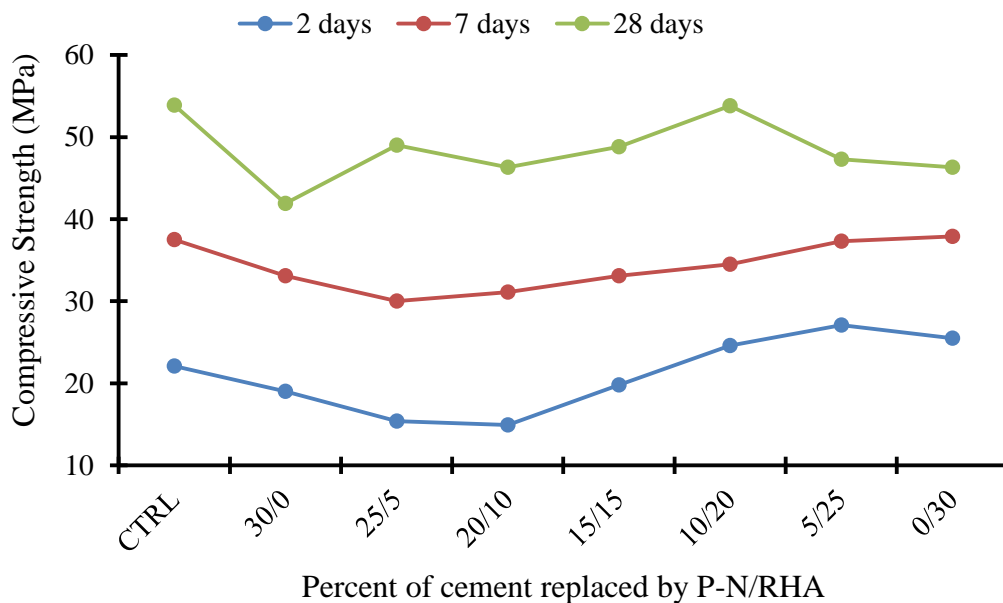


**Figure 5.5:** Compressive Strength versus percent of cement replaced by P-PN/RHA

### 5.3.5 Strength Activity Index (SAI)

SAI of binary and ternary materials used in this study was determined according to ASTM C 311 [78]. The SAI of the Pozzolan blended cement mortar was determined for each cement replacement level at 7 and 28 days curing period. **Figure 5.6**, show the Strength Activity Index of cement mortar blended with S-N and RHA at 7 and 28 days respectively. Observation indicated that, 7 days SAI of mortar blended with S-N/RHA in the ratio of 25/5, 20/10, 15/15 and 5/25 were lower compared to the minimum of 75% specified in ASTM C [57]. This could have aroused from upset or opposed hydration and pozzolanic reactions stemmed from different chemical energies of the S-N and RHA as observed in the compressive strength, Figure 5.4. But the higher SAI values were found at 30/0, 5/25 and 0/30 respectively indicating uninterrupted pozzolanic reactions in the microstructure.

Similar to 7 days, the 28 days SAI of blended cement mortar yield lower than the specified value of 75% at S-N/RHA replacement 25/5, 20/10, 15/15 respectively [57]. The causative being upset or conflicting hydration and pozzolanic reactions. At 30/0, 5/25 and 0/30% S-N/RHA replacement level, the 28 days a SAI of 86.5, 79.2 and 85.9% respectively were achieved, **Figure 5.6**. The increased SAI was associated to increased amount of reactive RHA and subtraction of contradicting S-N reactant. The general observation on **Figure 5.6** showed that, SAI improved when these pozzolan work alone. Thus, suggesting that it is better to select using S-N or RHA alone but not both although both materials are available. It also addressed that, blending cement with S-N and RHA together retard the setting time and strength development of cement strength.

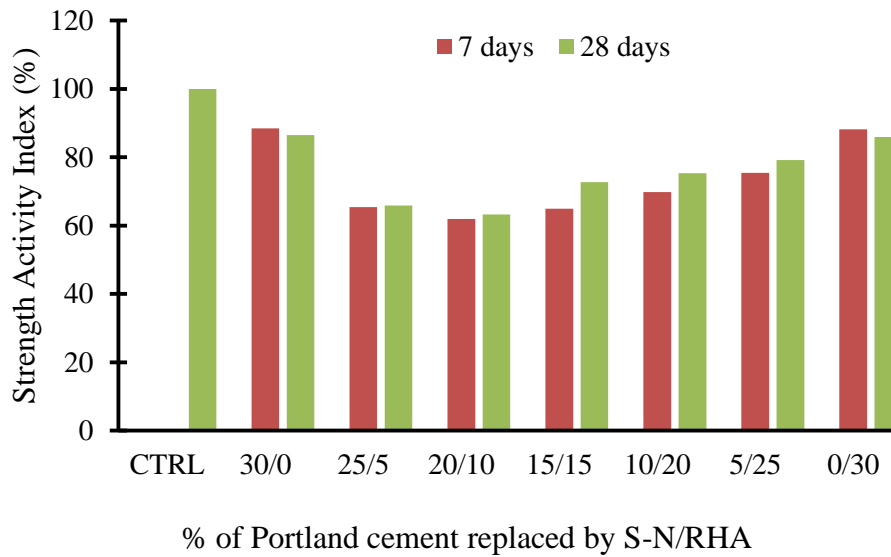


**Figure 5.6:** Strength Activity Index of cement blended with S-N/RHA

**Figure 5.7** show SAI at 7 and 28 days curing period of cement mortar blended with P-N/RHA. The 25/5 and 20/10 P-N/RHA mixes gave a 7 days SAI 69.8 and 72.4% below the minimum requirement of 75% specified by ASTM [57] owing to delayed pozzolanic reaction of P-N. For the cement mortar with 30% P-N, the SAI afforded was 77.0%. The P-N/RHA cement mortar blended at 15/15, 10/20, 5/25 and 0/30 presented a SAI of 77.0, 80.3, 86.8 and 88.2% respectively of the reference cement mortar at 7 days curing period. These trend was related to increased compressive strength following increasing amount of reactive RHA in the microstructure. The 28 days SAI appeared to have minimum SAI 77.7% and maximum 99.8% at 30% P-N and 10/20% P-N/RHA replacement respectively. The 28 days SAI was attributed to the increasing amount of amorphous RHA which improved pozzolanic reaction. The same was attributed to the reactions between the excess amorphous silica and alkali from P-N in the microstructure resulting into increased compressive strength and SAI. Thus, suggesting that P-N and RHA can be thought as ternary materials to improve performance of common Portland cement.

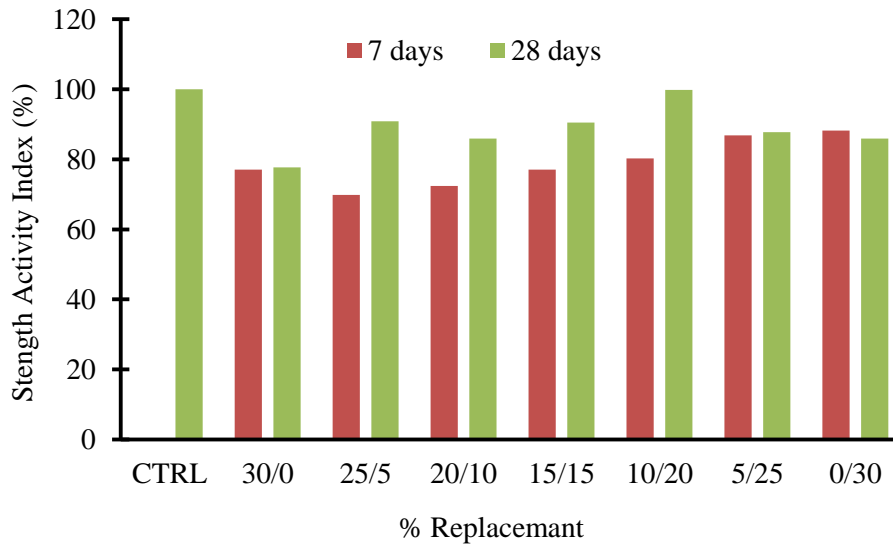


**Figure 5.7:** Strength Activity Index of cement blended with P-N/RHA

### 5.3.6 Effects of Pozzolan on Cumulative SAI of Binary and Ternary Materials.

**Figure 5.8** showed the cumulative SAI of cement mortar blended S-N, P-N and RHA between 7 and 28 curing days. The cumulative SAI was assessed by determining the cumulative sum of the difference between 7 and 28 days SAI. Cumulative SAI indicate whether the strength of blended cement was increasing or decreasing as Portland cement replacement level was increasing. The results showed that, the cumulative SAI increased constantly to 41 at 20% percent cement replacement by RHA. However, beyond 20% the rate decreased slowly and afford 67 at 40% RHA replacement level **Figure 5.8**. The same trend was found in **Figure 3.9(c)**, implying that as non-hydraulic materials was increased in the microstructure drained the CH needed for pozzolanic reactions. Also increased the inter-particle distances between hydration products hence leading to low bond strength in the cement-aggregate interface.

The results also showed that, the cumulative SAI of S-N bended cement increased gently to 23 at 20% replacement level, however at lower rate compared to RHA. This tendency denoted lower pozzolanic reactions the S-N possessed contrast to RHA. From 20 to 30% replacement level the rate of SAI development increased leading to a SAI of 38% then

increased to 40%, however at slow rate. The reason for this trend was stronger pozzolanic reaction attained between 20 to 40% replacement which reduced as percent of pozzolan increased in the microstructure. Beyond 30% the rate decreased slowly as replacement level was increasing (**Figure 5.8**) leading to low compressive strength as suggested in **Figure 3.9(a)**. This implied that, as S-N increased in the microstructure drained the CH needed for pozzolanic. Also set apart the hydration products hence leading to low bond strength within cement-aggregate interface.

Unlike S-N and RHA, the P-N blended cement showed delayed SAI development up to 10% replacement level which improved abruptly to 41 at 20% replacement level. Observation revealed stronger pozzolanic reaction due to balanced CH and the reactive silica of the P-N. However, beyond 20% cement replacement the rate decreased slowly giving a SAI of 55 at 40% replacement **Figure 5.8**, leading to low compressive strength as suggested before in **Figure 3.9(b)**. The results of both S-N, P-N and RHA materials suggested that cement can successful be blended with these pozzolans up to 30% optimum without compromising other properties.

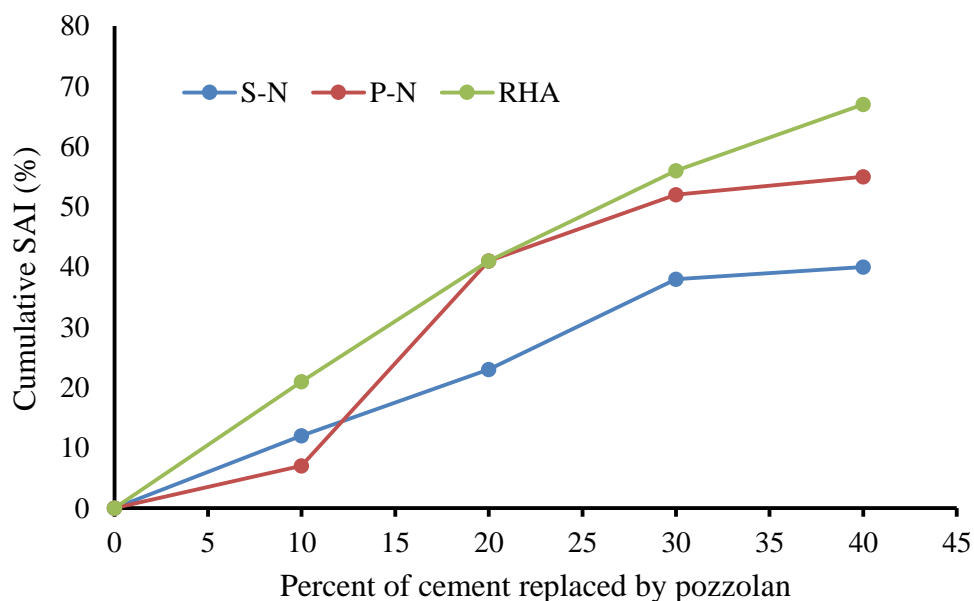


**Figure 5.8:** Cumulative SAI of binary materials versus percent of cement replaced

**Figure 5.9** showed the results of cumulative SAI for ternary materials where 30% of Portland cement were replaced with S-N/RHA and P-N/RHA. Cumulative SAI of Portland cement blende with S-N/RHA decreased from 0% for plain cement to - 2.0% at 25/5 S-N/RHA replacement **Figure 5.9**. The implication of high amount of non-hydraulic materials in the microstructure which retarded the pozzolanic reactions. Beyond 25/5 S-N/RHA replacement, SAI increased gently to 44.8% at S-N/RHA 0/30%. The indication of a steady pozzolanic reaction that produced additional C-S-H gel responsible for strength development. Contrary, the cumulative SAI for P-N/RHA blend revealed constant growth up to 81.7 % at 10/20 % P-N/RHA replacement level. This demonstrated a consensus between P-N and RHA reactant that permit pozzolanic reaction to continue and produced more C-S-H gel that contributed to the strength development. The C-S-H fill the gap between the aggregates, increased interfacial bod strength and reduced pores within the microstructure giving more strong mass. Generally blending of Portland cement with S-N/RHA does not bring any advantage but blending with P-N/RHA. Therefore it is more advantageous to employ S-N or RHA alone.

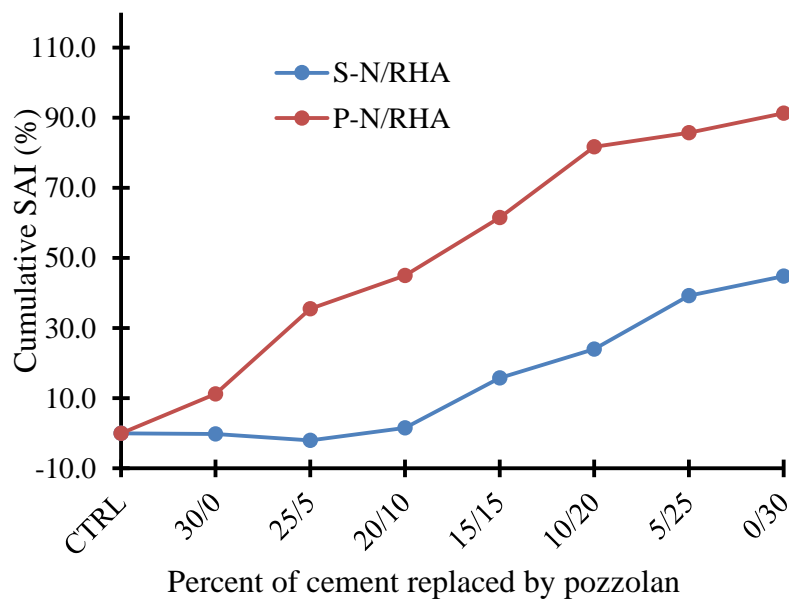


**Figure 5.9:** Cumulative SAI of ternary materials versus percent of cement replaced



## 5.4 Conclusions and Recommendations

### 5.4.1 Conclusions

With regard to test and analysis done it is worth to make the following conclusions: -

- 1) Water required for standard consistency paste of ternary materials increased as percent of RHA increased.
- 2) For cement blended with S-N/RHA had a maximum initial setting time of 151 minutes at 15/15% S-N/RHA replacement, the lower values being 99 and 86 minutes at 30/0% and 0/30% S-N/RHA.
- 3) Setting time of P-N/RHA blended cement increased on addition of 30% P-N to 188 minutes, beyond 30% setting time decreased with diminishing rate to 86 minutes at 0/30% P-N/RHA.
- 4) Soundness was found to be less than the limit of 10 mm specified by BS and flow decreased as percent of RHA increased in both cases.
- 5) The 28 days compressive strength of S-N/RHA blended cement was as high as 46.6 and 46.3 MPa at 30/0 and 0/30% S-N/RHA replacement level respectively.
- 6) All mixes of P-N/RHA yield a 28 days compressive strength above 42.5 MPa except at 30% P-N. The maximum compressive strength being 53.8 MPa attained at 10/20% P-N/RHA replacement level.
- 7) A 28 days SAI of S-N/RHA blended cement was higher 75 % recommended by ASTM at 30/0, 10/20, 5/25 and 0/30% S-N/RHA. Contrary, that of P-N/RHA were higher at all replacement levels.
- 8) The effect of ternary materials observed from cumulative SAI was the superposition of SAI of binary materials and RHA.

#### **5.4.2 Recommendations**

30% S-N, or P-N or RHA is recommended as the optimum replacement for Portland cement to reduce cement consumption and environmental degradation. It is also recommended not to mix S-N and RHA together but each materials can be used alone to enhance improved characteristics of the blended cement. Further research is needed to investigate the adverse reaction that causes the lower compressive strength at 25/5 to 10/20% S-N/RHA replacement.

## Chapter 6 CONCLUSION AND RECOMMENDATIONS

### 6.1 CONCLUSION

Scoria, pumice, and RHA materials were successfully characterized according to ASTM C 618 criteria and tested to establish their potentials as SCMs. Silica content was quite high as 40.0, 55.4 and 94.84% and basic oxides were 66.9, 76.44 and 94.84 respectively for S-N, P-N and RHA. Pozzolanic and strength activity index tests established these materials as good pozzolan. These materials showed high PAI of 82, 70.7, and 87.8% at 7 days: 89.0, 85.5, and 88.9% at 28 days in that order and meet the criteria for SCMs. The ultimate mean compressive strengths achieved for binary materials were 44.8, 43.0, and 42.5 MPa for pumice, RHA, and scoria respectively, after 28 days curing period. In addition, setting time of binary materials observed for all samples ranged from a minimum mean initial setting time of 80 min for S-N to maximum mean initial setting time of 154 min for RHA 600. Likewise, the final setting time ranged from a minimum mean final setting time of 156 min for S 900 to maximum final setting time of 190 min for RHA 600. Initial and final setting times for scoria, pumice, RHA were lower compared to those of Portland pozzolana cement (PPC), which were 166 and 285 min initial setting time and final setting times in that order.

Investigation on the influence of S-N and P-N pozzolanic binders on the key performance indicators of Portland cement concrete that Portland cement could be blended with S-N and P-N binders at 10% substitution level without compromising the compressive strength, modulus of rupture, flow, slump, permeability, thermal and volume stability and hence durability of the concrete. The optimum replacement level was therefore found to 10% for both S-N and P-N. Contrary to the expectations, S-N and P-N blended cement concrete at

10% substitution level showed slightly superior residual compressive strength after 600 °C temperature exposure compared to unblended PLC concrete. This implies that S-N and P-N could be used to blend cement used in the construction of structures in areas that are more prone to fire accidents. Moreover, the results show that S-N and P-N have greater potential in reducing the amount of cement used in construction, the energy consumed during clinkering process, and the CO<sub>2</sub> emitted by the cement industries. Therefore, these materials could be used for climate change mitigation.

The concrete shrinkage and expansion of 0.01% observed at all the substitution levels was within the acceptable limits of the standards. The coefficients of permeability decreased with the increase in the amount of S-N, reaching 4.9741E-08 m/s at 30% replacement level compared to 5.35714E-08 m/s for the control concrete. The correlation between modulus of rupture and compressive strength at all the substitution levels was much better for S-N concrete ( $R^2 = 0.9606$ ) than P-N ( $R^2 = 0.8229$ ). However, P-N concrete showed substantially higher modulus of rupture versus compressive strength at each cement replacement level compared to S-N. Therefore blending cement with P-N could be a breakthrough in solving the problem of brittleness in concrete materials.

For the case of ternary blended cement, it was found that water required for standard consistency paste increased as percent of RHA increased. The Portland cement blended with S-N/RHA had a maximum initial setting time of 151 and 188 minutes at 15/15 and 30/0% S-N/RHA and P-N/RHA respectively. The lower values being 99 and 86 minutes at 30/0% and 0/30% S-N/RHA and P-N/RHA respectively. The FST of ternary materials afforded a maximum of 185 and 222 minutes at 20/10 in both cases. Soundness was less than the limit of 10 mm specified by BS and flow decreased as percent of RHA increased in both cases. The 28 days compressive strength of S-N/RHA blended cement was as high as 46.6 and 46.3 MPa at 30/0 and 0/30% S-N/RHA replacement level respectively. Contrary, all mixes of P-N/RHA

yield a 28 days compressive strength above 42.5 MPa except at 30% P-N which gives 41.9 MPa. The maximum compressive strength being 53.8 MPa attained at 10/20% P-N/RHA replacement level. The 28 days SAI of S-N/RHA blended cement was as higher as 75% recommended by ASTM at 30/0, 10/20, 5/25 and 0/30% S-N/RHA. Contrary, that of P-N/RHA were higher at all replacement levels. The combination of all the above parameters demonstrated the suitability of S-N, P-N and RHA as potential SCMs.

## **6.2 RECOMMENDATIONS**

- 1 10% S-N, or P-N or RHA is recommended as the optimum replacement for Portland cement to reduce cement consumption and serves reducing environmental degradation without compromising other mortar and concrete properties.
- 2 Mixing of S-N and RHA together is not recommended but each materials can be used alone to enhance improved characteristics of the blended cement in ternary materials. But for the case of P-N in ternary blend, 10/20% P-N/RHA may be adopted yet achieving a good performance of cement mortar and concrete
- 3 Further research is needed to investigate the adverse reaction that causes the lower compressive strength at 25/5 to 10/20% S-N/RHA replacement.
- 4 S-N and P-N have greater potential in reducing the amount of cement used in construction, the energy consumed during clinkering process, and the CO<sub>2</sub> emitted by the cement industries. However RHA has that potential too, but need controlled burning.
- 5 Since the reason for the dramatic increase in modulus of rupture over 7 and 28 days curing periods at 20% substitution level for P-N was not fully understood, further investigation is need to unravel why this increase occurred for P-N and not for S-N materials.

## REFERENCES

- [1] A.M. Neville and J. J. Brooks, *Concrete Technology*, 2nd Editio. London: Pearson, 2010.
- [2] Mehta P. Kumar, “Advancements in Concrete Technology,” *Concr. Int.*, vol. 21, pp. 69–76, 1999.
- [3] Davidovits J., “Geopolymers and geopolymeric new material,” *J. Therm. Anal.*, vol. 35, pp. 29–41, 1998.
- [4] Ghassan K Al-chaar, Mouin Alkadi, and David A Yaksic, “The Use of Natural Pozzolan in Concrete as an Additive or Substitute for Cement Construction Engineering,” no. December, 2011.
- [5] Ghassan K. Al-chaar, Mouin Alkadi, and Panagiotis G Asteris, “Natural Pozzolan as a Partial Substitute for Cement in Concrete,” *open Constr. Build. Technol. J.*, vol. 7, pp. 33–42, 2013.
- [6] Alp İ., Devec H., Süngün Y.H, Yilmaz A.O, Mal A.K.E.S.İ, and Yilmaz E, “Pozzolanic characteristics of a natural raw materials for use in blended cements,” *Iran. J. Sci. Technol.*, vol. 33, no. B4, pp. 291–300, 2009.
- [7] K. M. A. Hossain, “Blended cement and lightweight concrete using scoria: mix design, strength, durability and heat insulation characteristics,” *Int. J. Phys. Sci.*, vol. 1, no. 1, pp. 5–16, 2006.
- [8] Green S., Brooke N., and McSaveney L., “Pumice aggregates for structural lightweight and internally cured concretes,” [www.perlite.co.nz/images/high-strength-lightweight-concrete.pdf](http://www.perlite.co.nz/images/high-strength-lightweight-concrete.pdf) (Accessed Jan 20, 2016)., ”.
- [9] Grasser Klaus and Minke Gernot, *Building with Pumice*. A Publication of Deustches Zentum Fur Entwicklungchnlogen-GATE Zusammenarbeit, 1990.
- [10] Della V., Kuhn I., and Hotza D., “Rice husk ash as an element source for active silica production,” *Mater. Lett.*, vol. 57, no. 4, pp. 818–821, 2002.
- [11] Della Viviana Possamai, Kühn Ingeborg, and Hotza Dachamir, “Processing and Characterization of Active Silica Obtained from Rice Husk Ash,” pp. 1–5, 2016.
- [12] Aiswarya S, Prince A. G, and Dilip C., “A Review on Use of Metakaolin in Cement Mortar and Concrete,” *Int. J. Innov. Res. Sci. Eng. Technol.*, vol. 3, no. 7, pp. 14697–14701, 2013.
- [13] John Newman; Ban Seng Choo., *Advanced Concrete Technology Constituent Materials*, 1st ed. Amsterdam, Boston London: Elsevier, 2003.
- [14] P. C. Hewlett, *Lea’s Chemistry of Cement and Concrete*, no. January. 2004.
- [15] Taylor H. F. W., *Cement chemistry*, 2 Edition. London and New York, 1997.
- [16] Sabir B.B, Wild S, and Bai J, “Metakaolin and calcined clays as pozzolans for concrete : a review,” *Cem. Concr. Compos. - Elsevier*, vol. 23, pp. 441–454, 2001.
- [17] A. Naceri and M. C. Hamina, “Effects of pozzolanic admixture ( waste bricks ) on mechanical response of mortar,” vol. 21, no. 1, pp. 1–8, 2008.
- [18] Abdul Wahab A., F. F. Abdul-hameed, and D. K. Al-dahan, “Evaluation of Al-Amij and Al-Hussainiyat Claystones ( Iraqi Western Desert ) for the Production of Pozzolana,” vol. 8, no. 1,

- pp. 59–73, 2012.
- [19] Moises Frias, E. Villar-Cocina, M.I. Sanchez de Rojas, and E. Valencia-Morales, “The effect that different pozzolanic activity methods has on the kinetic constants of the pozzolanic reaction in sugar cane straw-clay ash / lime systems : Application of a kinetic – diffusive model,” vol. 35, pp. 2137–2142, 2005.
- [20] Taylor Peter, Bektas Fatih, Yurdakul Ezgi, and and Ceylan Halil, “Optimizing Cementitious Content in Concrete Mixtures for Required Performance, National Concrete Pavement Technology Center Iowa State University,” 2012.
- [21] P. J. Tikalsky *et al.*, “Use of Raw or Processed Natural Pozzolans in Concrete Reported by ACI Committee 232,” *ACI 232.1R-00*, pp. 1–24, 2001.
- [22] Fathollah Sajedi and Hashim Abdul Razak, “The effect of chemical activators on early strength of ordinary Portland cement-slag mortars,” *Constr. Build. Mater.*, vol. 24, no. 10, pp. 1944–1951, 2010.
- [23] Mehta P.K. and Paulo J. M. Monteeiro, *Concrete Microstructure, Properties, and Materials*, 3rd ed. New York Chicago San Francisco Lisbon London Madrid Mexico City Milan New Delhi San Juan Seoul Singapore Sydney Toronto: McGraw-Hill, 2006.
- [24] ASTM C 595 - 03, *Standard Specification for*, vol. 14. .
- [25] ASTM C618, “Standard Specification for Coal Fly Ash and Raw or Calcined Natural Pozzolan for Use in Concrete,” 2005.
- [26] McCarter W. J and Tran D, “Monitoring pozzolanic activity by direct activation with calcium hydroxide,” *Constr. Build. Mater.*, vol. 10, no. 3, pp. 179–184, 1996.
- [27] ACI 232.1R-12, “Report on the Use of Raw or Processed Natural Pozzolans in Concrete,” 2012.
- [28] Ramezaniapour Ali Akbar, *Cement Replacement Materials*, 1 Edition. Berlin: Springer, 2014.
- [29] Jide Muli Akande, Chinuba Arum, and Fola Micah Omosogbe, “Determination of the Pozzolanic Properties of Olotu Marine Clay and Its Potentials for Cement Production,” *Mater. Sci. Appl.*, vol. 02, no. 01, pp. 53–58, 2011.
- [30] ACI 116R-00, “Cement and Concrete Terminology,” vol. 00, no. Reapproved, pp. 1–73, 2005.
- [31] Watcharapong Wongkeo and Arnon Chaipanich, “Compressive Strength of Blended Portland Cement Mortars Incorporating Fly Ash and Silica Fume at High Volume Replacement,” *Chiang Mai Univ. J. Nat. Sci.*, vol. 12, no. 2, pp. 121–130, 2013.
- [32] Obada Kayali, Naseer Haque M, and M Khatib Jamal, “Sustainability and Emerging Concrete Materials and Their Relevance to the Middle East,” pp. 103–110, 2008.
- [33] ACI 234R-06, “Guide for the Use of Silica Fume in Concrete,” 2006.
- [34] Xiuping Feng and Boyd Clark, “Evaluation of the Physical and Chemical Properties of Fly Ash Products for Use in Portland Cement Concrete,” in *World of Coal Ash (WOCA) Conference - May 9-12, 2011 in Denver, CO, USA*, 2011, pp. 1–8.
- [35] Mehta P. Kumar, “High-performance, high-volume fly ash concrete for sustainable development,” in *International Workshop on Sustainable Development and Concrete*

- Technology*, 2004, pp. 3–14.
- [36] Jatuphon Tangpagasit, Raungrut Cheerarot, Chai Jaturapitakkul, and I Kraiwood Kiattikomo, “Packing effect and pozzolanic reaction of fly ash in mortar,” vol. 35, pp. 1145–1151, 2005.
- [37] Payá J., Borrachero M. V., Monzó J., Peris-Mora E., and Amahjour F., “Enhanced conductivity measurement techniques for evaluation of fly ash pozzolanic activity,” *Cem. Concr. Res.*, vol. 31, no. 1, pp. 41–49, 2001.
- [38] Rajesh K., Amiy, K.S., Roy D.K., “Characterization and development of eco-friendly concrete using industrial waste - A Review,” *J. Urban Environ. Eng.*, vol. 8, pp. 98–108, 2014.
- [39] Fathollah Sajedi, “Effect of curing regime and temperature on the compressive strength of cement-slag mortars,” no. April, 2012.
- [40] Rodrigo Fernandez Lopez, “Calcined Clayey Soils as a Potential Replacement for Cement in Developing Countries,” vol. 4302, p. 178, 2009.
- [41] Erhan Güneyisi, Mehmet Gesoğlu, and Kasım Mermerdaş, “Improving strength, drying shrinkage, and pore structure of concrete using metakaolin,” *Mater. Struct.*, vol. 41, pp. 937–949, 2008.
- [42] Al-rawas Amer Ali and Hago Abdel Wahid, “Evaluation of field and laboratory produced burnt clay pozzolans,” vol. 31, pp. 29–35, 2006.
- [43] Samet B, Mnif T, and Chaabouni M, “Use of a kaolinitic clay as a pozzolanic material for cements : Formulation of blended cement,” vol. 29, pp. 741–749, 2007.
- [44] Chakchouk A, Samet B, and Mnif T, “Study on the potential use of Tunisian clays as pozzolanic material,” vol. 33, pp. 79–88, 2006.
- [45] ACI 234R-06, “Use of Raw or Processed Natural Pozzolans in Concrete,” *Am. Concr. Inst.*, pp. 1–24, 2001.
- [46] Sumrerng Rukzon, Prinya Chindapasirt, and Rattana Mahachai, “Effect of grinding on chemical and physical properties of rice husk ash,” *Int. J. Miner. Metall. Mater.*, vol. 16, no. 2, pp. 242–247, 2009.
- [47] W. Panpa and S. Jinawath, “Applied Catalysis B : Environmental Synthesis of ZSM-5 zeolite and silicalite from rice husk ash,” vol. 90, pp. 389–394, 2009.
- [48] Abdullahi M Usman, Raji A, and Nuhu H Waziri, “Characterisation of Girei Rice Husk Ash for Silica Potential,” vol. 8, no. 1, pp. 68–71, 2014.
- [49] Andrzej M. Brandt, *Cement-Based Composites - Materials, mechanical properties and performance*, Second Edi. Taylor & Francis Group, 2009.
- [50] Nair G. Deepa, K. S. Jagadish, and A. Fraaij, “Reactive pozzolanas from rice husk ash: An alternative to cement for rural housing,” *Cem. Concr. Res.*, vol. 36, no. 6, pp. 1062–1071, 2006.
- [51] Wansom Supaporn, Janjaturaphan Sirirat, and Sinthupinyo Sakprayut, “Pozzolanic Activity of Rice Husk Ash : Comparison of Various Electrical Methods,” *J. Miner. Mater.*, vol. 19, no. 2, pp. 1–7, 2009.
- [52] Givi A.N., Rashid A.S., Aziz F.N.A., Salleh M.A.M., “Contribution of Rice Husk Ash to the



- Properties of Mortar and Concrete : A Review,” *J. Am. Sci.*, vol. 6, no. 3, pp. 157–165, 2010.
- [53] Rajput Jayanti, Yadav R K, and Chandak R, “The Effect Of Rice Husk Ash Used As Supplementary Cementing Material On Strength Of Mortar,” *Int. J. Eng. Res. Appl.*, vol. 3, no. 3, pp. 133–136, 2013.
- [54] Karim M. R., Zain M. F M, and Jamil M., “Strength of mortar and concrete as influenced by rice husk ash: A review,” *World Appl. Sci. J.*, vol. 19, no. 10, pp. 1501–1513, 2012.
- [55] Kılıç A and Ati C D, “The effects of scoria and pumice aggregates on the strengths and unit weights of lightweight concrete,” vol. 4, no. 10, pp. 961–965, 2009.
- [56] Taha A., AL-Naaymi Ali, and Mohamed A., “Chemical , Physical and Geotechnical Properties Comparison between Scoria and Pumice Deposits in Dhamar – Rada Volcanic Field -SW Yemen,” *Aust. J. Basic Appl. Sci.*, vol. 7, no. 11, pp. 116–124, 2013.
- [57] ASTM C 618, “Standard Specification for Coal Fly Ash and Raw or Calcined Natural Pozzolan for Use in Concrete,” 2005.
- [58] Hieronimi A. Mboya, John Makunza, and Yazidi H. B. Mwishwa, “Assessment of Pumice Blocks in Comparison to Cement Sand Blocks and Burnt Blocks ‘ The Case of Mbeya City - Tanzania ,”” vol. 8, no. 1, pp. 43–55, 2011.
- [59] Green S., Brooke N., and McSaveney L., “Pumice Aggregates for Structural Lightweight and Internally Cured Concretes [www.perlite.co.nz/images/high-strength-lightweight-concrete.pdf](http://www.perlite.co.nz/images/high-strength-lightweight-concrete.pdf) (Accessed Jan 20, 2016).,” 2011.
- [60] Dugali S.K., *Building Materials*, 3 Edition. New Age International (P) Limited, Publisher, 2008.
- [61] Uzal B, Turanli L, Yücel H, Göncüoğlu M.C, and Çulfaz A, “Pozzolanic activity of clinoptilolite : A comparative study with silica fume , fl y ash and a non-zeolitic natural pozzolan,” *Cem. Concr. Res.*, vol. 40, pp. 398–404, 2010.
- [62] Terje Rein and Thorstensen P, “Inconsistencies in the pozzolanic strength activity index ( SAI ) for silica fume according to EN and ASTM,” 2014.
- [63] Luxan M P, Madruga F, and Saavedra J, “Rapid Evaluation of Pozzolanic Activity of Natural Products,” *Cem. Concr. Res.*, vol. 19, pp. 63–68, 1989.
- [64] Donatello S., Freeman-Pask A., T. M., and Cheeseman C. R., “Effect of milling and acid washing on the pozzolanic activity of incinerator sewage sludge ash,” *Cem. Concr. Compos.*, vol. 32, no. 1, pp. 54–61, 2010.
- [65] SS-EN 196-3:2005+A1:2008 (E), “Method of testing cement - Part 3: Determination of setting times and soundness,” no. 123867, 2015.
- [66] SS-EN 197-1, *Cement - Part 1: Composition, specification and conformity criteria for common cements*, no. 123867. 2011.
- [67] El-Dakroury A. and Gasser M.S., “Rice husk ash ( RHA ) as cement admixture for immobilization of liquid radioactive waste at different temperatures,” *J. Nucl. Mater.*, vol. 381, no. 3, pp. 271–277, 2008.
- [68] Juenger Maria, “Effects of Supplementary Cementing Materials on the Setting Time and Early

- Strength of Concrete (FHWA/TX-08/0-5550-1),” vol. 7, no. 82, 2008.
- [69] Kwabena A Boakye, Eugene Atiemo, James Sarfo-ansah, Augustine Osei-frimpong, and Albert A Adjaottor, “Improvement of Setting Times and Early Strength Development of Clay Pozzolana Cement through Chemical Activation,” vol. 1, no. 2, pp. 77–83, 2014.
- [70] Duggal S.K., *Building Materials*, 3 Edition. New Delhi: New Age International (P) Limited, 2008.
- [71] M. S. Mamlouk and J. P. Zaniewski, *Materials for Civil and Construction Engineers*, Third Edit. Upper Saddle River Boston Columbus San Francisco New York Indianapolis London Toronto Sydney Singapore Tokyo Montreal Dubai Madrid Hong Kong Mexico City Munich Paris Amsterdam Cape Town: Prentice Hall, Pearson, 2011.
- [72] N. Smaoui, M. A. Be´rube, B. Fournier, B. Bissonnette, and B. Durand, “Effects of alkali addition on the mechanical properties and durability of concrete,” vol. 35, pp. 203–212, 2005.
- [73] Mehdipour Iman and Khayat Kamal H, “Effect of supplementary cementitious material content and binder dispersion on packing density and compressive strength of sustainable cement paste,” *ACI Mater. J.*, vol. 113, no. 3, pp. 361–372, 2016.
- [74] Thomas A. Holm and Theodore W. Bremner, “State-of-the-Art Report on High-Strength , High-Durability Structural Low-Density Concrete for Applications in Severe Marine Environments Structures Laboratory,” no. August, 2000.
- [75] S. Kourounis, S. Tsvilis, P. E. Tsakiridis, G. D. Papadimitriou, and Z. Tsibouki, “Properties and hydration of blended cements with steelmaking slag,” vol. 37, pp. 815–822, 2007.
- [76] S. C. Bostanci, M. Limbachiya, and H. Kew, “Portland slag and composites cement concretes : engineering and durability properties,” vol. 112, pp. 542–552, 2016.
- [77] Bhanja S and Sengupta B, “Influence of silica fume on the tensile strength of concrete,” vol. 35, pp. 743–747, 2005.
- [78] ASTM C 311-05, “Standard Test Methods for Sampling and Testing Fly Ash or Natural Pozzolans for Use,” pp. 1–9, 2008.
- [79] V. Patel and N. Shah, “A Survey of High Performance Concrete Developments in Civil Engineering Field,” *Open J. Civ. Eng.*, vol. 3, no. June, pp. 69–79, 2013.
- [80] Hailong Ye, Aleksandra Radlinska, and Juliana Neves, “Drying and carbonation shrinkage of cement paste containing alkalis,” 2017.
- [81] Zongjin Li, Christopher Leung, and Yunping Xi, *Structural Renovation in Concrete*, 1 Edition. London and New York: Taylor & Francis, 2009.
- [82] Zongjin Li, *Advanced Concrete Technology*. New Jersey: John Wiley & Sons, 2011.
- [83] J. Sarfo-ansah, E. Atiemo, K. A. Boakye, D. Adjei, and A. A. Adjaottor, “Calcined Clay Pozzolan as an Admixture to Mitigate the Alkali-Silica Reaction in Concrete,” no. May, pp. 20–26, 2014.
- [84] A. N. Swaminathen and S. R. Ravi, “Use of Rice Husk Ash and Metakaolin as Pozzolonas for Concrete : A Review,” vol. 11, no. 1, pp. 656–664, 2016.
- [85] Khan M I and Lynsdale C J, “Strength , permeability , and carbonation of high-performance

- concrete,” vol. 32, pp. 123–131, 2002.
- [86] Kosmatka S., Kerkhoff B., and Panarese W. C., “Fly Ash , Slag , Silica Fume , and Natural Pozzolans,” *Chapter 3, Des. Control Concr. Mix. 15th Ed.*, no. 54048, pp. 57–72, 1996.
- [87] J. Setina, A. Gabrene, and I. Juhnevica, “Effect of pozzolanic additives on structure and chemical durability of concrete,” *Procedia Eng.*, vol. 57, pp. 1005–1012, 2013.
- [88] H. A. Mboya, J. K. Makunza, and Y. H. B. Mwishwa, “Assessment of Pumice Blocks in Comparison to Cement Sand Blocks and Burnt Blocks ‘ The Case of Mbeya City - Tanzania ,”” *J. Civ. Eng. Res. Pract.*, vol. 8, no. 1, pp. 43–55, 2011.
- [89] F. A. Oyawale, “Characterization of Rice Husk via Atomic Absorption Spectrophotometer for Optimal Silica Production,” vol. 2, no. 4, pp. 210–213, 2012.
- [90] G. A. Habeeb and H. Bin Mahmud, “Study on Properties of Rice Husk Ash and Its Use as Cement Replacement Material 3 . Experimental Work 2 . Scope of Work,” *Mater. Res.*, vol. 13, no. 2, pp. 185–190, 2010.
- [91] Njau K.N., Minja R.J.A, and Katima J.H.Y., ““Pumice soil: potential wetland substrate for treatment of domestic wastewater “Water Science and Technology,””” *IWA Publishing*, vol. vol 48, no. 5, pp. 85–92, 2008.
- [92] Ismail A. I. M., El-Shafey O. I., M. H. A. Amr, and El-Maghraby M. S., “Pumice Characteristics and Their Utilization on the Synthesis of Mesoporous Minerals and on the Removal of Heavy Metals,” *Int. Sch. Res. Not.*, vol. 2014, pp. 1–9, 2014.
- [93] BS EN 12350-1, “BS EN 12350-2:2009 Testing fresh concrete Part 2: Slump-test,” 2009.
- [94] SS-EN 196-2:, *Method of testing cement - Part 2: Chemical analysis of cement*, no. 123867. 2013.
- [95] ASTM D 854, “Standard Test for Specific Gravity of Soil Solids by Water Pycnometer,” 2003.
- [96] B8E1-1. Standard test method, “Standard test method specific gravity of solids & powders [www.yumpu.com /en/document/view/37351958/b8e1-1](http://www.yumpu.com/en/document/view/37351958/b8e1-1) (last visited on 21/June/2015),” no. 3, pp. 1–3, 1999.
- [97] SS-EN 196-6:2010, *Methods of testing cement - Part 6: Determination of Fineness*, no. 123867. 2010.
- [98] G. C. Cordeiro, R. D. T. Filho, L. M. Tavares, E. M. R. Fairbairn, and S.. Hempel, “Influence of particle size and specific surface area on the pozzolanic activity of residual rice husk ash Cement & Concrete Composites of residual rice husk ash,” no. MAY, 2011.
- [99] McCarthy M. J., Islam G. M. Sadiqul, L. J. Csetenyi, and M. R. Jones, “Evaluating Test Methods for Rapidly Assessing Fly Ash Reactivity for Use in Concrete,” in *World of Coal Ash Conference, April 22 - 25, 2013.*, 2013.
- [100] W. Mechti, T. Mnif, B. Samet, and M. J. Rouis, “Effects of the Secondary Minerals on the Pozzolanic Activity of Calcined Clay: Case of Quartz,” *Int. J. Res. Revies Appl. Sci.*, vol. 12, no. July, pp. 61–71, 2012.
- [101] ASTM C 187, “Standard Test Method for Normal Consistency of Hydraulic Cement 1,” pp. 10–12, 2004.

- [102] SS -EN 196-1, “Methods of testing cement – Part 1 : Determination of strength,” no. 123867, 2005.
- [103] I. Kett, *Engineered Concrete: Mix Design and Test Methods*, Second Edi. Boca Raton, London, New York: Taylor & Francis Group, 2010.
- [104] N. Y. Mostafa, S. A. S. El-hemaly, E. I. Al-wakeel, S. A. El-korashy, and P. W. Brown, “Characterization and evaluation of the pozzolanic activity of Egyptian industrial by-products I : Silica fume and dealuminated kaolin,” vol. 31, pp. 467–474, 2001.
- [105] R. Wassermann, A. Katz, and A. Bntur, “Minimum cement content requirements : a must or a myth ?,” *Mater. Struct.*, pp. 973–982, 2009.
- [106] D. Jelena, M. Snezana, I. Ivan, T. Nikola, “Properties of high-volume fly ash concrete and its role in sustainable development,” in *International conference-Contemporary achievement in civil engineering*, 2014.
- [107] A. Durán-Herrera, C. A. Juárez, P. Valdez, and D. P. Bentz, “Evaluation of sustainable high-volume fly ash concretes Cement & Concrete Composites,” vol. 33, pp. 39–45, 2011.
- [108] M. Schlaich and M. El Zareef, “Infra-lightweight concrete,” *Tailor Made Concr. Struct.*, pp. 707–714, 2008.
- [109] M. A. Rashid and M. A. Mansur, “Considerations in producing high strength concrete,” vol. 37, no. 1, pp. 53–63, 2009.
- [110] J. Kazjonovs, D. Bajare, and A. Korjakins, “Designing of High Density Concrete By Using Steel Treatment Waste,” *Mod. Build. Mater. Struct. Tech.*, 2010.
- [111] PD 6682-1:, “Aggregates — Part 1: Aggregates for concrete— Guidance on the use of BS EN 12620,” vol. 3, 2003.
- [112] BS EN 12620:, “Aggregates for concrete,” vol. 3, 2002.
- [113] BS EN 206-1, “Concrete —Part 1: Specification, performance, production and conformity,” vol. 3, 2000.
- [114] BS EN 12390-2:2000, “Testing hardened concrete - Part 2: Making and curing specimens for strength tests,” no. August, pp. 2–11, 2003.
- [115] BRE, *Design of normal concrete mixes*, 2nd Editio. London: BRE, 1997.
- [116] BS EN 1350-7, “Testing fresh concrete - Air content - Pressure method,” 2009.
- [117] BS EN 12350-6, “Testing fresh concrete - Density,” 2009.
- [118] BS 1881-116, “Testing concrete — Part 116: Method for determination of compressive strength of concrete cubes,” no. December, 1983.
- [119] BS EN 206, “Concrete — Specification , performance , production and conformity,” no. May, 2014.
- [120] SCCT, *CSI: 2010 - Construction Standard*, vol. 2. 2010.
- [121] J. H. Ideker, T. Fu, and T. Deboodt, “Development of Shrinkage Limits and Testing Protocols for ODOT High Performance Concrete,” Washington, 2013.
- [122] ASTM C157, “Standard Test Method for Length Change of Hardened Hydraulic-Cement Mortar and,” vol. 04, pp. 1–7, 2003.

- [123] L. Barcelo, M. Moranville, and B. Clavaud, "Autogenous shrinkage of concrete: A balance between autogenous swelling and self-desiccation," *Cem. Concr. Res.*, vol. 35, no. 1, pp. 177–183, 2005.
- [124] D. F. Velandia, C. J. Lynsdale, J. L. Provis, F. Ramirez, and A. C. Gomez, "Evaluation of activated high volume fly ash systems using Na<sub>2</sub>SO<sub>4</sub>, lime and quicklime in mortars with high loss on ignition fly ashes," *Constr. Build. Mater.*, vol. 128, pp. 248–255, 2016.
- [125] P. Technologies, C. E. Reductions, and I. C. Industry, "Existing and Potential Technologies for Carbon Emissions Reductions in the Indian Cement Industry Existing and Potential Technologies for Carbon Emissions Reductions in the Indian Cement Industry."
- [126] V. Jegatheesan, J. L. Liow, L. Shu, S. H. Kim, and C. Visvanathan, "The need for global coordination in sustainable development," *J. Clean. Prod.*, vol. 17, no. 7, pp. 637–643, 2009.
- [127] E. Benhelal, G. Zahedi, E. Shamsaei, and A. Bahadori, "Global strategies and potentials to curb CO<sub>2</sub> emissions in cement industry," *J. Clean. Prod.*, vol. 51, pp. 142–161, 2013.
- [128] N. M. Chanu and D. T. K. Devi, "Contribution Of Rice Husk Ash To The Properties Of Cement Mortar And Concrete," *I-7*, vol. 6, no. 3, pp. 157–165, 2013.
- [129] H. A. Mboya, C. K. King'ondou, K. N. Njau, and A. L. Mrema, "Measurement of Pozzolanic Activity Index of Scoria, Pumice, and Rice Husk Ash as Potential Supplementary Cementitious Materials for Portland Cement," *Adv. Civ. Eng. - Hindawi*, vol. 2017, 2017.
- [130] M. Processing, "USE OF PUMICE AND SCORIA AGGREGATES," vol. 50, no. 2, pp. 467–476, 2014.
- [131] BS EN 196 - 1, "Methods of testing cement – Part 1: Determination of strength," vol. (E), 2005.
- [132] British Standards Institution, "BS EN 206 Concrete — Specification, performance, production and conformity," *Bsi*, no. May, 2013.
- [133] R. Terje and T. Per, "Inconsistencies in the pozzolanic strength activity index (SAI) for silica fume according to EN and ASTM," *Mater. Struct.*, pp. 3979–3990, 2015.

## APPENDICES

**Appendix 1: Chemical composition in percentages (%) of Scoria, Pumice and RHA calcined at different temperatures.**

Sample	Temp	SiO <sub>2</sub>	Fe <sub>2</sub> O <sub>3</sub>	Al <sub>2</sub> O <sub>3</sub>	CaO	K <sub>2</sub> O	Na <sub>2</sub> O	MgO	SO <sub>3</sub>	Cl	P <sub>2</sub> O <sub>5</sub>	TiO <sub>2</sub>	MnO	L.o.I	Total
S 900	900	41.60	15.10	13.40	10.10	1.09	3.11	5.43	0.12	0.00	0.98	3.31	0.19	5.01	99.44
S 800	800	43.40	14.80	15.60	10.50	1.01	2.63	5.43	0.16	0.00	1.19	3.60	0.22	1.47	100.01
S 700	700	45.30	14.60	12.90	10.20	0.81	2.35	5.46	0.12	0.04	1.05	3.39	0.22	3.52	99.96
S 600	600	44.50	15.20	12.00	10.30	1.00	2.30	5.04	0.13	0.00	1.03	3.27	0.18	5.05	100.00
S-N	-	40.00	13.90	13.00	9.60	1.22	2.13	4.62	0.07	0.00	1.11	3.08	0.21	10.76	99.70
P 900	900	63.10	4.48	15.90	0.62	5.10	5.15	0.27	0.00	0.19	0.00	0.66	0.36	4.18	100.01
P 800	800	57.30	4.56	16.60	1.24	5.34	5.89	0.26	0.16	0.24	0.00	0.64	0.33	7.45	100.01
P 700	700	55.00	4.42	15.60	0.80	5.36	5.46	0.24	0.12	0.45	0.10	0.60	0.33	10.32	98.80
P 600	600	56.60	4.56	17.50	1.27	5.74	5.96	0.31	0.19	0.58	0.10	0.64	0.35	6.20	100.00
P-N	-	55.40	4.64	16.40	1.70	5.46	5.33	0.62	0.10	0.55	0.00	0.68	0.34	8.78	100.00
RHA 900	900	88.80	0.44	0.32	0.65	2.02	0.00	0.24	0.30	0.10	0.62	0.00	0.13	6.07	99.69
RHA 800	800	92.40	0.49	0.38	0.80	2.23	0.19	0.30	0.20	0.24	0.48	0.00	0.16	2.13	100.00
RHA 700	700	94.70	0.24	0.29	0.55	2.35	0.00	0.35	0.20	0.38	0.58	0.00	0.14	0.21	99.99
RHA 600	600	94.25	0.26	0.33	0.63	2.51	0.00	0.28	0.25	0.28	0.54	0.00	0.11	0.56	100.00
RHA-uc	-	93.50	0.53	0.00	0.67	2.45	0.19	0.38	0.24	0.36	0.73	0.00	0.12	0.86	100.03

**Appendix 2: Specific Gravity, Gross Density and Specific Surface Area**

<b>S/No</b>	<b>Sample No</b>	<b>Specific Gravity</b>	<b>Gross Density</b>	<b>Fineness</b>
			<b>kg/m<sup>3</sup></b>	<b>m<sup>2</sup>/kg</b>
1	S-N	2.93	2930	575
2	S 600	3.04	3040	456
3	S 700	2.97	2970	333
4	S 800	2.96	2960	314
5	S 900	2.95	2950	325
6	P-N	2.39	2390	506
7	P 600	2.43	2430	573
8	P 700	2.43	2430	447
9	P 800	2.41	2410	479
10	P 900	2.50	2500	369
11	RHA-uc	2.17	2170	611
12	RHA 600	2.14	2140	462
13	RHA 700	2.15	2150	309
14	RHA 800	2.21	2210	300
15	RHA 900	2.28	2280	282



**Appendix 3A: Conductivity and Pozzolanic Activity Index of Scoria**

<b>SCORIA (Conductivity (m/S))</b>											
Days	Time / hrs	S-N		S 600		S 700		S 800		S 900	
		PH	COND	PH	COND	PH	COND	PH	COND	PH	COND
1	1	11	5.94	11.18	5.44	11.31	5.65	10.99	4.61	11.22	5.3
	2	11.58	2.92	11.42	3.74	11.2	4.08	11.16	3.35	11.32	4.32
	24	10.81	1.78	11	2.45	11.11	2.63	10.94	2.29	11.08	3.37
3	72	10.6	1.47	10.95	2.12	10.87	2.27	10.82	2.18	11.28	3.16
7	168	10.6	1.33	10.85	1.76	10.97	1.75	10.87	1.93	11.07	3.06
14	336	10.28	1.08	10.51	1.46	10.58	1.4	10.55	1.9	11.15	2.99
28	672	9.83	0.84	10.63	1.12	10.42	0.81	10.68	1.58	11.27	2.73
<b>SCORIA (Pozzolanic Activity)</b>											
Days	Time (hrs)		PI		PI		PI		PI		PI
1	1		0		0		0		0		0
	2		50.842		31.25		27.788		27.332		18.491
	24		70.034		54.963		53.451		50.325		36.415
3	72		75.253		61.029		59.823		52.711		40.377
7	168		77.609		67.647		69.027		58.134		42.264
14	336		81.818		73.162		75.221		58.785		43.585
28	672		85.859		79.412		85.664		65.727		48.491

**Appendix 3B: Conductivity and Pozzolanic Activity Index of Pumice**

<b>PUMICE (Conductivity (m/S))</b>												
Days	Time / Hrs	P-N		P 600		P 700		P 800		P 900		
		PH	COND	PH	COND	PH	COND	PH	COND	PH	COND	
1	1	11.12	5.35	11.19	5.33	11.19	6.08	11.26	5.35	11.45	6.03	
	2	11.22	3.05	11.31	3.56	11.37	4.69	11.15	4.38	11.74	5.1	
	24	10.74	2.17	10.96	2.73	11.23	3.54	11.12	3.31	11.7	4.83	
3	72	10.62	2.03	11.13	2.51	11.24	3.54	11.35	3.23	11.79	4.62	
7	168	10.72	1.73	10.83	2.08	11.1	3.53	11.02	3.21	11.61	3.56	
14	336	10.75	1.5	10.88	1.9	11.1	3.23	10.96	3.17	11.57	3.35	
28	672	10.61	1.21	10.8	1.56	11.07	3.04	10.89	2.81	11.15	2.9	
			<b>PUMICE (Pozzolanic Activity)</b>									
Days	Time (hrs)		PI		PI		PI		PI		PI	
1	1		0		0		0		0		0	
	2		42.991		33.208		22.862		18.131		15.423	
	24		59.439		48.78		41.776		38.131		19.9	
3	72		62.056		52.908		41.776		39.626		23.383	
7	168		67.664		60.976		41.941		40		40.962	
14	336		71.963		64.353		46.875		40.748		44.444	
28	672		77.383		70.732		50		47.477		51.907	

**Appendix 3C: Conductivity and Pozzolanic Activity Index of RHA**

<b>RHA (Conductivity (m/S))</b>											
Days	Time / Hrs	RHA-uc		RHA 600		RHA 700		RHA 800		RHA 900	
		PH	COND	PH	COND	PH	COND	PH	COND	PH	COND
1	1	11.62	5.82	11.82	6.29	11.82	6.46	11.82	6.49	11.71	6.71
	2	11.31	2.22	11.7	4.96	11.76	5.34	11.81	5.57	11.8	5.87
	24	11.67	1.23	11.65	3.49	11.57	4.43	11.7	5.03	11.74	5.24
3	72	10.15	1.03	11.32	3.13	11.37	2.91	11.75	4.39	11.64	4.71
7	168	10.04	0.83	10.73	1.15	10.94	1.33	11.49	2.55	11.41	2.35
14	336	9.86	0.81	10.45	0.95	10.63	0.97	11.12	1.5	11.19	1.43
28	672	9.68	0.77	10.08	0.8	10.01	0.75	10.19	0.65	10.35	0.65
<b>RHA (Pozzolanic Activity)</b>											
Days	Time (hrs)	PI		PI		PI		PI		PI	
1	1	0		0		0		0		0	
	2	61.856		21.145		17.337		14.176		12.519	
	24	78.866		44.515		31.424		22.496		21.908	
3	72	82.302		50.238		54.954		32.357		29.806	
7	168	85.739		81.717		79.412		60.709		64.978	
14	336	86.082		84.897		84.985		76.888		78.689	
28	672	86.77		87.281		88.39		89.985		90.313	

**Appendix 4: Setting time, water cement ratio and soundness**

<b>Sample ID</b>	<b>% Replacement</b>	<b>Initial (min)</b>	<b>Final (min)</b>	<b>Water demand</b>	<b>W/B Ratio</b>	<b>Soundness (mm)</b>
PLC (42.5N)	0	78	126		0.27	1.0
PPC (42.5N)	0	166	285		0.33	2.0
S 900	10	70	161	130	0.26	1.0
S 900	20	94	158	130	0.26	1.0
S 900	30	82	150		0.28	1.0
S 900	40	112	153	135	0.27	1.0
S 800	10	89	143	130	0.26	0
S 800	20	125	136	135	0.27	0
S 800	30	98	145	140	0.28	0.5
S 800	40	99	134	140	0.28	0.5
S 700	10	100	136	130	0.26	0.5
S 700	20	86	144	135	0.27	1.0
S 700	30	90	130	140	0.28	0.5
S 700	40	120	165	140	0.28	1.0
S 600	10	85	130	140	0.28	1.0
S 600	20	97	132	140	0.28	0
S 600	30	103	137	145	0.29	1.0
S 600	40	98	128	145	0.29	0
S-N	10	89	135	140	0.28	0
S-N	20	71	123	140	0.28	1.0
S-N	30	62	109	145	0.29	0
S-N	40	98	132	145	0.29	0.5

<b>Sample ID</b>	<b>% Replacement</b>	<b>Initial (min)</b>	<b>Final (min)</b>	<b>Water demand</b>	<b>W/B Ratio</b>	<b>Soundness (mm)</b>
P 900	10	146	174	130	0.26	0.5
P 900	20	142	175	140	0.28	1.0
P 900	30	144	179	150	0.30	0.5
P 900	40	150	199	150	0.30	0.5
P 800	10	100	126	135	0.27	1.0
P 800	20	104	119	145	0.29	2.0
P 800	30	98	114	150	0.30	2.0
P 800	40	101	115	160	0.32	1.0
P 700	10	99	139	145	0.29	0.0
P 700	20	110	151	150	0.30	0.5
P 700	30	106	145	165	0.33	0.5
P 700	40	105	145	170	0.34	0.5
P 600	10	95	155	140	0.28	1.0
P 600	20	88	166	145	0.29	1.0
P 600	30	120	174	155	0.31	1.5
P 600	40	107	140	165	0.33	2.0
P-N	10	118	153	135	0.27	0.0
P-N	20	119	175	140	0.28	1.0
P-N	30	119	175	145	0.29	1.0
P-N	40	118	183	145	0.29	0.0
RHA 900	10	65	140	130	0.26	1.5
RHA 900	20	84	135	130	0.26	1.0
RHA 900	30	141	188	130	0.26	1.0

<b>Sample ID</b>	<b>% Replacement</b>	<b>Initial (min)</b>	<b>Final (min)</b>	<b>Water demand</b>	<b>W/B Ratio</b>	<b>Soundness (mm)</b>
RHA 900	40	128	168	130	0.26	0.5
RHA 800	10	107	133	145	0.29	1.0
RHA 800	20	111	160	160	0.32	0.5
RHA 800	30	95	142	170	0.34	0.5
RHA 800	40	106	179	185	0.37	1.0
RHA 700	10	105	148	150	0.3	1.0
RHA 700	20	108	150	160	0.32	1.0
RHA 700	30	126	162	175	0.35	0.5
RHA 700	40	130	180	190	0.38	0.5
RHA 600	10	142	188	145	0.29	1.0
RHA 600	20	131	162	160	0.32	0.5
RHA 600	30	166	186	170	0.35	0.5
RHA 600	40	176	224	190	0.38	0.5
RHA-uc	10	119	163	140	0.28	1.0
RHA-uc	20	111	157	155	0.31	0.5
RHA-uc	30	104	172	175	0.35	0.5
RHA-uc	40	152	199	190	0.38	0.5

**Appendix 5: Water cement ratio, % replacement, and calcining temperature**

% Replacement	WATER CEMENT RATIO															
	Control	SCORIA					PUMICE					RICE HUSK ACH				
	PLC	900	800	700	600	N	900	800	700	600	N	900	800	700	600	uc
10	0.26	0.26	0.26	0.26	0.28	0.28	0.26	0.27	0.29	0.28	0.27	0.26	0.29	0.28	0.29	0.28
20	0.26	0.26	0.27	0.27	0.28	0.28	0.28	0.29	0.30	0.29	0.28	0.26	0.32	0.28	0.32	0.31
30	0.26	0.26	0.28	0.28	0.29	0.29	0.30	0.30	0.33	0.31	0.29	0.26	0.34	0.29	0.35	0.35
40	0.26	0.27	0.28	0.28	0.29	0.29	0.30	0.32	0.34	0.33	0.29	0.26	0.37	0.29	0.38	0.38

## Appendix 6: Compressive Strength

Sample No/ID	Calcining Temp. (°C)	% Replac- ement	Compressive Strength (MPa)				
			2	7	28	56	90
PLC (42.5N)	-	-	22.1	37.5	53.9	54.9	56.7
S 900 - 10	900	10	6.8	18.0	18.4	27.5	27.7
S 900 - 20	900	20	6.5	13.5	16.0	27.7	28.2
S 900 - 30	900	30	5.3	8.3	11.9	17.4	18.2
S 900 - 40	900	40	6.9	10.2	13.0	18.5	21.1
S800 - 10	800	10	17.2	44.3	51.3	52.0	54.9
S800 - 20	800	20	22.0	43.0	47.3	43.3	48.1
S800 - 30	800	30	19.9	29.4	38.9	42.3	43.1
S800 - 40	800	40	14.4	26.4	28.5	32.7	32.2
S 700 - 10	700	10	21.0	34.7	42.9	42.6	77.0
S 700 - 20	700	20	19.7	27.0	37.3	39.0	74.8
S 700 - 30	700	30	18.3	24.9	37.6	32.7	32.7
S 700 - 40	700	40	12.8	20.1	29.5	27.6	27.0
S 600 - 10	600	10	24.3	43.3	54.0	57.2	57.3
S600 - 20	600	20	24.1	33.1	50.5	49.6	51.0
S 600 - 30	600	30	24.0	31.4	50.1	40.2	50.1
S 600 - 40	600	40	19.7	28.6	41.5	38.6	39.6
S-N - 10	100	10	30.6	46.8	61.0	65.7	65.8
S-N - 20	100	20	29.5	44.4	57.8	58.4	58.8
S-N - 30	100	30	24.3	38.0	46.6	50.0	51.1
S-N - 40	100	40	16.2	31.4	43.6	44.1	43.8



Sample No/ID	Calcining Temp. (°C)	% Replac- ement	Compressive Strength (MPa)				
			2	7	28	56	90
P 900 - 10	900	10	27.9	44.4	54.4	69.0	62.9
P 900 - 20	900	20	26.9	43.2	50.8	54.2	60.0
P 900 - 30	900	30	21.9	39.6	48.3	50.6	0.0
P 900 - 40	900	40	19.8	34.1	44.3	46.0	0.0
P 800 - 10	800	10	20.9	42.7	47.9	52.9	54.1
P 800 - 20	800	20	21.3	42.0	42.2	51.4	58.3
P 800 - 30	800	30	19.4	33.0	40.6	51.7	55.2
P 800 - 40	800	40	19.3	32.4	39.4	49.6	48.8
P 700 - 10	700	10	26.0	41.9	56.7	57.6	58.0
P 700 - 20	700	20	22.0	28.6	43.8	47.7	47.5
P 700 - 30	700	30	19.1	27.4	40.3	40.2	40.5
P 700 - 40	700	40	16.6	22.5	32.0	34.0	33.3
P 600 - 10	600	10	24.0	40.0	60.5	62.6	62.9
P 600 - 20	600	20	25.8	35.4	47.3	54.4	54.6
P 600 - 30	600	30	15.3	35.8	40.6	48.6	49.2
P 600 - 40	600	40	11.2	24.8	34.6	36.1	37.2
P-N - 10	100	10	25.3	38.9	51.9	52.9	52.3
P-N - 20	100	20	26.5	43.2	43.8	52.8	52.8
P-N - 30	100	30	19.0	33.1	41.9	46.7	46.6
P-N - 40	100	40	14.2	25.3	34.8	36.7	37.6
RHA 900 - 10	900	10	29.2	46.5	55.9	59.8	59.6
RHA 900 - 20	900	20	23.9	34.8	40.3	44.3	45.2

Sample No/ID	Calcining Temp. (°C)	% Replac- ement	Compressive Strength (MPa)				
			2	7	28	56	90
RHA 900 - 30	900	30	19.0	31.4	34.7	44.2	45.2
RHA 900 - 40	900	40	9.8	19.4	20.8	24.6	25.1
RHA 800 - 10	800	10	38.0	46.7	54.6	56.9	56.1
RHA 800 - 20	800	20	22.7	32.9	42.3	48.9	49.1
RHA 800 - 30	800	30	18.5	25.5	30.3	38.0	44.8
RHA 800 - 40	800	40	14.9	22.4	30.0	31.7	43.2
RHA 700 - 10	700	10	27.4	48.1	56.7	59.2	64.4
RHA 700 - 20	700	20	24.0	44.3	50.4	50.8	60.1
RHA 700 - 30	700	30	24.2	30.0	43.3	44.8	45.5
RHA 700 - 40	700	40	19.0	23.5	35.1	35.4	42.4
RHA 600 - 10	600	10	32.7	48.1	66.8	69.4	69.5
RHA 600 - 20	600	20	24.7	38.8	50.3	47.7	55.3
RHA 600 - 30	600	30	21.5	33.5	39.6	42.8	42.5
RHA 600 - 40	600	40	18.4	30.4	29.8	38.1	39.3
RHA-uc - 10	100	10	25.7	38.6	44.3	49.6	49.1
RHA-uc - 20	100	20	25.6	39.5	45.7	50.1	51.6
RHA-uc - 30	100	30	25.5	37.9	46.3	45.5	49.6
RHA-uc - 40	100	40	20.7	33.0	41.9	42.5	44.6

**Appendix 7: Strength Activity Index (SAI)**

Sample No/ID	Calcining Temp. (°C)	% Replacement	Strength Activity Index (%)				
			2	7	28	56	90
S 900 - 10	900	10	30.8	48.0	34.1	50.1	48.9
S 900 - 20	900	20	29.4	36.0	29.7	50.5	49.8
S 900 - 30	900	30	24.1	22.1	22.0	31.7	32.2
S 900 - 40	900	40	31.3	27.2	24.2	33.8	37.3
S800 - 10	800	10	77.9	118.2	95.1	94.7	96.9
S800 - 20	800	20	99.6	114.6	87.8	78.8	84.9
S800 - 30	800	30	90.2	78.3	72.2	77.1	76.1
S800 - 40	800	40	65.1	70.4	52.8	59.6	56.8
S 700 - 10	700	10	95.1	92.6	79.6	77.6	77.0
S 700 - 20	700	20	89.1	72.0	69.1	71.0	74.8
S 700 - 30	700	30	82.6	66.3	69.7	59.6	57.7
S 700 - 40	700	40	57.7	53.7	54.7	50.3	47.6
S 600 - 10	600	10	109.8	115.4	100.1	104.2	101.1
S600 - 20	600	20	109.1	88.3	93.7	90.3	90.1
S 600 - 30	600	30	108.9	83.7	92.9	73.2	88.4
S 600 - 40	600	40	89.1	76.3	76.9	70.4	69.9
S-N - 10	100	10	138.7	124.8	113.2	119.7	116.2
S-N - 20	100	20	133.4	118.4	107.3	106.5	103.7
S-N - 30	100	30	110.0	101.2	86.4	91.1	90.3
S-N - 40	100	40	73.4	83.7	80.9	80.3	77.2

Sample No/ID	Calcining Temp. (°C)	% Replacement	Strength Activity Index (%)				
			2	7	28	56	90
P 900 - 10	900	10	126.2	118.3	100.9	125.6	111.0
P 900 - 20	900	20	121.7	115.2	94.3	98.7	105.9
P 900 - 30	900	30	99.0	105.6	89.6	92.2	98.0
P 900 - 40	900	40	89.8	91.0	82.1	83.9	85.8
P 800 - 10	800	10	94.7	113.9	88.9	96.4	95.4
P 800 - 20	800	20	96.6	112.0	78.2	93.6	102.8
P 800 - 30	800	30	87.9	87.9	75.3	94.2	97.3
P 800 - 40	800	40	87.2	86.4	73.0	90.3	87.9
P 700 - 10	700	10	117.7	111.8	105.1	104.9	102.4
P 700 - 20	700	20	99.6	76.2	81.1	86.9	83.8
P 700 - 30	700	30	86.6	73.0	74.8	73.2	71.1
P 700 - 40	700	40	75.1	59.9	59.3	61.9	58.8
P 600 - 10	600	10	108.9	106.7	112.2	114.0	111.0
P 600 - 20	600	20	116.8	94.3	92.8	99.1	96.3
P 600 - 30	600	30	69.1	95.6	75.3	88.6	86.8
P 600 - 40	600	40	50.6	66.1	64.1	65.8	65.6
P-N - 10	100	10	114.3	103.7	96.2	96.4	92.3
P-N - 20	100	20	120.0	115.1	81.2	96.2	93.2
P-N - 30	100	30	85.8	88.2	77.7	85.0	82.2
P-N - 40	100	40	64.3	67.3	64.5	66.8	66.4
RHA 900 - 10	900	10	132.3	124.0	103.7	108.9	105.1
RHA 900 - 20	900	20	108.1	92.9	74.8	80.6	79.8

Sample No/ID	Calcining Temp. (°C)	% Replacement	Strength Activity Index (%)				
			2	7	28	56	90
RHA 900 - 30	900	30	86.0	83.7	64.3	80.5	79.8
RHA 900 - 40	900	40	44.3	51.6	38.6	44.8	44.3
RHA 800 - 10	800	10	172.1	124.4	101.2	103.6	99.1
RHA 800 - 20	800	20	102.6	87.7	78.5	89.1	86.6
RHA 800 - 30	800	30	83.8	68.1	56.2	69.2	79.1
RHA 800 - 40	800	40	67.4	59.8	55.6	57.7	76.3
RHA 700 - 10	700	10	124.0	128.3	105.1	107.8	113.6
RHA 700 - 20	700	20	108.5	118.1	93.5	92.6	106.1
RHA 700 - 30	700	30	109.6	80.1	80.4	81.6	80.3
RHA 700 - 40	700	40	86.0	62.7	65.1	64.5	74.8
RHA 600 - 10	600	10	147.9	128.2	123.8	126.4	122.6
RHA 600 - 20	600	20	111.9	103.3	93.3	86.9	97.0
RHA 600 - 30	600	30	97.2	89.4	73.5	78.0	75.7
RHA 600 - 40	600	40	83.4	81.1	55.3	69.4	69.3
RHA-uc - 10	100	10	116.2	103.0	82.1	90.3	86.6
RHA-uc - 20	100	20	115.8	105.3	84.8	91.3	91.0
RHA-uc - 30	100	30	115.7	101.0	85.8	82.9	87.5
RHA-uc - 40	100	40	93.8	87.9	77.7	77.4	78.7

**Appendix 8: Shrinkage (25 x 25 x 300 mm prism)**

<b>Sample ID/ Number</b>	<b>Initial Reading (mm)</b>	<b>Final Reading (mm)</b>	<b>Shrinkage (mm)</b>
BS			10 max
PLC	300.0	297.5	2.5
S 900 / 10%	295.0	294.0	1.0
S 900 / 20%	297.0	295.5	1.5
S 900 / 30%	301.5	300.0	1.5
S 900 / 40%	302.0	300.0	2.0
S 800 / 10%	-	-	
S 800 / 20%	302.3	302.0	0.3
S 800 / 30%	303.5	302.0	1.5
S 800 / 40%	302.6	301.0	1.6
S 700 / 10%	301.5	301.0	0.5
S 700 / 20%	299.5	299.5	0.0
S 700 / 30%	301.5	300.0	1.5
S 700 / 40%	299.3	299.0	0.3
S 600 / 10%	300.8	300.0	0.8
S 600 / 20%	300.0	298.0	2.0
S 600 / 30%	303.2	302.0	1.2
S 600 / 40%	301.6	301.0	0.6
S-N / 10%	301.8	301.0	0.8
S-N / 20%	303.0	302.0	1.0
S-N / 30%	301.5	301.0	0.5

<b>Sample ID/ Number</b>	<b>Initial Reading (mm)</b>	<b>Final Reading (mm)</b>	<b>Shrinkage (mm)</b>
S-N / 40%	301.5	301.0	0.5
P 900 / 10%	-	-	
P 900 / 20%	-	-	
P 900 / 30%	-	-	
P 900 / 40%	-	-	
P 800 / 10%	300.0	299.5	0.5
P 800 / 20%	299.0	298.5	0.5
P 800 / 30%	300.0	299.6	0.4
P 800 / 40%	-	-	
P 700 / 10%	300.0	299.8	0.2
P 700 / 20%	298.8	298.7	0.1
P 700 / 30%	300.0	300.0	0.0
P 700 / 40%	300.5	299.9	0.6
P 600 / 10%	301.0	300.0	1.0
P 600 / 20%	299.0	298.5	0.5
P 600 / 30%	299.5	299.0	0.5
P 600 / 40%	301.0	300.5	0.5
P-N / 10%	300.5	299.0	1.5
P-N / 20%	302.5	302.0	0.5
P-N / 30%	301.0	299.0	2.0
P-N / 40%	301.5	301.0	0.5
RHA 900 / 10%	299.5	299.0	0.5

<b>Sample ID/ Number</b>	<b>Initial Reading (mm)</b>	<b>Final Reading (mm)</b>	<b>Shrinkage (mm)</b>
RHA 900 / 20%	301.5	301.2	0.3
RHA 900 / 30%	299.0	298.7	0.3
RHA 900 / 40%	299.0	298.5	0.5
RHA 800 / 10%	301.0	299.5	1.5
RHA 800 / 20%	302.0	301.2	0.8
RHA 800 / 30%	300.0	299.6	0.4
RHA 800 / 40%	299.0	298.5	0.5
RHA 700 / 10%	300.5	299.0	1.5
RHA 700 / 20%	300.0	298.5	1.5
RHA 700 / 30%	300.0	298.5	1.5
RHA 700 / 40%	301.0	299.4	1.6
RHA 600 / 10%	303.0	302.4	0.6
RHA 600 / 20%	300.0	298.5	1.5
RHA 600 / 30%	300.5	298.8	1.7
RHA 600 / 40%	300.5	299.0	1.5
RHA-uc / 10%	300.5	299.8	0.7
RHA-uc / 20%	299.5	298.4	1.1
RHA-uc / 30%	300.5	300.1	0.4
RHA-uc / 40%	300.0	298.5	1.5